T.R.

GEBZE TECHNICAL UNIVERSITY

GRADUATE SCHOOL OF NATURAL AND APPLIED SCIENCES

ANALYTICAL REGULARIZATION ALGORITHM FOR SCATTERED FIELDS FROM ECCENTRICALLY MULTILAYERED CIRCULAR CYLINDERS

EMRAH SEVER

A THESIS SUBMITTED FOR THE DEGREE OF

DOCTOR OF PHILOSOPHY

DEPARTMENT OF ELECTRONIC ENGINEERING

GEBZE

2018

T.R.

GEBZE TECHNICAL UNIVERSITY

GRADUATE SCHOOL OF NATURAL AND APPLIED SCIENCES

ANALYTICAL REGULARIZATION ALGORITHM FOR SCATTERED FIELDS FROM ECCENTRICALLY MULTILAYERED CIRCULAR CYLINDERS

EMRAH SEVER

A THESIS SUBMITTED FOR THE DEGREE OF DOCTOR OF PHILOSOPHY

DEPARTMENT OF ELECTRONIC ENGINEERING

THESIS SUPERVISOR

PROF. DR. YURY A. TUCHKIN

GEBZE

2018

T.C.
GEBZE TEKNİK ÜNİVERSİTESİ
FEN BİLİMLERİ ENSTİTÜSÜ

EŞ MERKEZLİ OLMAYAN ÇOK TABAKALI DAİRESEL SİLİNDİRLERDEN SAÇILAN ALANLAR İÇİN ANALİTİK REGÜLARİZASYON ALGORİTMASI

EMRAH SEVER
DOKTORA TEZİ
ELEKTRONİK MÜHENDİSLİĞİ ANABİLİM DALI

DANIŞMANI
PROF. DR. YURY A. TUCHKIN

GEBZE
2018

GEBZE TEKNİK ÜNİVERSİTESİ	DOKTORA JÜRİ ONAY FORMU

GTÜ Fen Bilimleri Enstitüsü Yönetim Kurulu'nun 10/01/2018 tarih ve 2018/03 sayılı kararıyla oluşturulan jüri tarafından 22/01/2018 tarihinde tez savunma sınavı yapılan Emrah Sever'in tez çalışması Elektronik Mühendisliği Anabilim Dalında DOKTORA tezi olarak kabul edilmiştir.

JÜRİ

ÜYE (TEZ DANIŞMANI)	: Prof. Dr. Yury A. TUCHKIN
ÜYE	: Prof. Dr. Ali ALKUMRU
ÜYE	: Prof. Dr. Ahmet DEMİR
ÜYE	: Doç. Dr. Fatih DİKMEN
ÜYE	: Yrd. Doç. Dr. Fatih ERDEN

ONAY

Gebze Teknik Üniversitesi Fen Bilimleri Enstitüsü Yönetim Kurulu'nun ...../...../..... tarih ve ...../..... sayılı kararı.

SUMMARY

This thesis presents the theoretical explanation and application of the Analytical Regularization Method (ARM) to a few different 2-dimensional boundary value problems (BVP) of eccentrically layered circular boundaries. Since the circular boundaries are under consideration, the linear algebraic equation system of the unknowns can be constructed either by infinite series representation of the fields that is obtained from Helmholtz equation through separation of variables (SoV) or by discretizing the integral equation that is arrived by the Green's identities from Helmholtz equation. However, both methods, in general, result in an algebraic equation of the first kind, which is ill-conditioned in numerical sense. The direct solution of such a system may have nothing common to the exact solution. The user of such a system must do some extra checks to make sure of the numerical results. In this thesis, such a bad system is transformed into a linear algebraic equation system of the second kind, which is a well-conditioned one, by means of the Analytical Regularization Method. This powerful semi-analytical semi-numerical method has been applied to a wide range of the diffraction problems with an approximate three decades of history. Within the scope of this study, the method is applied to both corresponding algebraic systems of the fields of the eccentrically layered circular impedance and dielectric boundaries, which are obtained from the separation of variables method and the discretization of the boundary integral equations through the entire domain Galerkin method. It is shown by means of various numerical results the necessity and the advantage of using such a method and to avoid using an un-regularized system. In addition, it is shown that by using the entire domain Galerkin method for the "algebraization" of the integral equation and then using the convolution theorem, a super-algebraically convergent algorithm can be constructed for 2-dimensional boundary value diffraction problems.

Key Words: 2-dimensional boundary value problems, eccentrically layered circular cylinders, separation of variables, boundary integral equations, Analytical Regularization Method (ARM), super-algebraically convergence.

ÖZET

Bu tezde, Analitik Regülarizasyon Metodunun teorik açıklaması yapılmış ve çok tabakalı eş merkezli olmayan dairesel sınırlara sahip birkaç farklı empedans ve dielektrik sınır değer problemlerine uygulanması açıklanmıştır. Dairesel sınırlar söz konusu olduğunda, bilinmeyenlere ilişkin cebrik denklem sistemi hem Helmholtz denkleminden değişkenlerine ayrıştırma yöntemi ile elde edilen sonsuz seriler biçiminde ifade edilen alanlardan hem de Green özdeşlikleri aracılığı ile Helmholtz denkleminden elde edilen sınır integral denklemlerinin ayrıklaştırılmasından elde edilebilir. Fakat iki yöntem sonucunda elde edilen cebrik denklem sistemleri sayısal uygulamalar açısından kötü koşullu olan birinci tip denklem sistemleridir. Böyle bir sistemin doğrudan çözülmesi ile elde edilen sonucun gerçek çözüm ile hiçbir ilgisi olmayabilir. Bu türden bir sistemin kullanıcısı elde edilen sayısal sonuçların doğruluğunu ekstra kontroller ile test etmelidir. Bu tezde, bu türden kötü bir sistem Analitik Regülarizasyon yöntemi ile iyi koşullu olan ikinci tip bir sisteme dönüştürülmektedir. Bu yöntem yaklaşık olarak 30 yıllık geçmişi olan ve geniş bir sınıftaki kırınım problemlerine uygulanan güçlü, yarı analitik yarı nümerik bir yöntemdir. Bu çalışma kapsamında bu yöntem, eş merkezli olmayan, dairesel sınırlı empedans ve dielektrik sınırlara ilişkin, değişkenlere ayrıştırma yöntemi elde edilen seri gösterimlerden oluşan sistemlere ve Green özdeşlikleri ile elde edilen integral denklemlerin tüm bölge Galerkin metodu ile ayrıklaştırılması ile elde edilen sistemlere uygulanmıştır. Çok çeşitli sayısal sonuçlar ile böyle bir yöntemin kullanılmasının gerekliliği ve avantajları ve regülarize edilmemiş bir sistemden uzak durulmasının gerekliliği gösterilmiştir. Ayrıca integral denklemlerin tüm bölge Galerkin yöntemi ile cebrik denklemlere dönüştürülmesi ve konvolüsyon teoreminin kullanılması ile 2-boyutlu sınır değer kırınım problemleri için üstel yakınsak bir algoritmanın kurulabildiği gösterilmiştir.

Anahtar Kelimeler: 2-boyutlu sınır değer problemleri, eş merkezli olmayan dairesel katmanlı silindirler, değişkenlere ayrıştırma yöntemi, sınır integral denklemleri, Analitik Regülarizasyon Metodu (ARM), üstel yakınsaklık.

ACKNOWLEDGEMENTS

I would like to express my deepest and sincere gratitude to my supervisor, Prof. Dr. Yury Tuchkin, who not only shared his profound scientific knowledge with me but also taught me great lessons of life. I also would like to thank Assoc. Prof. Dr. Fatih Dikmen. He has been a very important part of this work from the beginning to the end. His support, suggestions, and encouragement gave me the drive to complete this work. I would particularly like to thank Prof. Dr. Gökhan Uzgören. I am grateful for his suggestions and encouragement that made great contributions both to my academic and daily life. I also acknowledge Prof. Dr. Ali Alkumru who made very important contributions to my scientific insight with his great courses.

I wish to express my warm and sincere thanks to my mother-in-love for all her help and support during the raising of my child. Everything would be much harder without her help. I am grateful to my parents for their love and support. Nor will I ever be able to thank enough to them for their contributions during all my life. I am deeply thankful to my wife and my daughter for their love and sacrifice. Their existence gives meaning to my studies.

In addition, I want to thank my dear friend Assist. Prof. Dr. Yusuf Acar who supported me with motivating words almost every week. Finally, I want to thank the former and current members of the Electronics Engineering Department of the Gebze Technical University.

TABLE of CONTENTS

LIST of ABBREVIATIONS and ACRONYMS

Abbreviations and Acronyms		**Explanations**
∇	:	Gradient
Δ	:	Laplacian
$\vec{E}$	:	Vector electric field
$\vec{H}$	:	Vector magnetic field
$\vec{K}$	:	Vector electric surface current density
$\vec{K}_m$	:	Vector magnetic surface current density
ε	:	Dielectric permittivity
μ	:	Magnetic permeability
ω	:	Angular frequency
k	:	Wave number
LAES1	:	Linear algebraic equation of the first kind
LAES2	:	Linear algebraic equation of the second kind
ARM	:	Analytic Regularization Method
PEC	:	Perfectly electric conductive
RCS	:	Radar cross-section
EFIE	:	Electric field integral equation
MFIE	:	Magnetic field integral equation
TM-z	:	Transverse Magnetic along *z*-axis
TE-z	:	Transverse Electric along *z*-axis
SoV	:	Separation of variables
2-D	:	2-dimensional
BVP	:	Boundary value problem
w.r.t.	:	with respect to
$C^{m,\alpha}(G)$	:	Normed space of real or complex-valued uniformly Hölder m^{th} order continuously differentiable functions defined on G

LIST of FIGURES

LIST of TABLES

1. INTRODUCTION

Analytical solution of the scattering fields of monochromatic waves by circular cylinders is well known in electromagnetics and new designs are done in nanotechnology, metamaterial science, bio-electromagnetics, acoustics, and power transmission lines based on this analytical solution [1]-[3]. That is why the researchers in these areas must rely on the solutions based on this analytical model. Also, it is known from the literature that the expression of the scattered field of such a system is obtained by means of the Green's identities in an integral form and, the discretization of this integral yields an infinite, ill-conditioned linear algebraic equation system of the first kind (LAES1) in the form of $Ax=b$. The numerical calculation of this system as $x=A^{-1}b$ involves extra efforts [4], since the inversion of matrix A is very sensitive to the truncation number and suffers from round-off errors. Therefore, this system is error prone and unstable even for concentrically layered circular cylinders when the size of the algebraic system is large. Because the entries of matrix consist of Bessel and Hankel functions that have extremely fast decaying and fast-growing behavior while their order increases. Therefore, large values of the algebraic system cause overflow and underflow in the computer during calculations. In non-concentric case, the situation is far worse than the concentric case. In this case, because of the overflow and underflow, the rank of the matrix becomes fixed and smaller than the size of the algebraic system and no longer depends on the size of the algebraic system and, as a result, the system becomes degenerated. Consequently, the solution of such a system results in numerical catastrophe and the solution obtained from such a numerical process may have nothing common to the exact solution.

Since the inversion of a matrix of a first kind system is very sensitive to the truncation number, it is necessary to transform such first kind system to a second kind one by means of a regularization method for obtaining a new system immune to round-off errors and obtain reliable results. In this thesis, because of its stability and reliability even at lower truncation numbers, some approaches based on the Analytical Regularization Method are preferred. In this method, one left side operator (L) and one right side operator (R) are chosen such that applying them to LAES1 yields a new linear algebraic equation system of the second kind (LAES2) in the form of $(I+K)y=g$ where $I+K = LAR$ and $g=Lb$. This new system is stable independently of the truncation

number even at lower truncation numbers. As a result, it is safe, stable and ensures the reliability of numerical calculations [5].

In the context of this thesis, firstly, the ARM procedure has been applied to the system of scattered fields of eccentrically layered dielectric circular cylinders similar to presented in [6] for two parallel perfectly electric conductive (PEC) circular cylinders. Then the numerical results of the radar cross-section (RCS) were compared with the configurations in [7]-[9] and these results are presented in [10]. Therein, it is shown that the RCS results are consistent with [7]-[9] and, in addition, the stability of the system is shown by means of the condition number of the system, which is a crucial indicator of the sensitivity of the matrix inversion. Later, the suggested ARM algorithm is applied to the algebraic system of the scattered fields of eccentrically layered dielectric circular cylinders [11], two parallel circular impedance cylinders [12] and a metamaterial covered two perfectly electric conductive circular cylinders [13]. In the numerical results of these papers, it is shown that the second kind system is always stable and reliable even at lower truncation numbers. Contrary to this, the first kind system is not stable, and one must make some extra measures such as the satisfaction of the boundary conditions to ensure the stability of the system and reliability of the results. The results presented therein show clearly, why such a regularization procedure is necessary for eccentrically layered circular cylinders and even for concentrically layered circular systems.

Secondly, the ARM procedure for the arbitrarily shaped boundaries with the entire domain Galerkin method is applied to the boundary integral equations of the type of Electric Field Integral Equation (EFIE) and Magnetic Field Integral Equation (MFIE) of the scattered field of single PEC boundary [14]-[16]. The considered EFIE and MFIE of one PEC boundary and one dielectric boundary are taken from [17] for TM (E-polarization) and TE (H-polarization). Then these equations are generalized for multiple dielectric and impedance boundaries by means of the equivalence principle. And then, by the information at hand, super-algebraically converging and numerically stable algorithms are constructed for two parallel impedance boundaries [18] and for two layered and two parallel dielectric boundaries [19].

Solution of the EFIE or MFIE is an important issue because in the case of circular boundaries the result of the separation of variables method, where all the fields are expressed in infinite series, is used. However, even if the circular shapes can be used for modeling most of important problems, the structures used in practical applications,

in general, have arbitrarily shaped boundaries. That is why, from one side some important research is being done for the systems of the structures that consist of circular cylinders and their regularization, from another side an important effort is made for the application of ARM to the systems of the arbitrarily shaped boundaries. As discussed above, for an obstacle that has an arbitrary shape, one needs a more general solution of the boundary integral equation of the scattered field such as EFIE, MFIE or a combination of them as Combined Field Integral Equation (CFIE), Combined Source Integral Equation (CSIE), Extended Boundary Condition (EBC) [17], Muller formulation [20], PMCHW formulation [21] and so on. It is well-known that the EFIE and MFIE themselves suffer from non-uniqueness of their solutions at frequencies associated with internal cavity resonances [22], [23]. The other above-mentioned formulations are constructed as eliminating the resonance solutions. Therefore, they are resonance-free and give a unique solution at all frequencies. However, in the scope of this work, the resonance frequencies are not considered, and the construction of the formulations is based on the EFIE and MFIE for all kinds of the boundaries and both polarizations. Such a formulation brings the possibility of comparable results in themselves since the EFIE and MFIE of a system have different kernels but the same unknowns.

It is well-known that the EFIE of a PEC cylinder is the Fredholm integral equation of the first kind while its MFIE is the Fredholm integral equation of the second kind for both polarizations [17]. Therefore, their discretization brings first and second kind algebraic systems respectively. For one dielectric boundary, EFIE and MFIE are the first kind integral equation for each polarization [24]. That is why the algebraic systems resulted from these equations must be regularized for having stable systems and reliable solutions. The situation is same for multiple dielectric boundaries. However, for impedance cylinders it depends on the value of the surface impedance for both polarizations.

The implementation procedure of the ARM in integral equations is technically different from series equations. Because in the case of series equations the fields are expressed in the infinite sum of cylindrical Bessel and Hankel functions with some unknowns correspond to transmission and reflection coefficients. The fields that are expressed in such a form are nothing but just the Fourier series expansion. Since the fundamental step of the ARM is to express the fields in the form of Fourier series and then use the equality of Fourier coefficients by applying the orthogonality property of

complex exponentials, this form is very convenient for the implementation of the ARM. However, for arbitrarily shaped boundaries, one must solve the EFIE or MFIE or a combination of them by applying the local singular expansion to the kernels and then remove the singularities of the Green's function and its derivatives that arise when the source and observation points coincide. For this purpose, an analytical function, which has a similar singularity of Green's function, is used. The Fourier coefficients of this function are known analytically, and the ARM is applied according to the behavior of these coefficients [5], [18], [19], [25].

For a PEC cylinder, in E-polarization case, the kernel of EFIE is the Green's function and MFIE has the kernel as first-order derivative of the Green's function w.r.t. the normal direction at the observation point. On the other hand, in H-polarization case, MFIE has the first-order derivative of the Green's function w.r.t. the normal direction at integration point and EFIE has a second-order derivative of the Green's function w.r.t. integration and observation point as kernel, respectively. The Green's function itself has logarithmic singularity while the distance between integration and observation points tends to zero. Therefore, it is not a smooth function on the boundary and it must be smoothened by extracting its singular part. Also, the first order derivative of the Green's function is finite but not infinitely smooth since the logarithm appears in its derivatives. Thus, the logarithmic part must be removed from this kernel as well, for having infinitely smooth functions. The second order derivative of the Green's function w.r.t. the normal derivative has the most singular part, and fortunately this singularity can be extracted by means of another form of the same above-mentioned analytical function. These are the four problematical kernels that can be encountered in any boundary integral equations of the 2-D boundary value problems and their singularities are handled in detail from the point of view of ARM algorithm in Chapter 2.2.5.

In the next chapter, Chapter 2, the mathematical background of the ARM is given, firstly, for the system that obtained from the series representation of the fields given in circular coordinates. It can be shown [4] that in the circular coordinates the series representation can be obtained from the integral equation by expanding zero-order Hankel function by means of the Graf's addition theorem [26]. By this means, the behavior of unknown coefficients of the fields represented in series whose asymptotic behavior is very crucial for specifying the regularization operators, are

expressed clearly. Secondly, the ARM procedure is given for 2-D BVP of Dirichlet, Neumann, third-kind and dielectric boundaries.

In Chapter 3, the numerical implementations of the theoretical information given in Chapter 2 are achieved by applying them to several kind of BVP. At first, in Chapter 3.1, the ARM algorithm that is explained in Chapter 2.1 is applied to the algebraic system of two parallel infinitely long circular impedance cylinders. Then, in Chapter 3.2, in the same manner, it is applied to several eccentrically layered circular dielectric cylinders. And then, in Chapter 3.3 and 3.4, the ARM algorithm for the boundary integral equations of arbitrarily shaped boundaries that are discussed in Chapter 2.2 and its subchapters is applied to two dielectric circular boundaries and two parallel circular impedance cylinders respectively. The numerical results that are obtained from the solution of the integral equations are validated in themselves by comparison of the EFIE and MFIE of the same unknowns, and also an extra check is done by comparison of the solution of the rigorous algorithm which is constructed by the ARM for the circular boundaries.

2. ANALYTICAL REGULARIZATION METHOD FOR 2-D BOUNDARY VALUE PROBLEMS

Analytical Regularization Method is an analytical and analytical-numerical method that can be used in diffraction theory to reduce ill-conditioned integral, integral-differential and series equations of the first kind to such equations of the second kind which makes it possible to solve these equations efficiently on the computer [5]. The regularization techniques based on the ARM are successfully used in scattering by two and three-dimensional body of revolution closed and unclosed screens, compact and periodic, dielectric and perfectly conducting obstacles [5], [27]-[33].

It is known that the monochromatic wave scattered by an obstacle in 2-dimensional coordinates satisfies the homogeneous Helmholtz equation

$$\Delta u^s(q) + k^2 u^s(q) = 0,\ q \in R^2 \setminus S \tag{2.1}$$

with the boundary condition

$$\alpha(q) u^t(q) + \beta(q) \frac{\partial u^t(q)}{\partial n} = f(q),\ q \in S \tag{2.2}$$

and the Sommerfeld radiation condition

$$\lim_{|q| \to \infty} |q|^{1/2} \left(\frac{\partial u^s(q)}{\partial |q|} - iku^s(q) \right) = 0 \tag{2.3}$$

where $u^t(q) = u^i(q) + u^s(q)$ is the total field, $u^s(q)$ is the scattered field and $u^i(q)$ is the incident field.

Also, it is known that for the coordinate problems, where the boundary and coordinate surfaces (or contours) coincide, the separation of variables method makes it possible to reduce the boundary value problem of (2.1)-(2.3) to an infinite algebraic system of the first kind of the form

$$Ax = b \tag{2.4}$$

For non-coordinate problems, the Helmholtz equation can be reduced to an integral representation by means of the Green's formulae. After imposing the boundary condition (2.2) and the radiation condition (2.3) to the integral representation, the boundary integral equation is obtained. The discretization, in another sense "algebraization", of the integral equation yields, again, an infinite algebraic equation of the first kind in the form of (2.4). The discretization can be made by means of various quadrature methods, Galerkin Method, Moment Method, and alike.

The numerical treatment of the boundary value diffraction problem (2.1)-(2.3) requires the numerical solution of (2.4). Since such an infinite dimensional equation cannot be solved numerically, finite dimensional approximations must be used. By the truncation of (2.4) the finite algebraic equation system of the form

$$A_N x_N = b_N \tag{2.5}$$

is arrived at and it is hoped that the solution x_N is the approximation of x, which becomes, conceptually, more accurate approach for increasing truncation number N. However, it is doubtful whether the x_N converges to x while $N \to \infty$. Even it may happen that the numerical solution of (2.5), say $\tilde{x}_N$, calculated on a computer which has a word length containing only a finite m_c number of binary digits, has nothing common with the exact solutions of (2.4) and (2.5). The main reason of such possibility is the presence of the round-off errors, amplification and propagation of such errors during the calculation process for ill-conditioned matrices. The method of numerical solving can be Gauss elimination, LU-decomposition or various iterative methods, but there is not qualitative difference from point of view of accuracy and stability of the solution [34].

To decide whether the finite-dimensional system (2.5) is worth solving at all, it is necessary to answer the following questions.

i) Does x_N converge to x when $N \to \infty$? If so, in what metric is this?
ii) Will the "numerical catastrophe" $\|x_N - \tilde{x}_N\|/\|x_N\| > 1$ come with growing N?

The second question is reasonable to consider only if the first question is answered positively in the relevant metric coordinated with the metric (specified by the physical nature of the boundary value problem) of the functional space where the initial boundary value problem solution is sought [5], [34], [35].

It is known that in the general case the first question is answered negatively, i.e. as N increases the solution of the system of the first kind, x_N, broadly speaking, does not converge to x in any metric. This is typical behavior of most parts of boundary value diffraction problems [36]. Nevertheless, let us assume that owing to the special properties of the operator A, this convergence takes place in the wanted metric. The standard definition of the condition number [37], [38] of the operator A_N is

$$\nu(A_N) = \|A_N\|_2 \left\|A_N^{-1}\right\|_2 \tag{2.6}$$

where the operator norm $\|\cdot\|_2$ is created by the Euclidean metric of real or complex-valued *N*-dimensional space. System of the first kind is characterized by $\|A_N\|_2 \to \infty$ or $\|A_N^{-1}\|_2 \to \infty$ when $N \to \infty$, i.e. the operators A or A^{-1} is unbounded in the operator norm constructed from the vector norm of l_2 space. Consequently, $\nu(A_N) \to \infty$ for $N \to \infty$ [5], [35].

It has been verified [37] that the number of correct binary digits in the solution $\tilde{x}_N$ does not exceed the value

$$m_r = m_c - \log_2 \nu(A_N) \tag{2.7}$$

where m_c is the binary length of the computer mantissa and m_r describes the number of significant digits in the element of $\tilde{x}_N$ vector that has the largest modulus. Correspondingly, a relative error of components smaller in module is far larger. Moreover, if these components decrease fast, only first few of them can carry right significant digits, the rest cannot be computed at all. In this case, the algorithm has the problem of renormalization of the unknown x vector and balancing of the initial system matrix [5], [35] (and the references cited therein).

Thus, if $m_r \le 0$, i.e. $m_c \le \log_2 \nu(A_N)$ the solution $\tilde{x}_N$ contains no significant digits to be true and the above-mentioned numerical catastrophe arises. In this case, the discrepancy $\delta^N \stackrel{\text{def}}{=} A_N \tilde{x}_N - b_N$ will be in the order of $\|\delta^N\|_2 \approx N 2^{-m_c} \|\tilde{x}_N\|_2$

value, which is evidently quite small. The accurate solution x_N rounded to m_c binary digits shows the same order discrepancy.

It is indicated in [5], [35] that the only practical way to recognize a numerical catastrophe is the direct calculation of $\nu(A_N)$ and m_r. Various indirect criteria, such as energy balance, stabilization of solution $\tilde{x}_N$ with increasing N, etc., may, as a rule, only give an illusion of solution correctness of the initial boundary value problem. Because in the former case, the energy conservation law may be satisfied with a very high accuracy even when $m_r \leq 0$ and $\tilde{x}_N$ having no significant digits to be true. In the latter case, after the inequality $m_r \leq 0$ is reached, the solution $\tilde{x}_N$ may be indifferent to N or vary very slowly, being prescribed by the rule of the arithmetical result rounding in the computer.

Let us now consider an alternative situation. Suppose that the original boundary value problem is equivalently reduced, in the l_2, to the infinite system of the algebraic equation of the form $Ax = b;\ x, b \in l_2$, but now the operator A has the form

$$A = I + H \tag{2.8}$$

where operator H is compact in the l_2 and I is the identity operator. Now, matrix A obeys the Fredholm alternative, and if A is not degenerated, then equation

$$(I + H)x = b \tag{2.9}$$

as a rule, has a unique solution. Thus, owing to the mentioned equivalence, there exist the bounded $A^{-1} = \|I + H\|^{-1}$ operator in l_2 space and the value

$$\nu_\infty = \|I + H\|_2 \left\|(I + H)^{-1}\right\|_2 < \infty \tag{2.10}$$

is correctly determined. Likewise, the procedure above, consider the truncated system

$$(I + H_N)x_N = b_N \tag{2.11}$$

Since H is compact, the sequence of finite-dimension matrix operators H_N can be chosen as

$$\|H - H_N\|_2 \to 0, \text{ when } N \to \infty \tag{2.12}$$

If (2.12) takes place then $\|x - x_N\| \to 0$. It means that answer of first question above is now positive. In space l_2 the limit

$$\nu_N = \lim_{N\to\infty} \nu(I + H_N) = \lim_{N\to\infty} \|I + H_N\|_2 \left\|(I + H_N)^{-1}\right\|_2 \to \nu_\infty \tag{2.13}$$

Hence, all ν_N are uniformly bounded for any sufficiently large N. For most practical problems in diffraction theory $\nu_N \ll 2^{m_c}$ for many modern computers in non-resonant cases.

The equation (2.9) is known as one of the second kind. The more general equation (2.4) which cannot be represented in the form of (2.9) is known as one of the first kind. The typical behavior of first kind and second kind systems are shown in Figure 2.1 (this picture is taken from [34]).

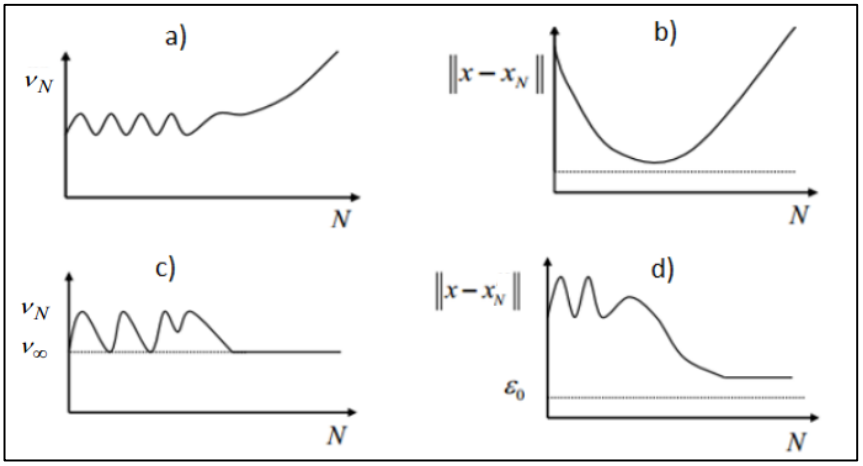

Figure 2.1: Correlation of condition number and error of numerical solution of truncated systems as functions of the truncated matrix dimension *N*. a) and b) are for equations of the first kind; c) and d) are for the second kind.

It is crucial to emphasize the importance of consideration of (2.9) just in space l_2. Because in this space the computer arithmetic provides numerical stability and convergence of $\tilde{x}_N$ to x within small deviations. For any other space, the qualitative

characteristics of the condition number and exact solution x_N are the same. But the computer treats such equations as one in l_2 and if the system might not be one of the second kind just in space l_2, then the numerical solution $\tilde{x}_N$ becomes unstable and divergent.

For solving a system of the first kind, Tikhonov regularization [39] is the most and known powerful tool. Firstly, well-skilled persons can use it and secondly, in general, it does not give all the necessary qualitative features of the solutions. Another way that is used in this thesis is based on the equivalent transform of the equation (2.4) of the first kind to an equation of the second kind (2.9), i.e. reducing the initial boundary value problem to the equation of the second kind. Because, as explained above, compared to equations of the first kind, the second-kind equations do not have the principal disadvantages preventing their effective solutions. Thus, in l_2 space it provides a good basis for efficient algorithms of numerical solutions of the problems. However, it is a mistake to think that such transformation is possible in the same space if the equation (2.4) is not of the Fredholm type. If such transform from (2.4) to (2.9) is constructed in the same functional space, there are only two possibilities; the resulting equation is not equivalent to the initial one or the equation (2.9) is not the second one, i.e. operator H is not compact in the same space [34].

The key point of the methods that transform the initial boundary value problem to the equation of the second kind is the regularization of the operator of the problem. From the point of view of the functional analysis, this idea is very simple and well-known [40]. Nevertheless, for constructing such a transform one must understand its mathematical background clearly. To this end, at first, the equation (2.4) must be reformulated as one given on a pair of functional spaces H_1 and H_2, i.e. $b \in H_2$, and $A: H_1 \to H_2$. Secondly, operator A must provide some special additive and multiplicative splittings as

$$A = A_0 + A_1 \tag{2.14}$$

where A_1 is the subordinate to the operator $A_0: H_1 \to H_2$ and spaces H_1 and H_2 should form set of correctness of A_0 in Tikhonov sense (see [39]). Thirdly, the operator A_0 must have the representation

$$A_0 = L^{-1}R^{-1} : H_1 \to H_2 \tag{2.15}$$

with known in closed analytical form operators L^{-1} and R^{-1} where

$$\begin{aligned} R^{-1} &: H_1 \to H_0, \;\; R : H_0 \to H_1 \\ L^{-1} &: H_0 \to H_2, \;\; L : H_2 \to H_0 \end{aligned} \tag{2.16}$$

and H_0 is some intermediate space and the operator $LA_1R: H_0 \to H_0$ is compact in H_0. Here the best choice of functional space is $H_0 = l_2$ because of the above-explained advantages of the equation (2.9) in the space l_2.

If the explained construction is implemented mathematically, it gives a direct and simple way of the transform of (2.4) to (2.9). Since the operator R^{-1} exist and bounded, any element $x \in H_1$ can be written as $x = Ry$ for some $y = R^{-1}x \in H_0$ defined as new unknown. Now applying the operator L to (2.4) from the left, and using the properties (2.14) and (2.15) results into the following equation of the second kind

$$\left(I + LA_1R\right) y = Lb, \;\; y, Lb \in l_2 \tag{2.17}$$

with compact operator $K = LA_1R$ in l_2 space.

The above-described construction by the operators L and R is known as Analytical Regularization Method. The equation (2.17) is the regularized equation of (2.4) and the pair (L, R) are called as double-sided regulators of the operator A given with the property (2.14). The graphical scheme of ARM for operator A is shown in Figure 2.2.

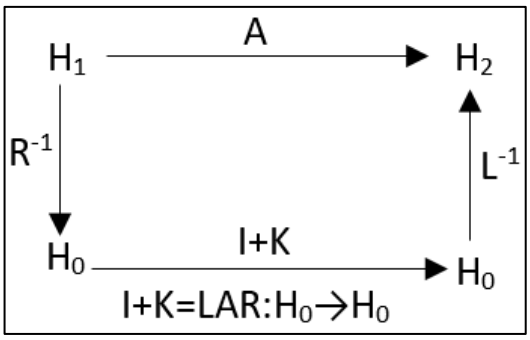

Figure 2.2: Graphical scheme of ARM.

As seen from above-explanations, the purpose of the ARM is reducing the equation of the first kind (2.4) to the equation of the second kind (2.17) by proper reposing of (2.4). So, there is a one-to-one correspondence between the solutions due to the operator R. Once the solution y is obtained from (2.17) then the solution x is obtained as $x = Ry$.

If H_0 is a Hilbert space, then by choosing a proper basis and matching the Fourier coefficients of the left- and right-hand side of the equations (2.17) one arrives, by virtue of the well-known isomorphism of Hilbert spaces [41], [42], to the equation of the second kind in the space l_2 where $y, b \in l_2$ and $K: l_2 \to l_2$ is a compact operator with necessity.

The necessity of application of ARM to the boundary value diffraction problems and the key steps of identifying the double-sided regulators for having a second kind system, which gives stable and convergent algorithms in computer arithmetic, have been explained in this part. But, note that the above-explained abstract construction does not answer how to build the operators or in which functional spaces the operators should be defined for the considered diffraction problems. There is no *priori* knowledge for construction of the operators L and R in closed form. In the next subchapters, the answers of these questions are given for some kind of boundary value diffraction problems.

2.1. ARM Algorithm for the Algebraic System of the Series Solution of Circular Boundaries

The geometrical structure of the circular boundaries, homogeneous along O_z axis, from the point of view of diffraction theory in 2-D, can be generalized as Figure 2.3.

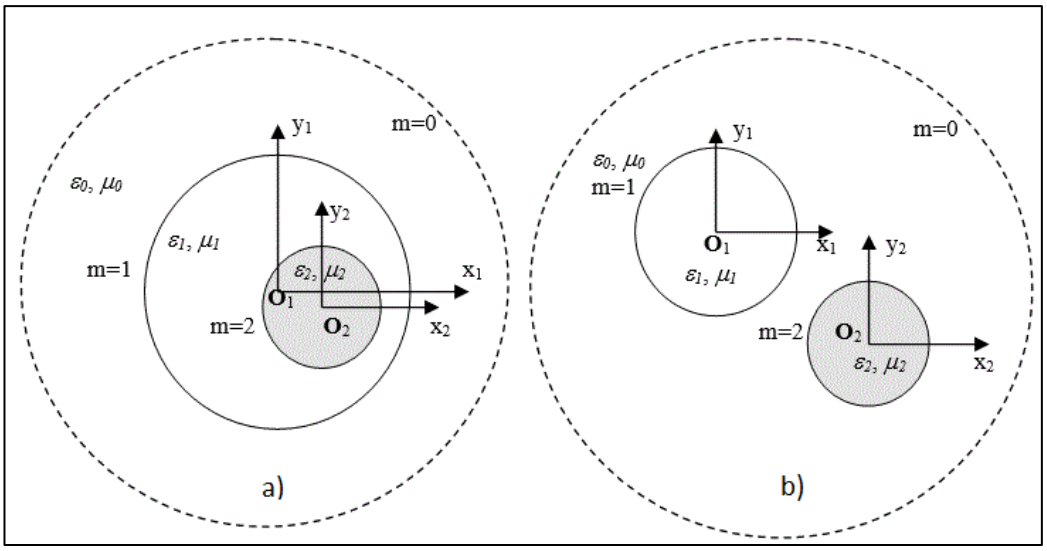

Figure 2.3: The Geometrical structure of the problem; a) Nested boundaries (inclusion) b) Parallel boundaries (neighbor). The dashed circles stand for the fictitious boundary at the infinity for m=0.

Here, the configuration a) stands for the nested circular cylinders, and b) stands for the parallel circular cylinders. The index m is used for denoting the boundaries but j is used for indexing the regions between boundaries. Any structure of a boundary value problem of circular boundaries, in 2-D, can be consist of only a), only b) or a combination of them. In this sense the information of implementing the ARM that is going to be given for the configurations in Figure 2.3 includes all possible situations of a boundary value diffraction problems of circular boundaries in 2-D.

For posing of the problem, first of all, the expression of the fields that satisfy homogeneous Helmholtz equation (2.1) related to the regions of Figure 2.3 must be given. The field representations for the coordinate problems, where the boundary of the scatterer and the coordinate coincides are well-known [7]-[9], [11]-[13], [43] for monochromatic waves scattering by eccentrically layered circular cylinders as in Figure 2.3. To this end, the equation (2.1) is solved by means of the separation of variables method and this solution yields the representation of the fields into infinite Fourier series expansions. For $e^{i\omega t}$ time dependency the reflected field (outgoing wave) and the transmitted field (incoming wave) from any mth boundary can be expressed in terms of its local polar coordinate system (ρ_m, φ_m) as follows.

$$u_z^{(ref,m)}\left(\rho_m,\varphi_m\right)=\sum_{n=-\infty}^{\infty} R_n^{(m)} H_n^{(2)}\left(k_j\rho_m\right)e^{in\varphi_m} \tag{2.18}$$

$$u_z^{(tr,m)}\left(\rho_m,\varphi_m\right)=\sum_{n=-\infty}^{\infty}T_n^{(m)}J_n\left(k_j\rho_m\right)e^{in\varphi_m} \tag{2.19}$$

Here $R_n^{(m)}$ and $T_n^{(m)}$ are unknown coefficients of the reflected and transmitted fields respectively. $H_n^{(2)}(t)$ in (2.18) is the second kind Hankel function and $J_n(t)$ in (2.19) is the Bessel function and k_j is the wave-number of j^{th} medium defined as

$$k_j=\omega\left\{\varepsilon_j\mu_j\right\}^{1/2},\quad j=1,2,3. \tag{2.20}$$

with the dielectric permittivity ε_j and magnetic permeability μ_j of the medium.

If the representation of the field between two boundaries is under consideration (i.e. $m=1$ and $m=2$), then the question of which coordinate system arises. Namely, which coordinate system should be chosen as reference for expressing the fields (here the incident field is not considered for Figure 2.3.b) since it is assumed that it comes from the boundary $m=0$ at infinity and it can be expressed in any local coordinate system without transformation). Same or different coordinates can be chosen for boundaries. But as it is explained in [11] same or different coordinates systems correspond to series expansion or integral formulation respectively. In addition, it is explained therein that from the solid mathematical background based on integral formulation [4] requires the choice of different local coordinates of boundaries for expression of the fields into Fourier series. Thus, for the analytical model used for circular boundaries through this thesis is based on this fact and all the fields, scattered or transmitted, are expressed in terms of local coordinates of their own scatterer. By virtue of this fact, the total fields between two regions of Figure 2.3.a) (region $j=1$) and of Figure 2.3.b) (region $j=0$) can be shown as follows.

$$\begin{aligned}u_z^{(1)}\left(q\right)&=u_z^{(tr,1)}+u_z^{(ref,2)}\\&=\sum_{n=-\infty}^{\infty}T_n^{(1)}J_n\left(k_1\rho_1\right)e^{in\varphi_1}+\sum_{n=-\infty}^{\infty}R_n^{(2)}H_n^{(2)}\left(k_1\rho_2\right)e^{in\varphi_2}\end{aligned} \tag{2.21}$$

$$u_z^{(0)}(q) = u_z^{(ref,1)}(q) + u_z^{(ref,2)}(q) + u_z^{inc}(q)$$
$$= \sum_{n=-\infty}^{\infty} R_n^{(1)} H_n^{(2)}(k_0\rho_1) e^{in\varphi_1} + \sum_{n=-\infty}^{\infty} R_n^{(2)} H_n^{(2)}(k_0\rho_2) e^{in\varphi_2} + u_z^{inc} \quad (2.22)$$

As seen from (2.21) and (2.22) the fields contain two parts that expressed in two different local coordinates (ρ_1, φ_1) and (ρ_2, φ_2) that belong to the boundary of scatterers. Namely, the reflected or transmitted field of a scatterer becomes incident field of the other scatterer.

For having the solution of the boundary value problem, the unknowns $R_n^{(m)}$ and $T_n^{(m)}$ must be calculated at first. For this end, the boundary conditions are subjected to each boundary and then arrived at an equation formed by the Fourier coefficients of the series. But, before writing this equation, a transformation of coordinates is necessary. Because, if the boundary condition is written on one boundary, say $m = 1$, then the field (transmitted for Figure 2.3.a) and reflected for Figure 2.3.b) that comes from boundary $m = 2$ and expressed in its local coordinate system must be transformed to the local coordinate system of the boundary $m = 1$. This transformation is done by means of the well-known Graf's addition theorem for cylindrical Bessel functions [6], [26], [44] that are summarized as

$$Z_n(k\rho_p) e^{in\varphi_p} = \begin{cases} \sum_{s=-\infty}^{\infty} e^{i(n-s)\theta_{pq}} J_{n-s}(kd_{pq}) Z_s(k\rho_q) e^{is\varphi_q}; & d_{pq} < \rho_q \\ \sum_{s=-\infty}^{\infty} e^{i(n-s)\theta_{pq}} Z_{n-s}(kd_{pq}) J_s(k\rho_q) e^{is\varphi_q}; & d_{pq} > \rho_q \end{cases} \quad (2.23)$$

where $Z_n(t)$ stands for $J_n(t)$ or $H_n^{(2)}(t)$, θ_{pq} is the angle of the vector $\boldsymbol{d_{pq}}$ that directed from the center point $\mathbf{O_p}$ to the center point $\mathbf{O_q}$ w.r.t. the *x*-axis of the global coordinate system, and $d_{pq} = |\boldsymbol{d_{pq}}| = |\mathbf{O}_p - \mathbf{O}_q|$ is the distance between these local origins. The equations given in (2.23) are used for transformation of the fields that are expressed in local coordinate system (ρ_p, φ_p) to the fields expressed in local coordinate system (ρ_q, φ_q). It is clear that $d_{pq} = d_{qp}$ and $\theta_{pq} = \pi + \theta_{qp}$.

By the help of the equation (2.23) the boundary conditions, peculiar to the kind of the boundary (PEC, dielectric or impedance), are imposed and then arrived at the final infinite-dimensional equation of the first kind in form of (2.4).

Now let us consider the configurations in Figure 2.3.a) and Figure 2.3.b) as two different problems and construct their algebraic equation system by assuming that all regions are filled by homogeneous dielectric materials. Even though the formulation is explained by dielectric mediums, the main idea of constructing the system and its regularization operators are very similar for all kind of boundaries. After constructing the system, asymptotic behavior of the entries of the matrix is analyzed to reveal its ill-conditioned behavior that shows it is a system of the first kind. Then, the next step is identifying the double-sided regularization operators L and R for reducing this system equivalently to an equation of the second kind in form of (2.17). For this end, as explained in Chapter 2, at first, the new unknown of the equation (2.17) is constructed as $y = R^{-1}x$, and secondly, the operator L^{-1} is constructed as it results in $LAR = I + K$. However, now the matter is the construction of the operator R^{-1}. It will be explained below in details but now, it is enough to say that it is determined according to the asymptotic behavior of the unknowns $R_n^{(m)}$ and $T_n^{(m)}$. In some sense, it is a proper scaling of unknowns which is, at first, done in [6] for two perfectly conductive circular cylinders.

Now let us consider the boundary value problem of the structure of infinitely long circular cylinders along the *z*-axis that is given in Figure 2.3.a) illuminated by E-polarized (TM-*z*) plane wave. It is well known that for the considered configuration, the electric field of a TM-*z* wave has only *z*-component and the other components can be represented by means of this component, with $e^{i\omega t}$ time dependency [45], as follows

$$E_\rho = E_\varphi = H_z = 0;\ H_\varphi = \frac{1}{i\omega\mu}\frac{\partial E_z}{\partial \rho};\ H_\rho = -\frac{1}{i\omega\mu}\frac{1}{\rho}\frac{\partial E_z}{\partial \varphi} \tag{2.24}$$

Therefore, the electric field of the incident plane wave also has only the *z*-component as $E_z^{inc}(\rho,\varphi) = e^{ik\rho cos(\varphi-\varphi_0)}$ with the incidence angle φ_0 and it has the following expression in terms of cylindrical harmonics with Bessel functions [45], [46].

$$E_z^{inc}(\rho,\varphi) = \sum_{n=-\infty}^{\infty} i^n J_n(k\rho) e^{in(\varphi-\varphi_0)} \tag{2.25}$$

On a dielectric boundary, the tangential components of the electric field and magnetic fields are continuous. Since $E_\varphi = H_z = 0$, then electric field has only E_z, and magnetic field has only H_φ components as tangential. That is why, in TM-z case, the following boundary conditions are valid on a dielectric boundary.

$$E_z^{(2)} - E_z^{(1)} = 0; \quad H_\varphi^{(2)} - H_\varphi^{(1)} = 0 \tag{2.26}$$

where the superscripts (1) and (2) indicate the inner and outer regions of the boundary respectively and, E_z and H_φ are the total tangential electric and magnetic fields in these regions.

By imposing the boundary conditions (2.26) on each boundary at $\rho_1 = a$ and $\rho_2 = b$ and using the equations (2.21), (2.22) as the total fields and substituting (2.25) as the incident field then arrived at the equations of electric fields on the boundary $m = 1$,

$$\begin{aligned} &\left\{ \sum_{n=-\infty}^{\infty} R_n^{(1)} H_n^{(2)}\left(k_0\rho_1\right) e^{in\varphi_1} + \sum_{n=-\infty}^{\infty} i^n J_n(k_0\rho_1) e^{in(\varphi_1-\varphi_0)} \right\}_{\rho_1=a} - \\ &\left\{ \sum_{n=-\infty}^{\infty} T_n^{(1)} J_n\left(k_1\rho_1\right) e^{in\varphi_1} + \sum_{n=-\infty}^{\infty} R_n^{(2)} H_n^{(2)}\left(k_1\rho_2\right) e^{in\varphi_2} \right\}_{\rho_1=a} = 0 \end{aligned} \tag{2.27}$$

and on the boundary $m = 2$,

$$\begin{aligned} &\left\{ \sum_{n=-\infty}^{\infty} T_n^{(1)} J_n\left(k_1\rho_1\right) e^{in\varphi_1} + \sum_{n=-\infty}^{\infty} R_n^{(2)} H_n^{(2)}\left(k_1\rho_2\right) e^{in\varphi_2} \right\}_{\rho_2=b} - \\ &\left\{ \sum_{n=-\infty}^{\infty} T_n^{(2)} J_n\left(k_2\rho_2\right) e^{in\varphi_2} \right\}_{\rho_2=b} = 0 \end{aligned} \tag{2.28}$$

As seen in (2.27) and (2.28) there are the terms written in local coordinates (ρ_1, φ_1) and (ρ_2, φ_2). That's why it is necessary to transform the local coordinate (ρ_2, φ_2) to (ρ_1, φ_1) in (2.27) and vice versa for (2.28). As explained above, this transformation is achieved by means of the addition theorems given in (2.23) as follows.

$$H_n^{(2)}\left(k_1\rho_2\right)e^{in\varphi_2}=\sum_{s=-\infty}^{\infty}e^{i(n-s)\theta_{21}}J_{n-s}(k_1d_{21})H_s^{(2)}(k_1\rho_1)e^{is\varphi_1};\ \mathrm{d}_{21}<a \tag{2.29}$$

$$J_n\left(k_1\rho_1\right)e^{in\varphi_1}=\sum_{s=-\infty}^{\infty}e^{i(n-s)\theta_{12}}J_{n-s}(k_1d_{12})J_s(k_1\rho_2)e^{is\varphi_2};\ \mathrm{d}_{12}<b \tag{2.30}$$

Note that both equations are obtained by means of the first line of (2.23) for $d_{21}<a$ and $d_{12}<b$. However, the same result in (2.30) is obtained if the inner circle does not include the center of the host circle, i.e. when $d_{12}>b$. If these relations are substituted into (2.27) and (2.28), respectively, and by making the change $s=n$ and $n=s$ then the equations become as

$$\begin{aligned}&\left\{\sum_{n=-\infty}^{\infty}R_n^{(1)}H_n^{(2)}\left(k_0a\right)e^{in\varphi_1}+\sum_{n=-\infty}^{\infty}i^nJ_n(k_0a)e^{in(\varphi_1-\varphi_0)}\right\}-\\&\left\{\sum_{n=-\infty}^{\infty}T_n^{(1)}J_n\left(k_1a\right)e^{in\varphi_1}+\sum_{n=-\infty}^{\infty}R_n^{(21)}H_n^{(2)}\left(k_1a\right)e^{in\varphi_1}\right\}=0\end{aligned} \tag{2.31}$$

$$\begin{aligned}&\left\{\sum_{n=-\infty}^{\infty}T_n^{(12)}J_n\left(k_1b\right)e^{in\varphi_2}+\sum_{n=-\infty}^{\infty}R_n^{(2)}H_n^{(2)}\left(k_1b\right)e^{in\varphi_2}\right\}-\\&\left\{\sum_{n=-\infty}^{\infty}T_n^{(2)}J_n\left(k_2b\right)e^{in\varphi_2}\right\}=0\end{aligned} \tag{2.32}$$

where

$$R_n^{(21)}=\sum_{s=-\infty}^{\infty}R_s^{(2)}e^{i(s-n)\theta_{21}}J_{s-n}(k_1d_{21}) \tag{2.33}$$

$$T_n^{(12)}=\sum_{s=-\infty}^{\infty}T_s^{(1)}e^{i(s-n)\theta_{12}}J_{s-n}(k_1d_{12}) \tag{2.34}$$

In all above equations, the subscripts (12) and (21) are kept on the purpose of expressing the transformation from coordinate O_1 to coordinate O_2 and from O_2 to O_1, respectively.

Now, by using the relation of tangential magnetic field and electric field given in (2.24) and the boundary condition of magnetic fields in (2.26) the following

equations of magnetic field, similar to electric field equations, are obtained on the boundary $m = 1$,

$$\begin{aligned}&\left\{\sum_{n=-\infty}^{\infty} R_n^{(1)} H_n'^{(2)}\left(k_0 a\right) e^{in\varphi_1} + \sum_{n=-\infty}^{\infty} i^n J_n'(k_0 a) e^{in(\varphi_1-\varphi_0)}\right\} - \\ &\frac{1}{\eta_{r1}}\left\{\sum_{n=-\infty}^{\infty} T_n^{(1)} J_n'\left(k_1 a\right) e^{in\varphi_1} + \sum_{n=-\infty}^{\infty} R_n^{(21)} H_n'^{(2)}\left(k_1 a\right) e^{in\varphi_1}\right\} = 0\end{aligned} \tag{2.35}$$

and on the boundary $m = 2$,

$$\begin{aligned}&\frac{1}{\eta_{r1}}\left\{\sum_{n=-\infty}^{\infty} T_n^{(12)} J_n'\left(k_1 b\right) e^{in\varphi_2} + \sum_{n=-\infty}^{\infty} R_n^{(2)} H_n'^{(2)}\left(k_1 b\right) e^{in\varphi_2}\right\} - \\ &\frac{1}{\eta_{r2}}\left\{\sum_{n=-\infty}^{\infty} T_n^{(2)} J_n'\left(k_2 b\right) e^{in\varphi_2}\right\} = 0\end{aligned} \tag{2.36}$$

where $\eta_{ri} = \sqrt{\mu_{ri}/\varepsilon_{ri}}$ is the relative intrinsic impedance of the i^{th} medium with the relative parameters μ_{ri} and ε_{ri}. Here $F'(z) = dF/dz$ denotes the derivative w.r.t. the argument where F stands for $J_n(z)$ and $H_n^{(2)}(z)$.

Collecting equations (2.31), (2.32), (2.35), (2.36) and by using the orthogonality property of the complex exponentials, one arrives at a system of the equation of Fourier coefficients, with the definition $T_n^{(0)} = e^{in(\pi/2-\varphi_0)}$, as follows

$$R_n^{(1)} H_n^{(2)}\left(k_0 a\right) - \left\{R_n^{(21)} H_n^{(2)}\left(k_1 a\right) + T_n^{(1)} J_n\left(k_1 a\right)\right\} = -T_n^{(0)} J_n\left(k_0 a\right) \tag{2.37}$$

$$R_n^{(1)} H_n'^{(2)}\left(k_0 a\right) - \frac{1}{\eta_{r1}}\left\{R_n^{(21)} H_n'^{(2)}\left(k_1 a\right) + T_n^{(1)} J_n'\left(k_1 a\right)\right\} = -T_n^{(0)} J_n\left(k_0 a\right) \tag{2.38}$$

$$T_n^{(12)} J_n\left(k_1 b\right) + R_n^{(2)} H_n^{(2)}\left(k_1 b\right) - T_n^{(2)} J_n\left(k_2 b\right) = 0 \tag{2.39}$$

$$\frac{1}{\eta_{r1}}\left\{T_n^{(12)} J_n'\left(k_1 b\right) + R_n^{(2)} H_n'^{(2)}\left(k_1 b\right)\right\} - \frac{1}{\eta_{r2}}\left\{T_n^{(2)} J_n'\left(k_2 b\right)\right\} = 0 \tag{2.40}$$

Now there is the system of the equations (2.37), (2.38), (2.39) and (2.40) and the unknowns $R_n^{(1)}$, $T_n^{(1)}$, $R_n^{(2)}$, $T_n^{(2)}$. But, is clear that, for every fixed "*n*" it is possible to eliminate at first two unknowns by proper scaling and extraction operations. This elimination procedure is applied here, but, not with purpose the of eliminating some unknowns. Instead, it is aimed to have a system that consists of the functions that are familiar from analysis of circular coaxial cable problems [8], [44]. For this end, at first, $T_n^{(1)}$ is eliminated by multiplying the first and the second equations by $J'_n(k_1a)/\eta_1$ and $J_n(k_1a)$, respectively, and then extracting the resultant equations. This procedure is correct due to the fact that functions $J_n(t)$ and $J'_n(t)$ have not common root, i.e. $|J_n(t) + J'_n(t)| > 0$ for any t. Analogously, $R_n^{(1)}$ is eliminated in a very similar way, with the fact that $\left|H_n^{(2)}(t) + H'^{(2)}_n(t)\right| > 0$, and arrived at another equation. If the same procedure is followed for $R_n^{(2)}$, $T_n^{(2)}$ then the following equation system in form of $Ax = b$ is obtained [11]

$$\underbrace{\left[\begin{array}{cc|cc} P_n^{(1,0)}(a) & [0] & W_{n,s}^{\{21\}(1)}(a) & [0] \\ [0] & P_n^{(1,0)}(a) & T_{n,s}^{\{21\}(1,0)}(a) & [0] \\ \hline [0] & Q_{n,s}^{\{12\}(2,1)}(b) & P_n^{(2,1)}(b) & [0] \\ [0] & W_{n,s}^{\{12\}(1)}(b) & [0] & P_n^{(2,1)}(b) \end{array}\right]}_{A} \underbrace{\left[\begin{array}{c} R_n^{(1)} \\ T_n^{(1)} \\ R_n^{(2)} \\ T_n^{(2)} \end{array}\right]}_{x} = \underbrace{\left[\begin{array}{c} -T_n^{(0)}Q_n^{(1,0)}(a) \\ -T_n^{(0)}W_n^{(0)}(a) \\ [0] \\ [0] \end{array}\right]}_{b} \tag{2.41}$$

where the terms denoted by the top script $\{pq\}$ are the interaction blocks that are the results of the addition theorems and are in the form of the following expression

$$F_{n,s}^{\{pq\}} = F_n \sum_{s=-\infty}^{\infty} e^{i(s-n)\theta_{pq}} J_{s-n}(k_1 d_{pq}) \tag{2.42}$$

with the following definitions that are familiar from coaxial circle problems

$$
\begin{aligned}
P_n^{(j,l)}(\rho) &= \beta_j H_n^{(1)}(k_l\rho) J_n'(k_j\rho) - \beta_l H_n^{(1)\prime}(k_l\rho) J_n(k_j\rho),\\
Q_n^{(j,l)}(\rho) &= \beta_j J_n(k_l\rho) J_n'(k_j\rho) - \beta_l J_n'(k_l\rho) J_n(k_j\rho),\\
T_n^{(j,l)}(\rho) &= \beta_j H_n^{(1)}(k_l\rho) H_n^{(1)\prime}(k_j\rho) - \beta_l H_n^{(1)\prime}(k_l\rho) H_n^{(1)}(k_j\rho),\\
W_n^{(j)}(\rho) &= -P_n^{(j,j)}(\rho) = 2i\beta_j / \pi k_j\rho, \quad \beta_j = 1/\eta_{rj},
\end{aligned}
\tag{2.43}
$$

If one follows all the steps of the formulation given for the configuration of Figure 2.3.a) analogously for Figure 2.3.b) then arrives the following linear algebraic equation system

$$
\underbrace{\left[\begin{array}{cc|cc}
P_n^{(1,0)}(a) & [0] & Q_{n,s}^{\{21\}(1,0)}(a) & [0] \\
[0] & P_n^{(1,0)}(a) & W_{n,s}^{\{21\}(0)}(a) & [0] \\
\hline
Q_{n,s}^{\{12\}(2,0)}(b) & [0] & P_n^{(2,0)}(b) & [0] \\
W_{n,s}^{\{12\}(0)}(b) & [0] & [0] & P_n^{(2,0)}(b)
\end{array}\right]}_{A}
\underbrace{\left[\begin{array}{c} R_n^{(1)} \\ T_n^{(1)} \\ \hline R_n^{(2)} \\ T_n^{(2)} \end{array}\right]}_{x}
=
\underbrace{\left[\begin{array}{c} -T_n^{(0)} Q_n^{(1,0)}(a) \\ -T_n^{(0)} W_n^{(0)}(a) \\ \hline -T_n^{(0)} Q_n^{(2,0)}(b) \\ -T_n^{(0)} W_n^{(0)}(b) \end{array}\right]}_{b}
\tag{2.44}
$$

which is again in the same form of (2.41), with the same definitions in (2.43). Note that since in this case, the distance between the local origins is greater than the radius of the circles, i.e. $d > a$ and $d > b$, then the term $H_{s-n}^{(2)}(k_0 d_{pq})$ appears instead of $J_{s-n}(k_1 d_{pq})$ in equation (2.42).

The vertical and horizontal lines that are seen in the matrix of the system (2.41) and (2.44) are used to outline the self and interaction blocks corresponding to the configurations Figure 2.3.a) and Figure 2.3.b), respectively. Now, let us use each part of the matrix that are separated by these lines as one block and construct the following common block-form of these systems as

$$
A_{mm'}^{jj'} = \left[\begin{array}{cc} \left[\Pi_m^j\right] & \left[\Upsilon_{m'm}^{j}\right] \\ \left[\Upsilon_{mm'}^{j'}\right] & \left[\Pi_{m'}^{j'}\right] \end{array}\right];\quad x_{mm'} = \left[\begin{array}{c} \left[\xi_m\right] \\ \left[\xi_{m'}\right] \end{array}\right];\quad b_{mm'}^{jj'} = \left[\begin{array}{c} \left[\tau_m^j\right] \\ \left[\tau_{m'}^{j'}\right] \end{array}\right]
\tag{2.45}
$$

where each entry in $A_{mm'}^{jj'}$ is a 2×2 block-matrix that corresponds to one part in the matrix A of the system (2.41) and (2.44). The subscripts m, m' and superscript j, j' are the indices of circular boundaries and their host media, respectively. The diagonal elements of $A_{mm'}^{jj'}$ denoted by Π correspond to the self-blocks of each boundary m and m', and the non-diagonal elements denoted by Υ are the interaction blocks of these boundaries. The entries in the column of unknowns, related to the boundaries, have the form as $\xi_m = \left[R_n^{(m)}, T_n^{(m)}\right]^T$ and the entries of the right-hand side are in the form as $\tau_m^j = \left[-T_n^{(0)} Q_n^{(j,0)}(\rho_m),\ -T_n^{(0)} W_n^{(0)}(\rho_m)\right]^T$ if the incident wave exist, otherwise they are zero.

The aim of the block representation as in (2.45) is to give a compact scheme for constructing the systems of more complicated configurations. It helps to construct the algebraic system of more complicated configurations of circular boundaries easily by simply substituting the corresponding self or interaction blocks into the matrix, as it will be shown in the Chapters 3.1 and 3.2. The system of two parallel impedance cylinders, which will be considered in Chapter 3.1, has the same properties without having the functions in (2.43) since these functions are obtained from the relation of the dielectric boundary conditions.

In the case of TE-*z* wave incidence, in contrast to the TM-*z* wave, the magnetic field has the only *z*-component H_z, and in this case the incidence field has only the component $H_z^{inc} = e^{ik\rho cos(\varphi - \varphi_0)}$. Analogous to (2.24) all other components are expressed in terms of H_z as follows.

$$H_\rho = H_\varphi = E_z = 0;\ E_\varphi = -\frac{1}{i\omega\varepsilon}\frac{\partial H_z}{\partial \rho};\ H_\rho = \frac{1}{i\omega\varepsilon}\frac{1}{\rho}\frac{\partial H_z}{\partial \varphi} \tag{2.46}$$

If the relations between tangential components (H_φ, E_z) in (2.24) and (E_φ, H_z) in (2.46) are compared then it is clear that the formulation for TE-*z* polarization is obtained for both systems simply by putting η_{rj} instead of $1/\eta_{rj}$, i.e. $1/\beta_j$ instead of β_j, in equations (2.43). Therefore, for both polarizations the algebraic systems of the diffraction boundary value problem of the configurations of Figure 2.3(A) and Figure 2.3(B) are in the form of $Ax = b$ as (2.41) and (2.44) respectively.

Now it is possible to solve the systems (2.41) or (2.44) with unknown coefficients $R_n^{(1)}$, $T_n^{(1)}$, $R_n^{(2)}$, $T_n^{(2)}$. It is clear that, these systems should be one of the first kind, but, with the purpose to reveal this, let's analyze the systems by considering the entries of the matrix A while the Fourier index $n \to \infty$. Since all the functions that form the matrix consist of the Bessel and Hankel function and their derivatives, at first, it is necessary to show the asymptotic behavior of these functions while $n \to \infty$. The asymptotic expansion of these functions for large orders [26] are as follows

$$J_n(z) = \frac{1}{n!}\left(\frac{z}{2}\right)^n \left[1 + \mathcal{O}\left(\frac{z^2}{n}\right)\right];\ n \to \infty \tag{2.47}$$

$$J'_n(z) = \frac{1}{2}\frac{1}{(n-1)!}\left(\frac{z}{2}\right)^{n-1} \left[1 + \mathcal{O}\left(\frac{z^2}{n}\right)\right];\ n \to \infty \tag{2.48}$$

$$H_n^{(2)}(z) = \frac{i}{\pi}(n-1)!\left(\frac{z}{2}\right)^{-n} \left[1 + \mathcal{O}\left(\frac{z^2}{n}\right)\right];\ n \to \infty \tag{2.49}$$

$$H'^{(2)}_n(z) = -\frac{i}{2\pi}n!\left(\frac{z}{2}\right)^{-n-1} \left[1 + \mathcal{O}\left(\frac{z^2}{n}\right)\right];\ n \to \infty \tag{2.50}$$

and by means of the asymptotic Stirling formula $n! \sim (2\pi n)^{1/2}(n/e)^n$ [26] the upper bounds for Bessel and Hankel functions can be estimated as

$$\begin{aligned} |J_n(t)| &\sim \frac{1}{\sqrt{2\pi n}}\left(\frac{et}{2n}\right)^n \le \frac{e^{|\mathrm{Im}\, t|}}{n!}\left|\left(\frac{t}{2}\right)^n\right|; \\ H_n^{(1,2)}(t) &\sim \sqrt{\frac{2}{\pi n}}\left|\left(\frac{2n}{et}\right)^n\right| \le (n-1)!e^{-|\mathrm{Im}\, t|}\left|\left(\frac{2}{t}\right)^n\right| \end{aligned} \tag{2.51}$$

By using the equations (2.47)-(2.50) the asymptotic behavior of the functions $P_n^{(j,l)}(\rho)$, $Q_n^{(j,l)}(\rho)$, $R_n^{(j,l)}(\rho)$, $T_n^{(j,l)}(\rho)$ in (2.43) can be written as

$$P_n^{(j,l)}(\rho)=\frac{i}{\pi\rho}\left(\frac{k_j\rho}{k_l\rho}\right)^n\left[\frac{1}{\mu_j}+\frac{1}{\mu_l}\right]+\mathcal{O}\left(\frac{1}{n}\right);\ n\to\infty \tag{2.52}$$

$$Q_n^{(j,l)}(\rho)=\frac{1}{n!(n-1)!}\left(\frac{k_j\rho}{2}\right)^n\left(\frac{k_l\rho}{2}\right)^n\frac{1}{\rho}\left[\frac{1}{\mu_j}-\frac{1}{\mu_l}\right]\left[1+\mathcal{O}\left(\frac{1}{n}\right)\right];\ n\to\infty \tag{2.53}$$

$$R_n^{(j,l)}(\rho)=-\frac{i}{\pi\rho}\left(\frac{k_j\rho}{k_l\rho}\right)^n\left[\frac{1}{\mu_j}+\frac{1}{\mu_l}\right]\left[1+\mathcal{O}\left(\frac{1}{n}\right)\right];\ n\to\infty \tag{2.54}$$

$$T_n^{(j,l)}(\rho)=\frac{n!(n-1)!}{\pi^2\rho}\left(\frac{k_j\rho}{2}\right)^{-n}\left(\frac{k_l\rho}{2}\right)^{-n}\left[\frac{1}{\mu_j}-\frac{1}{\mu_l}\right]\left[1+\mathcal{O}\left(\frac{1}{n}\right)\right];\ n\to\infty \tag{2.55}$$

and analogous to (2.51) their upper limits can be estimated quite simply.

As can be seen from the asymptotic forms (2.47)-(2.51) for large indexes, the function of Bessel and its derivative decay very fast ($\sim O(1/n!)$), and on the other hand Hankel function and its derivative grow very fast ($\sim O(n!)$), while the index $n\to\infty$. The asymptotic behavior of the matrix entries given by (2.52)-(2.55) shows that the function $Q_n(\rho)$ decays approximately with the order of $(1/n!)^2$ and, $T_n(\rho)$ grows with the order of $(n!)^2$. On the other side, the functions $P_n(\rho)$ and $R_n(\rho)$ may decay or grow algebraically depends on the ratio k_j/k_l. All explanation given here shows that the systems (2.41) and (2.44) are evidently the systems of the first kind with dramatically growing or decaying matrix elements. That is why such systems cannot be reduced to the system of the second kind by simple division operations.

Such an infinite-size system can be solved numerically only by some truncation procedure. However, due to the above-explained facts, the inversion of the matrix A is very sensitive to the truncation number of the algebraic system and produces very large condition numbers that are calculated by (2.6) which points to the absence of the correct solution. That is why, for having numerically stable system and reliable solutions, the systems such as (2.41) and (2.44) need to be transformed into a second kind one as in form of (2.17). This can be achieved by means of the ARM. But for this purpose, at first, the structure of unknown coefficients $R_n^{(m)}$, $T_n^{(m)}$ must be known for

defining new unknowns $\tilde{R}_n^{(m)}$, $\tilde{T}_n^{(m)}$ by a scaling operator R^{-1} as $y = R^{-1}x$. It is explained in [11] based on the integral formulation of the scattered field in [4] that the nature of the coefficients $R_n^{(m)}$, $T_n^{(m)}$ have the form

$$\begin{bmatrix} R_n^{(m)} \\ T_n^{(m)} \end{bmatrix} = c_1^{(m)}(n) \begin{bmatrix} J_n(k_j\rho_m) \\ H_n^{(2)}(k_j\rho_m) \end{bmatrix} - c_2^{(m)}(n) \begin{bmatrix} J'_n(k_j\rho_m) \\ H'^{(2)}_n(k_j\rho_m) \end{bmatrix} \tag{2.56}$$

where $c_1^{(m)}(n)$ and $c_2^{(m)}(n)$ are some coefficients related to the Fourier coefficients of the scattered field and its normal derivative respectively. So, as seen from (2.56) the unknown coefficients $R_n^{(m)}$, $T_n^{(m)}$ have similar asymptotic behavior of J_n(t) (or J'_n(t)) and $H_n^{(2)}(t)$ (or $H'^{(2)}_n(t)$) respectively, that are given in (2.47)-(2.50). Thus, based on this information, the first step of having a well-conditioned formulation can be achieved by specifying the new unknowns, with the diagonal right-hand side matrix operator R^{-1}, as

$$\underbrace{\begin{bmatrix} R_n^{(m)} \\ T_n^{(m)} \end{bmatrix}}_{y} = \underbrace{\begin{bmatrix} [F_1(n)] & [0] \\ [0] & [F_2(n)] \end{bmatrix}}_{R^{-1}} \underbrace{\begin{bmatrix} R_n^{(m)} \\ T_n^{(m)} \end{bmatrix}}_{x} \tag{2.57}$$

with proper choice of the functions $F_1(n)$ and $F_2(n)$ that are selected according to the asymptotic behaviors of (2.56). By considering the formulas in (2.47)-(2.50) it is clear that there are a few possible choices of $F_1(n)$ and $F_2(n)$ which are given in the Table 2.1 that have similar asymptotic behavior for large arguments. In addition, a proper combination of possible choices can be used which will be met in the problem of scattering by impedance cylinders in Chapter 3.1.

Table 2.1: The possible choices of the elements of right-hand side regulator.

$F_1(n)$	$1/J_n$, $1/J'_n$, $H_n^{(1)}$, $H'^{(1)}_n$, $H_n^{(2)}$, $H'^{(2)}_n$
$F_2(n)$	J_n, J'_n, $1/H_n^{(1)}$, $1/H'^{(1)}_n$, $1/H_n^{(2)}$, $1/H'^{(2)}_n$

Note that the key point of the selection of the operator R^{-1} is creating new unknowns by eliminating the asymptotically bad behavior of the old coefficients by a scaling operation. It is clear that for all of the circular configurations, the construction of new unknowns is just as explained here. However, the left-side regularization operator is chosen, depending on the nature of the operator A, as it yields that $LAR = I + K$ where K is a compact operator in space l_2.

In [6] $1/H_n'^{(2)}$ (as $1/F_1(n)$) is chosen as the operator R^{-1} for the problem of scattering by two perfectly conductive circular cylinders without a left side operator L. In the scope of this thesis, in addition to this, the left-hand side operator L is also selected as it produces a second kind system and the problem is generalized to a few different circular geometries with different boundary conditions [11]-[13]. The chosen operators and the numerical results for these configurations will be given in the application of the ARM in Chapters 3.1 and 3.2.

2.2. ARM Algorithm for the Algebraic System of Boundary Integral Equations

Here, some definitions and explanations that are used in [34] common to each boundary integral equations are represented and the concept of the ARM for integral equations is given through therein defined operators.

For the purpose, the Hilbert space $l_2(\lambda)$ of infinite sequences $\{c_n\}$ as

$$l_2(\lambda) = \left\{ \{c_n\}_{n=-\infty}^{\infty} : \sum_{n=-\infty}^{\infty} |c_n|^2 \tau_n^{2\lambda} < \infty \right\};\ \tau_n = \max\left(1, |n|^{1/2}\right) \tag{2.58}$$

is considered with evidently defined its scalar product and norm. As well, the notation H^{λ} is used for well-known Sobolev spaces of functions, which Fourier coefficients belong to $l_2(\lambda)$. For any arbitrary, and smooth, simple contour *S*, that is shown as in Figure 2.4, it is understood the Sobolev spaces on contour *S* for the parametrization proportional to the arc-length of this contour.

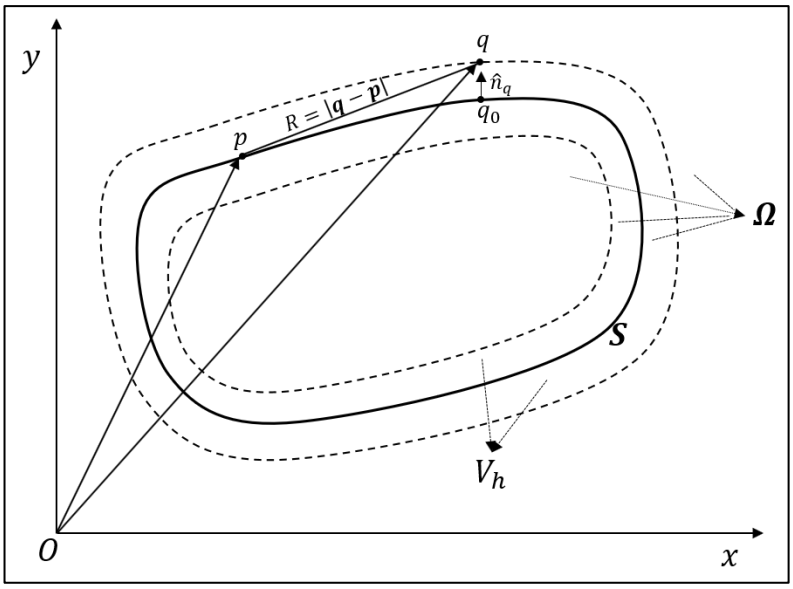

Figure 2.4: Cross-sectional view of the cylindrical obstacle of arbitrary shape with related definitions.

Let the non-self-crossing S is a class of $C^{2,\alpha}$ [47] and it is situated strongly inside a two-dimensional domain Ω as presented in Figure 2.4. For the potentials of single and double layers of diffraction theory [47] in Ω, the following notations are used

$$P[v](q) \overset{def}{=} \int_S v(p) G_2(q,p)\, dl_p, \quad q \in \Omega \setminus S \tag{2.59}$$

$$Q[u](q) \overset{def}{=} \int_S u(p) \frac{\partial G_2(q,p)}{\partial n_p} dl_p, \quad q \in \Omega \setminus S \tag{2.60}$$

where $G_2(q,p)$ is the Green's function of the domain R^2 that satisfies the same boundary conditions on the boundary ∂Ω. Here $\hat{n}_p$ is the unit outward normal vector at the point $p \in \partial\Omega$ and functions $u = u(p)$ and $v = v(p)$ have the properties as $u \in C^{1,\alpha}(S)$ and $v \in C^{0,\alpha}(S)$ [47].

In small enough open vicinity $V = V_h$ of S such that $V_h \cap S = \emptyset$ any point $q \in V_h$ has unique representation as $q = q_0 \pm h\hat{n}_q$, where $q_0 \in S$, $\hat{n}_q$ is the unit outward normal vector at the point q_0 and $h > 0$ is a unique scalar value. Thus, the normal derivatives of the potentials P and Q that is denoted with the prefix ∂_n can be defined in V as

$$\left[\partial_n Pv\right](q) = \left(\partial/\partial n_q\right)\left[Pv\right](q) \tag{2.61}$$

$$\left[\partial_n Qu\right](q) = \left(\partial/\partial n_q\right)\left[Qu\right](q) \tag{2.62}$$

For any function $f(q)$, the notation

$$f^{(\pm)}(q) = \lim_{h\to+0} f\left(q \pm h n_q\right), \quad q \in S \tag{2.63}$$

is used for limiting values, and the notation

$$\overline{f}(q) = f(q), \quad q \in S \tag{2.64}$$

is used for direct values, under the assumption that $f^{(\pm)}$ and $\bar{f}$ exist.

The relations between limiting and direct values of the potentials (2.59)-(2.62) are the same as for classic potentials [48], [49] and for the functions $v(p)$ and $u(p)$ that have at least the properties $v \in C^{0,\alpha}(S)$ and $u \in C^{1,\alpha}(S)$, the following identities are valid.

$$\left[P^{(+)}v\right](q) = \left[P^{(-)}v\right](q) = \left[\bar{P}v\right](q), \ q \in S \tag{2.65}$$

$$\left[\partial_n P^{(\pm)}v\right](q) = \left[\partial_n \overline{P}v\right](q) \pm \frac{1}{2}v(q), \ q \in S \tag{2.66}$$

$$\left[Q^{(\pm)}u\right](q) = \left[\bar{Q}u\right](q) \mp \frac{1}{2}u(q), \ q \in S \tag{2.67}$$

$$\left[\partial_n Q^{(+)}u\right](q) = \left[\partial_n Q^{(-)}u\right](q), \ q \in S \tag{2.68}$$

Let's now suppose that the contour S is parametrized by a vector function $\eta(\theta) = \left(x(\theta), y(\theta)\right)$ that has the properties as $\eta(\theta) \epsilon C^{2,\alpha}[-\pi, \pi]$ and

$$\left(\partial/\partial\theta\right)^K \eta(-\pi+0) = \left(\partial/\partial\theta\right)^K \eta(\pi-0), \quad K = 0,1,2... \tag{2.69}$$

and provides a one-to-one correspondence between the points on the contour S and the values $\theta\epsilon(-\pi,\pi]$. Owing to the one-to-one correspondence of the parametrization, the relation

$$l(\theta) \overset{def}{=} \left\{\left[x'(\theta)\right]^2 + \left[y'(\theta)\right]^2\right\}^{1/2} > 0 \tag{2.70}$$

is valid where $(\cdot)^K$ means the K^{th} and $'$ the first order derivative w.r.t. the argument.

Throughout the chapter, for any two functions $\alpha(\theta)$ and $\beta(\theta)$ of arbitrary nature, their inner product and composition will be denoted as

$$\langle \alpha \cdot \beta \rangle(\theta) = \alpha(\theta)\beta(\theta) \tag{2.71}$$

$$(\alpha \circ \beta)(\theta) = \alpha\left(\beta(\theta)\right) \tag{2.72}$$

and, for the direct and inverse Fourier transforms on $[-\pi,\pi]$ the notations F and F^{-1} are used, respectively. Also, I denotes the identity matrix and for the notation of diagonal matrix T_n the expression

$$T = diag\left\{\tau_n\right\}_{n=-\infty}^{\infty}, \quad \tau_n = \max(1,|n|^{1/2}) \tag{2.73}$$

is used.

Using these notations, the identities having a view of pseudo-differential operator of the corresponding integral and differentially integral operators can be derived as

$$\left[\overline{P}v\right] \circ \eta = -\frac{1}{2}\left[F^{-1}T^{-1}\left(I - 2M^P\right)T^{-1}F\left(l \cdot \langle v \circ \eta \rangle\right)\right] \tag{2.74}$$

$$\left[\overline{Q}u\right] \circ \eta = \left[F^{-1}T^{-1}M^Q TF\left(u \circ \eta\right)\right] \tag{2.75}$$

$$\left[\partial_n \overline{P}v\right]\circ\eta = \left\langle l^{-1}\cdot\left[F^{-1}TM^{\partial_n P}T^{-1}F\left\langle l\cdot(v\circ\eta)\right\rangle\right]\right\rangle \tag{2.76}$$

$$\left[\partial_n Q^{(\pm)}u\right]\circ\eta = \frac{1}{2}\left\langle l^{-1}\cdot\left[F^{-1}T\left(I+2M^{\partial_n Q}\right)TF\left(u\circ\eta\right)\right]\right\rangle \tag{2.77}$$

In the equations (2.74)-(2.77) the argument $\theta\epsilon[-\pi,\pi]$ is omitted for the sake of simplicity.

For the matrix M that denotes one of the matrices M^P, M^Q, $M^{\partial_n P}$, $M^{\partial_n Q}$ it can be shown that

$$\sum_{s=-\infty}^{\infty}\sum_{n=-\infty}^{\infty}\left(1+|s|\right)\left(1+|n|\right)\left|m_{sn}\right|^2 < \infty \tag{2.78}$$

where m_{sn} are the matrix elements of M. It means that m_{sn} are decaying when $s,n\to\infty$ even faster than the elements of a Hilbert-Schmidt matrix. In particular, such matrix M defines a compact matrix operator in l_2.

In order to understand the way of the representations (2.74)-(2.77), the derivation and their correctness let's consider the simplest case of potential $\bar{P}v$ in (2.74). Namely, it can be shown [50] that

$$[Pv\circ\eta](\theta) = \int_{-\pi}^{\pi} G_2\left(\eta(\theta),\eta(\tau)\right)l(\tau)v\left(\eta(\tau)\right)d\tau,\quad \theta\in[-\pi,\pi] \tag{2.79}$$

and function $G_2\left(\eta(\theta),\eta(\tau)\right)$ allows the representation

$$G_2\left(\eta(\theta),\eta(\tau)\right) = L(\theta-\tau)+p(\theta,\tau) \tag{2.80}$$

where

$$L(t) = \frac{1}{2\pi}\left\{-\frac{1}{2}+\ln\left|2\sin\frac{t}{2}\right|\right\} \tag{2.81}$$

$$-\frac{1}{2}+\ln\left|2\sin\frac{t}{2}\right|=-\frac{1}{2}\sum_{n=-\infty}^{\infty}\frac{e^{\mathrm{int}}}{\tau_n^2};\quad t\in[-\pi,\pi] \tag{2.82}$$

and $p(\theta,\tau)$ has continuous first partial derivatives and $(\partial^2/\partial\theta\partial\tau)p(\theta,\tau)\in L_2$ (L_2: space of square integrable functions). It means, in particular, that

$$\sum_{s=-\infty}^{\infty}\sum_{n=-\infty}^{\infty}\tau_n^4\tau_s^4\left|p_{sn}\right|^2<\infty \tag{2.83}$$

where p_{sn} are Fourier coefficients of $p(\theta,\tau)$ and definition of τ_n is given in (2.73). The identity (2.74) and the inequality (2.78) for $M=M^P$ follows immediately [50] from (2.79)-(2.83).

The most complicated proof is required for the identity (2.77). First of all [50],

$$\left(\partial_n Q^{(\pm)}u\circ\eta\right)(\theta)=A(\theta)+B(\theta) \tag{2.84}$$

$$A(\theta)=\frac{1}{l(\theta)}\frac{d^2}{d\theta^2}\int_{-\pi}^{\pi}u\left(\eta(\tau)\right)\ln\left|2\sin\frac{\theta-\tau}{2}\right|d\tau+\frac{1}{l(\theta)}\int_{-\pi}^{\pi}u\left(\eta(\tau)\right)d\tau \tag{2.85}$$

$$B(\theta)=\frac{1}{l(\theta)}\int_{-\pi}^{\pi}u\left(\eta(\tau)\right)W(\theta,\tau)\,d\tau \tag{2.86}$$

where $W(\theta,\tau)$ has singularities proportional to $\ln|2sin(\theta-\tau)/2|$ only. Calculation of the limits $\partial_n Q^{(\pm)}u$ in form of (2.84)-(2.86) is relatively simple in a point on local flat part of the contour when the contour is parametrized by its arc-length, but the proof becomes rather non-trivial in general case [28, 50].

In equation (2.85) the operation $d^2/d\theta^2$ cannot be moved inside the integral because it makes the result of the integral divergent. Nevertheless, under the supposition of $u\in C^{1,\alpha}(S)$, the expression for $A(\theta)$ is correct when the differential and integral operators are applied in the written order.

Due to the above-explained properties of $W(\theta,\tau)$, its Fourier coefficients w_{sn} satisfy the inequality

$$\sum_{s=-\infty}^{\infty}\sum_{n=-\infty}^{\infty}\left|w_{sn}\right|^2<\infty \tag{2.87}$$

Taking together the equations (2.81), (2.82) and (2.84)-(2.86) one arrives into the equation (2.77). The other formulas like (2.75) and (2.76) can be proved in a very similar way as (2.74) and (2.77).

In the next subchapters, the two-dimensional BVPs, whose posing is similar to that in [47] are considered by the ARM algorithm based on the above-given details.

2.2.1. ARM for Dirichlet Boundary Value Problem

This problem arises in the case of a TM wave incidence on a PEC cylinder. Let a closed non-self-crossing contour $S \subset \Omega = R^2$ is given that has the property as $S \in C^{2,\alpha}$. The contour is parametrized by the above described function $\eta(\theta) = \big(x(\theta), y(\theta)\big)$ for $\theta\epsilon(-\pi,\pi]$. In addition, let $V^{(-)}$ is an open bounded domain with boundary $\partial V^{(-)} = S$ and $V^{(+)}$ is the complementary to $\overline{V^{(-)}} = V^{(-)} \cup S$ in the domain R^2. Namely,

$$\partial V^{(-)} = S;\;\; V^{(+)} = R^2 \setminus \overline{V^{(-)}} \tag{2.88}$$

It is necessary to find the unknown function $u^s(q)$ in $q\epsilon R^2 \setminus S$, (i.e. scattering field in physical sense) which is one of the kind

$$u^s\left(q\right) \in C^2\left(R^2 \setminus S\right) \cap C^{1,\alpha}\left(\overline{V^{(+)}}\right) \cap C^{1,\alpha}\left(\overline{V^{(-)}}\right) \tag{2.89}$$

The condition (2.89) means, in particular, that $u^s(q)$ and all its derivatives of the first order are continuous in $\overline{V^{(+)}}$ and $\overline{V^{(-)}}$, but the limiting values $u^{s(+)}(q)$ and $u^{s(-)}(q)$ as well as $\partial_n u^{s(+)}(q)$ and $\partial_n u^{s(+)}(q)$ for $q\epsilon S$ are not necessarily equal where

$$\partial_n u^{s(\pm)}\left(q\right) = \left(\frac{\partial u^s}{\partial n_q}\right)^{(\pm)}, \quad q \in S \tag{2.90}$$

In addition, the function $u^s(q)$ must satisfy the homogeneous Helmholtz equation in $V^{(\pm)}$ i.e.

$$\left(\Delta + k^2\right)u^s\left(q\right) = 0, \quad q \in R^2 \backslash S \tag{2.91}$$

and the well-known Sommerfeld radiation condition

$$\lim_{|q|\to\infty} |q|^{1/2}\left(\frac{\partial u^s\left(q\right)}{\partial |q|} - iku^s\left(q\right)\right) = 0 \tag{2.92}$$

Also, $u^{s(\pm)}(q)$ should obey the Dirichlet boundary condition

$$u^{s(+)}\left(q\right) = u^{s(-)}\left(q\right) = -u^i\left(q\right), \quad q \in S \tag{2.93}$$

where $u^i(q)$ is a known function (having a sense of an incident field values on S).

Utilization of the Green's formulae technique gives the identity [47]-[50]

$$\left[\overline{P}\,\delta\partial_n u^s\right]\left(q\right) = -u^{(i)}\left(q\right), \quad q \in S \tag{2.94}$$

where $\delta\partial_n u^s(q) = \partial_n u^{s(+)}(q) - \partial_n u^{s(-)}(q)$, $q \epsilon S$.

Taking the identity (2.94) as a hint, one can consider the integral equation with unknown function $v(q) \in C^{0,\alpha}(S)$,

$$\left[\overline{P}v\right]\left(q\right) = -u^i\left(q\right), \quad q \in S \tag{2.95}$$

with a hope that function

$$U\left(q\right) = \left[Pv\right]\left(q\right), \quad q \in R^2 \backslash S \tag{2.96}$$

provides a solution of the Dirichlet BVP (this hope is not fulfilled always).

As it follows from (2.80), (2.81) the kernel of $\bar{P}$ is square integrable and, consequently, equation (2.95) is one of the first kind in space $L_2(S)$. As mentioned in Chapter 2, such equation posed in L_2 has rather "pathological" features. In particular, it does not obey to the Fredholm alternative and may have many or any solutions. In order to guarantee the unique solution let's apply the ARM to (2.95) as explained in Chapter 2.

Making the composition of both sides of (2.95) with the parametrization $\eta(\theta)$ and taking into account the representation (2.74), the following equation is obtained

$$-\frac{1}{2}\left[F^{-1}T^{-1}\left(I-2M^{P}\right)T^{-1}F\left(l\cdot\langle v\circ\eta\rangle\right)\right]=-\left(u^{i}\circ\eta\right) \tag{2.97}$$

Now it is evident that (2.97) is in form of (2.14) with the following double-sided operators

$$L^{-1}=-\frac{1}{2}F^{-1}T^{-1} \tag{2.98}$$

$$R^{-1}=T^{-1}F \tag{2.99}$$

that have the properties given in (2.16) where the linear (incomplete) spaces

$$\begin{aligned} H_1 &= H^{-1/2}(S)\cap C^{0,\alpha}(S)\\ H_2 &= H^{1/2}(S)\cap C^{1,\alpha}(S) \end{aligned} \tag{2.100}$$

are chosen for a suitable numerical implementation of the ARM with Sobolev spaces $H^{-1/2}(S)$ and $H^{1/2}(S)$ [34, 47]. This choice is applicable under the assumption $S \in C^{2,\alpha}$ [34].

Applying to (2.97) from the left-side by the operator $L=-2TF$ and introducing new unknown vector column z_D and right hand side f_D as

$$z_D=T^{-1}F\left\langle l\cdot\left(v\circ\eta\right)\right\rangle \tag{2.101}$$

$$f_D = -2TF\left(u^i \circ \eta\right) \tag{2.102}$$

then arrived at the final equation

$$\left(I - 2M^P\right) z_D = f_D, \quad z_D, f_D \in l_2 \tag{2.103}$$

Thus, the equation (2.95) is equivalently reduced to the infinite algebraic system (2.103) in l_2, with compact operator $H = -2M^P$ whose Fourier coefficients satisfy the inequality (2.78).

2.2.2. ARM for Neumann Boundary Value Problem

This boundary value problem is encountered in the case of a TE polarized plane wave incidence on a PEC cylinder.

The posing of the Neumann BVP is very similar to the Dirichlet BVP. Herein the Neumann boundary condition

$$\partial_n u^{s(+)}(q) = \partial_n u^{s(-)}(q) = -\partial_n u^i(q), \quad q \in S \tag{2.104}$$

is used instead of (2.93) that of Dirichlet boundary condition. This small change results in the qualitative difference between the solution properties and the way of its construction on the basis of the ARM. It is shown in [28], [50] that every solution $u^s(q)$ of the Neumann BVP can be represented, if exist, as

$$u^s(q) = -\left[Q\delta u^s\right](q), \quad q \in R^2 \setminus S \tag{2.105}$$

where

$$\delta u^s(q) = u^{s(+)}(q) - u^{s(-)}(q), \quad q \in S \tag{2.106}$$

Consequently, from (2.77) and (2.89) as shown in [47], [50] the following identity is correct.

$$\left[\partial_n Q^{(\pm)} \delta u^s\right](q) = \partial_n u^i(q), \quad q \in S \tag{2.107}$$

In the same manner, as done for identity (2.94), the new unknown $u(q)$ that satisfies the equation

$$\left[\partial_n Q^{(+)} u\right](q) = \partial_n u^i(q), \quad q \in S \tag{2.108}$$

can be introduced with the hope that the function

$$U(q) = -[Qu](q), \quad q \in R^2 \backslash S \tag{2.109}$$

gives a solution of the Neumann BVP.

The qualitative properties of (2.108) are opposite of (2.95). Namely, if the equation (2.108) is posed in space L_2, then the inverse operation to $\partial_n Q^{(\pm)}$ becomes bounded and even compact, but the $\partial_n Q^{(\pm)}$ itself is unbounded in L_2. Formulas (2.6) and (2.7) dictate the same numerical instability that is discussed for equation (2.95). But now not because of $\|A_N\|$ in (2.6), but due to $\|A_N^{-1}\|$ which tends to infinity when $N \to \infty$. Thus, again it is needed to choose a set of correctness, to provide additive and multiplicative splitting of $\partial_n Q^{(\pm)}$ and so on. Now, opposite to (2.100),

$$\begin{aligned} H_1 &= H^{1/2}(S) \cap C^{1,\alpha}(S) \\ H_2 &= H^{-1/2}(S) \cap C^{0,\alpha}(S) \end{aligned} \tag{2.110}$$

can be chosen [47], [50].

Formula (2.77) reduces the equation (2.108) to

$$F^{-1} T \left(I + 2M^{\partial_n Q}\right) T F(u \circ \eta) = 2\langle l \cdot u \circ \eta \rangle \tag{2.111}$$

The regularization of the (2.111) can be done easily with the operators

$$L^{-1} = F^{-1}T \tag{2.112}$$

$$R^{-1} = TF \tag{2.113}$$

Applying the operator $L = T^{-1}F$ from the left to the equation (2.111) and introducing new vector of unknowns z_N and g as

$$z_N = TF\left(u \circ \eta\right) \tag{2.114}$$

$$g = 2T^{-1}F\left\langle l \cdot \left(u \circ \eta\right)\right\rangle \tag{2.115}$$

then arrived at the equation

$$\left[I + 2M^{\partial_n Q}\right] z_N = g; \quad z_N, g \in l_2 \tag{2.116}$$

which is one of the second kind with compact operator $H = 2M^{\partial_n Q}$ in l_2.

2.2.3. ARM for Boundary Integral Equation of Third Kind BVP

The third kind boundary condition also called as impedance boundary condition or mixed boundary condition which defines a relation between the total tangential field and its normal derivative on the boundary is

$$\alpha\left(q\right)u^t\left(q\right) + \beta\left(q\right)\frac{u^t\left(q\right)}{\partial n} = 0; \;\; q \in S \tag{2.117}$$

where $u^t(q) = u^i(q) + u^s(q)$ is the total field, and $\alpha(q)$ and $\beta(q)$ are supposed to be infinitely smooth functions of point $q \in S$ and they are normalized as $|\alpha(q)|^2 + |\beta(q)|^2 = 1$. It is clear that the choice as $\alpha(q) = 1$ and $\beta(q) = 0$ corresponds to the Dirichlet boundary condition, and $\alpha(q) = 0$ and $\beta(q) = 1$ corresponds to Neumann boundary condition. That is why the consideration of the boundary value problem in sense of ARM is very similar to those problems. It will be shown that, depending on

the value of these parameters, this problem can be reduced the Dirichlet or Neumann BVPs.

Utilization of the theory of Green's formulae technique [47], [50] gives the following integral equation of the scattered field that satisfies the homogeneous Helmholtz equation (2.91)

$$u^s(q) = -\left[Q^{(+)}u\right](q) + \left[P^{(+)}v\right](q);\ q \in V^{(+)} \tag{2.118}$$

$$\partial_n u^s(q) = -\left[\partial_n Q^{(+)}u\right](q) + \left[\partial_n P^{(+)}v\right](q);\ q \in V^{(+)} \tag{2.119}$$

where, $u(q) = u^{s(+)}(q)$ and $v(q) = \partial_n u^{s(+)}(q)$.

Even if the relations (2.118) and (2.119) are given for the scattered field, the same relations can be obtained simply for the total field as well. From the relation of the fields given above, the scattered field can be written as

$$u^s(q) = u^t(q) - u^i(q) \tag{2.120}$$

If the equation (2.120) is substituted into (2.118) and (2.119), and then by using the relations (2.65)-(2.68) the boundary integral equations

$$\frac{1}{2}u(q) + \left[\overline{Q}u\right](q) - \left[\overline{P}v\right](q) = u^i(q);\ q \in S \tag{2.121}$$

$$\frac{1}{2}v(q) + \left[\partial_n Q^{(+)}u\right](q) - \left[\partial_n \overline{P}v\right](q) = \partial_n u^i;\ q \in S \tag{2.122}$$

are obtained for the total field, where now, $u(q) = u^{t(+)}(q)$ and $v(q) = \partial_n u^{t(+)}(q)$. The system of the equations (2.121) and (2.122) can be used for finding the unknowns $u(q)$ and $v(q)$. However, the relation (2.117) gives a possibility to express one unknown in terms of the other one, for example, as

$$u^t(q) = -\frac{\beta(q)}{\alpha(q)} \frac{\partial u^t(q)}{\partial n_q} \tag{2.123}$$

and then eliminate it from one of the equations. In this case, one of the two equations can be used for finding the corresponding unknown and then the other is obtained simply by means of the relation (2.117). Before doing this, the system must be analyzed from the point of the ARM. It is clear, as it is explained in [51], that the regularization process depends on the value

$$\eta(q) = \frac{\beta(q)}{\alpha(q)} \tag{2.124}$$

Also, it is explained in [51] that the case of

$$\left|\beta(q)\right| \geq \beta_0 > 0; \ q \in S \tag{2.125}$$

corresponds to the, so called, regular case where β_0 is some, not very small, constant and the alternative condition to (2.125) is

$$\left|\alpha(q)\right| \geq \alpha_0 > 0; \ q \in S \tag{2.126}$$

when $\eta(q)$ can be very small and even equal to zero.

In an analysis of E-polarized (TM-*z*) wave diffraction, $\eta(q)$ given by (2.124) corresponds to the impedance value. In this case, if the diffraction by a well-conductive cylinder is considered then $\eta(q) = 0$ and the equation (2.121) reduces to the same kind of equation of the Dirichlet boundary value problem and it can be solved in the same manner as (2.95). This equation is also called as electric field integral equation of scattering by PEC cylinder of TM-*z* polarization.

If the equation (2.122) is used for the purpose, with the condition of $\eta(q) = 0$, it reduces to

$$\frac{1}{2} v(q) - \left[\partial_n \overline{P} v\right](q) = \partial_n u^i; \ q \in S \tag{2.127}$$

which is the magnetic field integral equation of TM-*z* wave scattering by PEC cylinder. By means of the equation (2.76), it can be represented in the form of operators as

$$\left(I - 2M^{\partial_n P}\right) = 2\partial_n u^i \tag{2.128}$$

which is a second kind equation and obtained simply by multiplying by two without the need of using regularization operators. This happens because of the natural properties of the normal derivative of the single layer potential $\partial_n P$ that are given by (2.66) and (2.76).

If an H-polarized (TE-*z*) wave diffractions is considered, then the ratio $\eta(q) = \alpha(q)/\beta(q)$ defines an impedance on the surface. In this case, opposite to TM-*z* polarization, for very small or zero values of the impedance, the equation (2.122) reduced to the equation of the Neumann BVP and its regularization and solution can be obtained in the same way as explained for (2.108). This integral equation is called as the EFIE of the TE-*z* wave scattering by PEC cylinder.

If the equation (2.121) is considered for the solution of BVP in TE-*z* polarized wave, for very small or zero value of impedance, the integral equation

$$\frac{1}{2}u(q) + \left[\overline{Q}u\right](q) = u^i(q);\ \ q \in S \tag{2.129}$$

is obtained. With the properties of double-layer potential given by (2.67) and (2.75) the view in form of operators

$$\left(I + 2M^{Q}\right) = 2u^i \tag{2.130}$$

is obtained as a second kind equation which is the result of the properties of double layer potential.

All the cases theoretically discussed here will be analyzed numerically in Chapter 3.4 where the solution of the boundary integral equation of two parallel impedance cylinders is under consideration for TM-*z* and TE-*z* wave incidence.

2.2.4. ARM for Boundary Integral Equation of Dielectric BVP

Consider the dielectric body given in Figure 2.5 with the same domains $V^{(\pm)}$ that is discussed previously. Unlike the above situations, domains $V^{(+)}$ and $V^{(-)}$ have different material parameters resulting into different but constant wavenumbers $k^{(+)}$ and $k^{(-)}$ respectively.

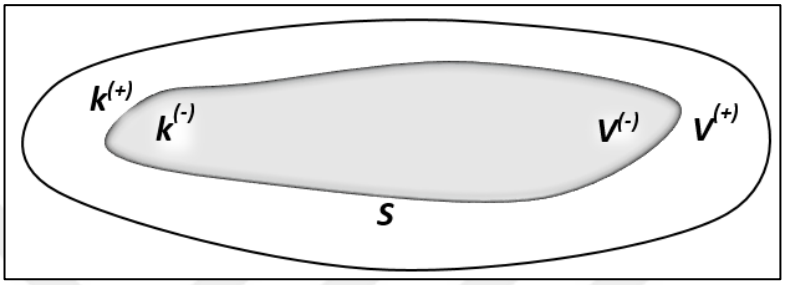

Figure 2.5: The schematic view of the arbitrarily shaped dielectric obstacle.

Analogous to the above BVPs, it is necessary to find the scattered field $u^{(s)}(q)$, $q \in V^{(+)} \cup V^{(-)}$ which belongs to the same class (2.89) but satisfies two Helmholtz equations with different wave numbers.

$$\left(\Delta + k^2\right) u^s\left(q\right) = 0, \;\; q \in V^{(-)} \bigcup V^{(+)} \tag{2.131}$$

$$k\left(q\right) = \begin{cases} k^{(+)}, & q \in V^{(+)} \\ k^{(-)}, & q \in V^{(-)} \end{cases} \tag{2.132}$$

In addition, it satisfies the dielectric boundary conditions

$$u^{s(-)}\left(q\right) = u^{s(+)}\left(q\right) + u^i\left(q\right), \;\; q \in S \tag{2.133}$$

$$\partial_n u^{s(-)}\left(q\right) = \partial_n u^{s(+)}\left(q\right) + \partial_n u^i\left(q\right), \;\; q \in S \tag{2.134}$$

and the Sommerfeld radiation condition (2.92) in the unbounded domain $V^{(+)}$. Analogous to (2.59) and (2.60) the potentials

$$\left[P_{(\pm)}v\right](q)=\int_S G_{2(\pm)}(q,p)v(p)dl_p,\ q\in V^{(\pm)} \tag{2.135}$$

$$\left[Q_{(\pm)}u\right](q)=\int_S \frac{\partial G_{2(\pm)}(q,p)}{\partial n_p}u(p)dl_p,\ q\in V^{(\pm)} \tag{2.136}$$

can be defined. Here and below the subscript $(\pm)$ is used for the values and functions associated with the domains $V^{(\pm)}$ respectively. By using the standard Green's formulae technique, the integral equations for scattered fields are obtained as

$$u^s(q)=\left[Q_{(-)}u^{s(-)}\right](q)-\left[P_{(-)}\partial_n u^{s(-)}\right](q);\ q\in V^{(-)} \tag{2.137}$$

$$u^s(q)=-\left[Q_{(+)}u^{s(+)}\right](q)+\left[P_{(+)}\partial_n u^{s(+)}\right](q);\ q\in V^{(+)} \tag{2.138}$$

Note that the field expressed by (2.137) is the total field inside the region $V^{(-)}$ since it is supposed that the incident field source is posed in the domain $V^{(+)}$. On the other side, the field given by (2.138) is the only scattered field. For having an equation expressed in terms of the total field, the relation

$$u^s(q)=u^t(q)-u^i(q);\ q\in V^{(+)} \tag{2.139}$$

is substituted into the equation and then the following relations are obtained in terms of the total field and its normal derivative.

$$u^t(q)-\left[Q_{(-)}u^{t(-)}\right](q)+\left[P_{(-)}\partial_n u^{t(-)}\right](q)=0;\ q\in V^{(-)} \tag{2.140}$$

$$\partial_n u^t(q)-\left[\partial_n Q_{(-)}u^{t(-)}\right](q)+\left[\partial_n P_{(-)}\partial_n u^{t(-)}\right](q)=0;\ q\in V^{(-)} \tag{2.141}$$

$$u^t(q)+\left[Q_{(+)}u^{t(+)}\right](q)-\left[P_{(+)}\partial_n u^{t(+)}\right](q)=u^i(q);\ q\in V^{(+)} \tag{2.142}$$

$$\partial_n u^t(q)+\left[\partial_n Q_{(+)}u^{t(+)}\right](q)-\left[\partial_n P_{(+)}\partial_n u^{t(+)}\right](q)=\partial_n u^i(q);\quad q\in V^{(+)} \tag{2.143}$$

where the values $u^t(q)$ and $\partial_n u^t(q)$ are the values in the domain but $u^{t(\pm)}(q)$ and $\partial_n u^{t(\pm)}(q)$ are the values on the boundary. The reason for expressing the integral representations in terms of the total field as (2.140)-(2.143) is to have similar integral equation forms that used in [17]. Therein the boundary integral equations are given in terms of the surface currents where the surface currents correspond to the total field on the surface. Also, in [17] the integral equations are classified as EFIE and MFIE for both polarizations and these equations are used in the following Chapters 3.3 and 3.4 where the application of ARM is investigated.

Now let's obtain the boundary integral equations from the integral representations (2.140)-(2.143) by passing the limit values given in (2.65)-(2.68). These operations yields the integral equations

$$\frac{1}{2}u^t(q)-\left[\overline{Q}_{(-)}u^t\right](q)+\left[\overline{P}_{(-)}\partial_n u^t\right](q)=0;\ q\in S \tag{2.144}$$

$$\frac{1}{2}u^t(q)+\left[\overline{Q}_{(+)}u^t\right](q)-\left[\overline{P}_{(+)}\partial_n u^t\right](q)=u^i(q);\ q\in S \tag{2.145}$$

$$\frac{1}{2}\partial_n u^t(q)-\left[\partial_n Q_{(-)}^{(-)}u^t\right](q)+\left[\partial_n P_{(-)}\partial_n u^t\right](q)=0;\ q\in S \tag{2.146}$$

$$\frac{1}{2}\partial_n u^t(q)+\left[\partial_n Q_{(+)}^{(+)}u^t\right](q)-\left[\partial_n \overline{P}_{(+)}\partial_n u^t\right](q)=\partial_n u^i(q);\ q\in S \tag{2.147}$$

on the boundary S. In these equations the superscripts $(\pm)$ of the fields are omitted since the total field on the outer side of the boundary is equal to the total field on the inner side in accordance with the dielectric boundary conditions (2.133) and (2.134).

The equation set (2.144), (2.145) are called as EFIEs and (2.146), (2.147) are called as MFIEs of TM-*z* wave scattering by the dielectric body. For the TE-*z* polarization, the opposite is said. This is the result of field formulation which leads four equations in two unknowns [22]. Thus, any of two equations or any proper

combination of them can be used for finding the unknowns. Here, the EFIE or MFIE formulations i.e. (2.144) and (2.145) or (2.146) and (2.147) are used for the solution of the system since this kind formulation is used in [18] and [19] which is followed from [17].

Now let's, at first, consider the equation set (2.144) and (2.145) in a proper form for analysis as

$$\begin{aligned} u^t(q)+2\left[\overline{Q}_{(+)}u^t\right](q)-2\left[\overline{P}_{(+)}\partial_n u^t\right](q)&=2u^i(q)\\ u^t(q)-2\left[\overline{Q}_{(-)}u^t\right](q)+2\left[\overline{P}_{(-)}\partial_n u^t\right](q)&=0 \end{aligned} \tag{2.148}$$

and in the matrix form as

$$\begin{bmatrix} A_{11} & A_{12} \\ A_{21} & A_{22} \end{bmatrix}\begin{bmatrix} u^t(q) \\ \partial_n u^t(q) \end{bmatrix}=\begin{bmatrix} b_1 \\ b_2 \end{bmatrix} \tag{2.149}$$

where the unknown vector and the known right-hand-side vector are as follows.

$$\begin{bmatrix} x_1 \\ x_2 \end{bmatrix}=\begin{bmatrix} u^t(q) \\ \partial_n u^t(q) \end{bmatrix};\ \begin{bmatrix} b_1 \\ b_2 \end{bmatrix}=\begin{bmatrix} u^i(q) \\ [0] \end{bmatrix} \tag{2.150}$$

If the equations (2.148)-(2.150) examined then it is clear that the matrix element A_{11} is a diagonal one but A_{22} is not. So, for having a full diagonal matrix, the block matrix A_{22} must be diagonalized. As it is seen from (2.148) it has the same kind equation of the Dirichlet BVP and thus, its regularization can be done in the same manner. So, the double-sided regulators are constructed as

$$L^{-1}=\begin{bmatrix} I & [0] \\ [0] & L_D^{-1} \end{bmatrix};\ R^{-1}=\begin{bmatrix} I & [0] \\ [0] & R_D^{-1} \end{bmatrix} \tag{2.151}$$

where I is the identity matrix and the operators that subscripted by D are the operators of the Dirichlet BVP given by (2.98) and (2.99).

The consideration of the equations (2.146) and (2.147) analogous to (2.148) yields to

$$\begin{aligned} &\partial_n u^t(q) - 2\left[\partial_n \overline{P}_{(+)} \partial_n u^t\right](q) + 2\left[\partial_n Q^{(+)}_{(+)} u^t\right](q) = 2\partial_n u^i(q) \\ &\partial_n u^t(q) + 2\left[\partial_n P_{(-)} \partial_n u^t\right](q) - 2\left[\partial_n Q^{(-)}_{(-)} u^t\right](q) = 0 \end{aligned} \tag{2.152}$$

with similar matrix form but with the inverse order of the unknowns. In this case, again, the matrix element A_{11} is a diagonal one and, the block matrix A_{22} must be diagonalized for having a full diagonal matrix. But now, A_{22} has an equation of the same kind as Neumann BVP and its regularization must be done similar to that. That's why the regularization operators have the following matrix forms

$$L^{-1} = \begin{bmatrix} I & [0] \\ [0] & L_N^{-1} \end{bmatrix};\ R^{-1} = \begin{bmatrix} I & [0] \\ [0] & R_N^{-1} \end{bmatrix} \tag{2.153}$$

where the operators denoted by the subscript of N are the operators of Neumann BVP given by (2.112) and (2.113) respectively.

As can be seen from (2.148) and (2.152), the regularization procedure changes depend on the chosen equation set. However, even if the procedure that is explained here is only for the EFIE and MFIE system, there is not a big difference for any combination of the equations (2.144)-(2.147). A different but qualitatively same procedure of regularization that explained in all details can be found in [24, 34] for dielectric boundaries.

Before finishing this part, it is crucial to underline that the solutions of the integral equation set (2.144)-(2.147) are not resonance-free and thus, may not be unique due to the facts that explained in [22] and in Chapter 3.4 of the [17]. For obtaining resonance-free solutions, there are several methods mentioned in the introduction part, which make a proper combination of the equations (2.144)-(2.147)

and guarantee a unique solution. However, the resonance solutions are beyond the scope of this work and the resonance frequencies are not considered here.

2.2.5. Singularity Properties of the Kernels of Potentials

The first and the basic step of the ARM is the local singular expansion of the kernels of the single and double layer potentials (2.59), (2.60) and their normal derivatives (2.61), (2.62) (if used in the formulation then the consideration of the tangential derivatives may be required which is out of the scope of this thesis).

It is seen from (2.59) that the kernel of the single layer potential is the two-dimensional free-space Green's function which, for the $e^{i\omega t}$ time dependency, is

$$K_P = G_2(q, p) = \frac{1}{4i} H_0^{(2)}(kR) = \frac{1}{4i}\left[J_0(kR) - iY_0(kR)\right] \tag{2.154}$$

where free space denotes not only vacuum but any homogeneous medium. Here $H_0^2(\cdot)$, $J_0(\cdot)$ and $Y_0(\cdot)$ are the zero order second kind Hankel, Bessel, and Neumann functions respectively and R is the distance between the points q and p that has the definition

$$R = \left|\vec{q} - \vec{p}\right| = \left\{\left(x_q - x_p\right)^2 + \left(y_q - y_p\right)^2\right\}^{1/2} \tag{2.155}$$

It is well-known that the $J_0(kR)$ is infinitely smooth function of R that has the expression [26]

$$J_0(kR) = 1 - \frac{(kR)^2}{4} + \frac{(kR)^4}{64} + \cdots \tag{2.156}$$

but $Y_0(kR)$ has logarithmic singularity when $R = 0$ and it has the following expansion [26]

$$Y_0(kR) = \frac{2}{\pi}\ln\left(\frac{kR}{2}\right)J_0(kR) + \frac{2\gamma}{\pi}J_0(kR) + \frac{(kR)^2}{2} - \cdots \tag{2.157}$$

and in terms of the Chebyshev polynomials $T_{2n}(\cdot)$ with known coefficients b_n up to 25 digits which is given in [52]

$$Y_0(kR) = \frac{2}{\pi}\ln\left(\frac{kR}{2}\right)J_0(kR) + \frac{2\gamma}{\pi}J_0(kR) + \sum_{n=0}^{\infty} b_n T_{2n}\left(\frac{kR}{8}\right) \tag{2.158}$$

Here $\gamma = 0.57721566490$ ... is the Euler constant.

By substituting (2.158) into (2.154) yields

$$G_2(kR) = -\frac{1}{2\pi}\ln\left(\frac{kR}{2}\right)J_0(kR) + \left(\frac{1}{4i} - \frac{\gamma}{2\pi}\right)J_0(kR) - \frac{1}{4}\sum_{n=0}^{\infty} b_n T_{2n}\left(\frac{kR}{8}\right) \tag{2.159}$$

For the points $q = \eta(\theta) = \big(x(\theta), y(\theta)\big)$ and $p = \eta(\tau) = \big(x(\tau), y(\tau)\big)$ the relation (2.155) can be rewritten as

$$R(\theta,\tau) = \left|\eta(\theta) - \eta(\tau)\right| = \left\{\big(x(\theta) - x(\tau)\big)^2 + \big(y(\theta) - y(\tau)\big)^2\right\}^{1/2} \tag{2.160}$$

Now, let us introduce the notations

$$\theta_1 = \theta;\ \theta_2 = \tau;\ \ \delta = \theta - \tau; \tag{2.161}$$

and

$$x_j^{(K)} = \left[\frac{d^{(K)}}{d\theta^{(K)}}x(\theta)\right]_{\theta=\theta_j};\ y_j^{(K)} = \left[\frac{d^{(K)}}{d\theta^{(K)}}y(\theta)\right]_{\theta=\theta_j},\ \ j = 1,2 \tag{2.162}$$

Now it is evident from (2.160) and (2.161) that $R \to 0$ when $\delta \to 0$ and $\delta \to \pm 2\pi$ with the property of the parametrization function $\eta(\theta)$ that given in (2.69). Thus, the

considered function may have the singularities only in such points where $\sin\left(\frac{\delta}{2}\right)=0$ which are the same points of $\delta=0,\pm 2\pi$. That is why, to investigate the behavior of the considered functions, the case $\delta\to 0$ is considered. For this end, at first, it is necessary to consider the corresponding behavior of the function (2.160). For this purpose let's define the Taylor series of

$$\delta_x = x_2 - x_1 = x_1'\delta + \frac{1}{2}x_1''\delta^2 + \frac{1}{6}x_1'''\delta^3 + \frac{1}{24}x_1^{(4)}\delta^4 + \mathcal{O}\left(\delta^5\right) \tag{2.163}$$

$$\delta_y = y_2 - y_1 = y_1'\delta + \frac{1}{2}y_1''\delta^2 + \frac{1}{6}y_1'''\delta^3 + \frac{1}{24}y_1^{(4)}\delta^4 + \mathcal{O}\left(\delta^5\right) \tag{2.164}$$

By means of these Taylor series, one can calculate that

$$R^2 = R^2(\theta,\tau) = \delta^2 l^2\left[1 + a\delta + b\delta^2 + c\delta^3 + \mathcal{O}\left(\delta^4\right)\right] \tag{2.165}$$

where $l = l(\theta)$ is the arc length defined by (2.70).

Now, by using the relation (2.165), the term that has the logarithmic singularity can be written as

$$\begin{aligned}\ln\left[kR(\theta,\tau)\right] &= \frac{1}{2}\ln\left[k^2R^2(\theta,\tau)\right] = \frac{1}{2}\ln\delta^2 + \varphi(\theta,\tau)\\ &= \ln|\delta| + \varphi(\theta,\tau)\end{aligned} \tag{2.166}$$

where $\varphi(\theta,\tau)$ is some infinitely differentiable function in the domain $|\theta-\tau|\le 2\pi$. Substituting the equations (2.156) and (2.157) into (2.154) and then using the relation (2.166) one can obtain the singular expansion

$$K_P = G_2\left[kR(\theta,\tau)\right] = \frac{1}{2\pi}\ln|\delta|\left\{1 + \sum_{n=2}^{N} A_n(\theta)\delta^n\right\} + F_N(\theta,\tau) \tag{2.167}$$

where $F_N(\theta,\tau)$ is some function that has continuous derivatives of the order not bigger than N. This expression is valid for arbitrary integer $N\ge 2$.

It is clear that the function $G_2\big(kR(\theta,\tau)\big)$ is the periodic function of θ and τ with the smooth parametrization function $\eta(\theta)$ that has the property (2.69). Also, it is evident that it is infinitely differentiable except at the points where $\delta = 0, \pm 2\pi$. As stated above, these points are the same as where the periodic function $\sin\left(\frac{\delta}{2}\right) = 0$. Furthermore, this function can be expanded into Taylor series for $\delta \to 0$ as

$$\begin{aligned}\sin\left(\frac{\delta}{2}\right) &= \frac{\delta}{2} - \left(\frac{\delta}{2}\right)^3 \frac{1}{3!} + \left(\frac{\delta}{2}\right)^5 \frac{1}{5!} - \cdots \\ &= \frac{\delta}{2}\left[1 + \alpha\delta^2 + \beta\delta^4 + \mathcal{O}\left(\delta^6\right)\right]\end{aligned} \tag{2.168}$$

By comparing the equations (2.166) and (2.168) one can easily see that

$$\ln\left|2\sin\left(\frac{\theta-\tau}{2}\right)\right| = \ln|\delta| + \psi(\theta,\tau) \tag{2.169}$$

where $\psi(\theta,\tau)$ some infinitely differentiable function in the domain $|\theta - \tau| \le 2\pi$. In addition, it can be found in [53] that, this function has the following Fourier series expansion

$$\ln\left|2\sin\left(\frac{\theta-\tau}{2}\right)\right| = -\frac{1}{2}\sum_{n=-\infty}^{\infty} \frac{e^{in(\theta-\tau)}}{|n|};\ n \neq 0,\ \theta,\tau \in [-\pi,\pi] \tag{2.170}$$

which can be written in another form [35], by the help of τ_n that has the definition in (2.73), as

$$-\frac{1}{2} + \ln\left|2\sin\left(\frac{\theta-\tau}{2}\right)\right| = -\frac{1}{2}\sum_{n=-\infty}^{\infty} \frac{e^{\mathrm{in}(\theta-\tau)}}{\tau_n^2};\ \theta,\tau \in [-\pi,\pi] \tag{2.171}$$

Now it is evident that by means of this expression, the singularity of the kernel (2.167) can be extracted and even the periodicity is preserved since they have the same singularity at same points. Because as shown in above chapters by the operators, the

integrals are discretized by expanding all the corresponding functions into their one or two-dimensional Fourier series and then reduced to the algebraic systems of their Fourier coefficients by the help of the orthogonality of the complex exponentials [5], [51], [54]. That is why the singular kernel is splitting into the smooth and singular parts and then the singularity is extracted with the help of the Fourier series expression given by (2.171). After all these statements, it is evident that one can express the kernel given by (2.167) as

$$K_P = G_2\left[kR(\theta,\tau)\right] = \frac{1}{2\pi}\left\{-\frac{1}{2} + \ln\left|2\sin\left(\frac{\theta-\tau}{2}\right)\right| + p(\theta,\tau)\right\} \tag{2.172}$$

which is, in some sense, the proof of the expressions (2.80)-(2.82).

Now let's analyze the kernel of the double layer potential given by (2.60) which is the normal derivative of the Green's function as

$$K_Q = \frac{\partial G_2(kR)}{\partial n_p} = \nabla_p\left[G_2(kR)\right]\cdot\hat{n}_p \tag{2.173}$$

where ∇_p stands for the gradient subjected to coordinates of $p(\tau) = \left(x(\tau), y(\tau)\right) = \left(x_p, y_p\right)$ and $\hat{n}_p = \left(n_x(\tau), n_y(\tau)\right)$ is the unit outward normal vector at point p whose components are

$$\hat{n}_p = n_x(\tau)\hat{e}_x + n_y(\tau)\hat{e}_y;\ n_x(\tau) = \frac{y'(\tau)}{l(\tau)};\ n_y(\tau) = -\frac{x'(\tau)}{l(\tau)} \tag{2.174}$$

If the gradient operator is subjected to the Green's function in (2.173) it results in

$$\begin{aligned}\nabla_p\left[G_2(kR)\right] &= \frac{\partial G_2(kR)}{\partial x_p}\hat{e}_x + \frac{\partial G_2(kR)}{\partial y_p}\hat{e}_y \\ &= \frac{\partial G_2(kR)}{\partial(kR)}\frac{\partial(kR)}{\partial x_p}\hat{e}_x + \frac{\partial G_2(kR)}{\partial(kR)}\frac{\partial(kR)}{\partial y_p}\hat{e}_y \\ &= k\frac{\partial G_2(kR)}{\partial(kR)}\left[\frac{\partial R}{\partial x_p}\hat{e}_x + \frac{\partial R}{\partial y_p}\hat{e}_y\right] = k\frac{\partial G_2(kR)}{\partial(kR)}\nabla_p R\end{aligned} \tag{2.175}$$

If R is considered as a vector that directed from point p to point q then it can be written in vector form as

$$\vec{R} = \left\{ \left(x_q - x_p \right) \hat{e}_x + \left(y_q - y_p \right) \hat{e}_y \right\} \tag{2.176}$$

By taking into consideration this new form and the definition (2.155), then the equation (2.175) becomes

$$\nabla_p \left[G_2 \left(kR \right) \right] = k \frac{\partial G_2 \left(kR \right)}{\partial \left(kR \right)} \frac{\vec{R}}{R} \tag{2.177}$$

By substituting this equation and (2.154) into (2.173) one arrives at

$$\frac{\partial G_2 \left(kR \right)}{\partial n_p} = \frac{k}{4i} \frac{\partial H_0^{(2)} \left(kR \right)}{\partial \left(kR \right)} \frac{\vec{R} \cdot \hat{n}_p}{R} = \frac{ik^2}{4} \frac{1}{kR} H_1^{(2)} \left(kR \right) \vec{R} \cdot \hat{n}_p \tag{2.178}$$

with the well-known identity [26]

$$\frac{\partial H_0^{(2)} \left(z \right)}{\partial z} = -H_1^{(2)} \left(z \right) \tag{2.179}$$

Here $H_1^{(2)}(z)$ is the first order second kind Hankel function and has the form

$$H_1^{(2)} \left(z \right) = J_1 \left(z \right) - iY_1 \left(z \right) \tag{2.180}$$

where its parts are the first order Bessel and Neumann functions that have the expansions

$$J_1 \left(kR \right) = \frac{kR}{2} - \frac{\left(kR \right)^3}{16} + \frac{\left(kR \right)^5}{64} - \cdots \tag{2.181}$$

$$Y_1(kR)=\frac{2}{\pi}\left\{-\frac{1}{kR}+\left[\ln\left(\frac{kR}{2}\right)+\gamma\right]J_1(kR)-\frac{kR}{4}+\frac{5(kR)^3}{48}+\mathcal{O}\left((kR)^5\right)\right\} \quad (2.182)$$

and in terms of the Chebyshev polynomials $T_{2n+1}(\cdot)$ with known coefficients c_n up to 25 digits that are given in [52]

$$Y_1(kR)=\frac{2}{\pi}\left\{-\frac{1}{kR}+\left[\ln\left(\frac{kR}{2}\right)+\gamma\right]J_1(kR)\right\}+\sum_{n=0}^{\infty}c_n T_{2n+1}\left(\frac{kR}{8}\right) \quad (2.183)$$

By substituting these equations into (2.178) and using the equations (2.174) and (2.176)

$$\begin{aligned} K_Q &= \frac{ik^2}{4}\frac{H_1^{(2)}(kR)}{kR}\vec{R}\cdot\hat{n}_p \\ &= \frac{k^2}{2\pi}\left\{-\frac{1}{(kR)^2}+\left[\ln\left(\frac{kR}{2}\right)+\gamma+i\frac{\pi}{2}\right]\frac{J_1(kR)}{kR}-\frac{1}{4}+\frac{5(kR)^2}{48}+\mathcal{O}\left((kR)^4\right)\right\}\vec{R}\cdot\hat{n}_p \end{aligned} \quad (2.184)$$

is obtained. Even it seems that (2.184) has the logarithmic and $1/R^2$ singularities, because of the factor $\vec{R}\cdot\hat{n}$, it becomes finite but not infinitely smooth yet. This can be shown by investigating the limit cases $\delta\to 0$ for the terms $\vec{R}\cdot\hat{n}_p$ and R by using their expressions given above and the Taylor series given in (2.163) and (2.164). Let's start with $\vec{R}\cdot\hat{n}_p$.

$$\begin{aligned} \vec{R}\cdot\hat{n}_p &= \frac{\left[x(\theta)-x(\tau)\right]y'(\tau)-\left[y(\theta)-y(\tau)\right]x'(\tau)}{l(\tau)} \\ &= \frac{\left[x'(\theta)\delta+\frac{x''(\theta)}{2}\delta^2+\mathcal{O}\left(\delta^3\right)\right]y'(\tau)}{l(\tau)}- \\ &\quad \frac{\left[y'(\theta)\delta+\frac{y''(\theta)}{2}\delta^2+\mathcal{O}\left(\delta^3\right)\right]x'(\tau)}{l(\tau)} \\ &= \frac{1}{2}\left(\frac{x''(\tau)y'(\tau)-y''(\tau)x'(\tau)}{l(\tau)}\right)\delta^2+\mathcal{O}\left(\delta^3\right) \end{aligned} \quad (2.185)$$

If the Taylor series of the function R that is given by (2.165) is used then

$$\lim_{\delta\to 0}\frac{\vec{R}\cdot\hat{n}_p}{R^2}=\frac{1}{2}\left(\frac{x''y'-y''x'}{l}\right)\delta^2\frac{1}{l^2\delta^2}=\frac{1}{2}\left(\frac{x''y'-y''x'}{l^3}\right) \tag{2.186}$$

is obtained. Thus, this ratio has a limit and it is infinitely smooth. This brings a very important result from the point of the application of ARM. Because similar to done the kernel of (2.172), by adding and extracting the canonic function (2.170) properly then an infinitely smooth kernel for double layer potential can be constructed.

It is evident that all the steps performed for the kernel of (2.60) are valid for the kernel of (2.61)

$$K_{\partial_n P}=\frac{\partial G_2(kR)}{\partial n_q} \tag{2.187}$$

with very slight differences as $n_p \to n_q$ and $\nabla_p R=-\nabla_q R$.

But the situation is quite different for the kernel of (2.62) that has the form

$$K_{\partial_n Q}=\frac{\partial^2 G_2(kR)}{\partial n_q \partial n_p} \tag{2.188}$$

which also, can be written as

$$\begin{aligned}\frac{\partial^2 G_2(kR)}{\partial n_q\partial n_p}&=\hat{n}_q\cdot\nabla_q\left\{\left[\hat{n}_p\cdot\nabla_p G_2(kR)\right]\right\}\\&=\hat{n}_q\cdot\nabla_q\left\{\left[\hat{n}_p\cdot\left(\nabla_p R\right)\right]\frac{\partial G_2(kR)}{\partial R}\right\}\\&=\hat{n}_q\cdot\nabla_q\left\{\left[\hat{n}_p\cdot\left(-\hat{R}\right)\right]\frac{\partial G_2(kR)}{\partial R}\right\}\\&=\hat{n}_q\cdot\left\{\nabla_q\left[\hat{n}_p\cdot\left(-\hat{R}\right)\right]\frac{\partial G_2(kR)}{\partial R}+\left[\hat{n}_p\cdot\left(-\hat{R}\right)\right]\nabla_q\left[\frac{\partial G_2(kR)}{\partial R}\right]\right\}\end{aligned} \tag{2.189}$$

where $\hat{R}=\vec{R}/R$ is the normalized unit vector. For the Green's function in (2.154)

$$\frac{1}{4i}\frac{\partial^2 H_0^{(2)}(kR)}{\partial n_q \partial n_p} = \frac{1}{R^2}\left(\hat{n}_q \cdot \vec{R}\right)\left(\hat{n}_p \cdot \vec{R}\right)\frac{k^2}{4i}H_0^{(2)}(kR) - \left[\frac{2}{R^2}\left(\hat{n}_q \cdot \hat{R}\right)\left(\hat{n}_p \cdot \hat{R}\right) - \left(\hat{n}_q \cdot \hat{n}_p\right)\right]\frac{k^2}{4i}\frac{H_1^{(2)}(kR)}{kR} \tag{2.190}$$

is obtained with the help of the relation of the differential equation of Hankel function

$$\frac{d^2 H_0^{(2)}(z)}{dz^2} = -\frac{1}{z}\frac{dH_0^{(2)}(z)}{dz} - H_0^{(2)}(z);\ \frac{dH_0^{(2)}(z)}{dz} = -H_1^{(2)}(z) \tag{2.191}$$

The singularity properties of the functions $H_0^{(2)}(kR)$ and $H_1^{(2)}(kR)/kR$ are given in (2.159) and (2.184) respectively where $H_0^{(2)}(kR)$ has a logarithmic singularity and $H_1^{(2)}(kR)/kR$ has a singularity proportional to $1/R^2$ and a logarithmic singularity. However, in (2.190) these terms are multiplied by some factors as $\left(\hat{n}_q \cdot \hat{R}\right)\left(\hat{n}_p \cdot \hat{R}\right)$ and $\left(\hat{n}_q \cdot \hat{n}_p\right)$. That is why it is necessary to investigate the limit case of these factors for $\delta \to 0$ as well. By the help of the Taylor expansions (2.163)-(2.165) (similar to (2.185), (2.186)) one can obtain the limits easily as

$$\lim_{\substack{\delta\to 0\\ \theta\to\tau}}\left(\hat{n}_q \cdot \vec{R}\right) = \frac{1}{l(\theta)}\left\{\frac{1}{2}\delta^2 M^{1,2} + \frac{1}{6}\delta^3 M^{1,3} + \mathcal{O}\left(\delta^4\right)\right\} \tag{2.192}$$

$$\lim_{\substack{\delta\to 0\\ \theta\to\tau}}\left(\hat{n}_p \cdot \vec{R}\right) = -\frac{1}{l(\tau)}\left\{\frac{1}{2}\delta^2 M^{1,2} + \frac{1}{6}\delta^3 M^{1,3} + \mathcal{O}\left(\delta^4\right)\right\} \tag{2.193}$$

$$\lim_{\substack{\delta\to 0\\ \theta\to\tau}}\left(\frac{1}{R^2}\right) = \frac{1}{l(\theta)l(\tau)\delta^2}\left\{1 - a\delta + \mathcal{O}\left(\delta^2\right)\right\} \tag{2.194}$$

$$\lim_{\substack{\delta\to 0\\ \theta\to\tau}}\left(\hat{n}_q \cdot \hat{n}_q\right) = \frac{1}{l(\theta)l(\tau)}\left\{l(\theta)l(\tau) + \delta P^{1,2} + \frac{1}{2}\delta^2 P^{1,3} + \frac{1}{6}\delta^3 P^{1,4} + \mathcal{O}\left(\delta^4\right)\right\} \tag{2.195}$$

with the following definitions

$$M^{i,j} = x^{(i)}(\theta)y^{(j)}(\theta) - y^{(i)}(\theta)x^{(j)}(\theta)$$
$$P^{i,j} = x^{(i)}(\theta)x^{(j)}(\theta) - y^{(i)}(\theta)y^{(j)}(\theta) \tag{2.196}$$

Now let's instead of (2.190) consider the function

$$D(\theta,\tau) = 2\pi l(\theta)l(\tau)K_{\partial_n Q} = 2\pi l(\theta)l(\tau)\left[\frac{1}{4i}\frac{\partial^2 H_0^{(2)}(kR)}{\partial n_q \partial n_p}\right] \tag{2.197}$$

which results in a proper formula from the point of singularity extraction. By collecting the formulae (2.159), (2.183) and (2.190) yields

$$\begin{aligned}
D(\theta,\tau) = &-\frac{i\pi}{2}k^2 l(\theta)l(\tau)\left(\hat{n}_q\cdot\hat{R}\right)\left(\hat{n}_p\cdot\hat{R}\right)\\
&\left\{\left(J_0(kR)-\frac{2J_1(kR)}{kR}\right)\left(1-i\frac{2\gamma}{\pi}\right)-i\sum_{n=0}^{\infty}\left[b_n T_{2n}\left(\frac{kR}{8}\right)-\frac{2}{kR}\sum_{n=0}^{\infty}c_n T_{2n+1}\left(\frac{kR}{8}\right)\right]\right\}\\
&-\frac{i\pi}{2}k^2 l(\theta)l(\tau)\left(\hat{n}_q\cdot\hat{n}_p\right)\left\{\frac{J_1(kR)}{kR}\left(1-i\frac{2\gamma}{\pi}\right)-\frac{i}{kR}\sum_{n=0}^{\infty}c_n T_{2n+1}\left(\frac{kR}{8}\right)\right\}\\
&-k^2 l(\theta)l(\tau)\left(\hat{n}_q\cdot\hat{R}\right)\left(\hat{n}_p\cdot\hat{R}\right)\left(J_0(kR)-\frac{2J_1(kR)}{kR}\right)\ln\left(\frac{kR}{2}\right)\\
&-k^2 l(\theta)l(\tau)\left(\hat{n}_q\cdot\hat{n}_p\right)\frac{J_1(kR)}{kR}\ln\left(\frac{kR}{2}\right)\\
&-k^2 l(\theta)l(\tau)\frac{1}{(kR)^2}\left[2\left(\hat{n}_q\cdot\hat{R}\right)\left(\hat{n}_p\cdot\hat{R}\right)-\left(\hat{n}_q\cdot\hat{n}_p\right)\right]
\end{aligned} \tag{2.198}$$

If the expansion of the functions that are given in (2.156)-(2.158), (2.181)-(2.183) and the limit values (2.192)-(2.195) are considered carefully then it is evident that the parts in the first two rows are infinitely smooth, the third row is finite, the fourth row has logarithmic singularity and the last one has a singularity proportional $1/\delta^2$. It is known from above explanations that the logarithmic singularity can be extracted by means of the canonic function (2.170). Also, it is evident from the Taylor series of (2.168) that

$$\left[2\sin\left(\frac{\theta-\tau}{2}\right)\right]^{-2} \tag{2.199}$$

has the same singularity as $1/\delta^2$ when $\delta \to 0$. Moreover, the following relation is valid [50]

$$\left[2\sin\left(\frac{\theta-\tau}{2}\right)\right]^{-2} = -\frac{\partial^2}{\partial\theta^2}\ln\left|2\sin\left(\frac{\theta-\tau}{2}\right)\right| \tag{2.200}$$

The Fourier coefficients of the function (2.200) can be obtained quite simply by differentiating the Fourier series in (2.170) w.r.t. θ which results in another Fourier series as

$$-\frac{\partial^2}{\partial\theta^2}\left[-\frac{1}{2}\sum_{n=-\infty}^{\infty}\frac{e^{in(\theta-\tau)}}{|n|}\right] = \frac{1}{2}\sum_{n=-\infty}^{\infty}|n|e^{in(\theta-\tau)} \tag{2.201}$$

This formula explains the appearance of the part of the kernel that is shown in (2.85).

All of the explanations till know express that the canonic function (2.170) and its another form (2.200) whose Fourier coefficients are known analytically are quite proper functions to remove the logarithmic and $1/\delta^2$ singularities. Namely, extraction and addition of these functions results in infinitely smooth functions whose limits are finite for $\delta \to 0$. Some of these limits can be calculated quite simply from the above given formulae and explanations. But, some parts of the limit of the function $D(\theta,\tau)$ in (2.198) cannot be obtained from the information given here which is calculated in [50] and is going to be represented below.

After smoothing of the kernels with the help of the functions (2.170) and (2.200) the following limits that are necessary for numerical calculations are valid for $\delta \to 0$.

$$\lim_{\substack{\delta\to 0\\ \theta\to\tau}}\left[K_p + \frac{1}{2\pi}\ln\left(2\sin\left(\frac{\theta-\tau}{2}\right)\right)J_0(kR)\right] = \frac{1}{4i} - \frac{\gamma}{2\pi} + \ln\left(\frac{kl}{2}\right) \tag{2.202}$$

$$\lim_{\substack{\delta\to 0\\ \theta\to\tau}}\left[K_Q + \frac{1}{2\pi}\ln\left(2\sin\left(\frac{\theta-\tau}{2}\right)\right)\frac{J_1(kR)}{kR}\vec{R}\cdot\hat{n}_p\right] = \frac{1}{2\pi l(\tau)}\left[\frac{M^{1,2}}{2l^2}\right] \tag{2.203}$$

$$\lim_{\substack{\delta\to 0\\ \theta\to\tau}}\left[K_{\partial_n P}-\frac{1}{2\pi}\ln\left(2\sin\left(\frac{\theta-\tau}{2}\right)\right)\frac{J_1(kR)}{kR}\vec{R}\cdot\hat{n}_p\right]=-\frac{1}{2\pi l(\theta)}\left[\frac{M^{1,2}}{2l^2}\right] \tag{2.204}$$

$$\lim_{\substack{\delta\to 0\\ \theta\to\tau}}\left[\begin{array}{l} D(\theta,\tau)+\\ k^2 l(\theta)l(\tau)\left(\hat{n}_q\cdot\hat{n}_p\right)\frac{J_1(kR)}{kR}\ln\left(2\sin\left(\frac{\theta-\tau}{2}\right)\right)-\left[2\sin\left(\frac{\theta-\tau}{2}\right)\right]^{-2}\end{array}\right] \tag{2.205}$$
$$=-\frac{(kl)^2}{2}\left(\ln\left(\frac{kl}{2}\right)+\frac{i\pi}{4}+\frac{\gamma}{2\pi}-\frac{1}{4}\right)+\left(\frac{P^{1,3}}{6l^2}-\frac{P^{2,2}}{4l^2}+\frac{1}{2}\frac{M^{1,2}}{l^4}\right)-\frac{1}{12}$$

From the expressions (2.202)-(2.205) it is evident that corresponding to the any part which is seen as

$$\ln\left(\frac{kR}{2}\right)f(\theta,\tau) \tag{2.206}$$

in the kernels, a new part in the form

$$\ln\left(\left|2\sin\left(\frac{\theta-\tau}{2}\right)\right|\right)f(\theta,\tau) \tag{2.207}$$

is extracted (and of course, the same term is added which is not seen in the expressions). At this point, it is necessary to make some critics about the behavior of $f(\theta,\tau)$ corresponding to (2.202)-(2.205). In (2.202) $f(\theta,\tau)=J_0(kR)$ which equals one for zero argument. This means extracting only the term $\ln|2sin[(\theta-\tau)/2]|$ without the factor $f(\theta,\tau)$ constructs, again, infinitely smooth parts by removing the logarithmic singularity. Moreover, the situation is a bit different for the kernels K_Q and $K_{\partial_n P}$ which have not singularities because of the factors $\left(\hat{n}_q\cdot\hat{R}\right)$ and $\left(\hat{n}_p\cdot\hat{R}\right)$ that go to zero faster than the logarithm. However, as stated above, even these kernels are not singular, they are finite. Nevertheless, by subjecting the extraction operation as (2.203) and (2.204) constructs infinitely smooth parts.

By doing so in the kernels, yields the product

$$\ln\left(\frac{\left(\frac{kR}{2}\right)}{\left|2\sin\left(\frac{\theta-\tau}{2}\right)\right|}\right) f(\theta,\tau) \tag{2.208}$$

which consists of infinitely smooth factors. Substitution of the limit values (2.165) and (2.168) into (2.208) and considering the case $\delta \to 0$ results in

$$\ln\left(\frac{kl}{2}\right) \lim_{\delta\to 0} f(\theta,\tau) \tag{2.209}$$

and these limit values are seen in (2.202)-(2.205). In addition to this, making the extraction operations by keeping the factors $f(\theta,\tau)$ with logarithmic functions requires the use of the convolution operation that brings the possibility of constructing exponentially converging algorithms [55], [56].

In this subchapter, at first, some BVPs are constructed by means of the integral equations that are in form of single and double layer potentials and their derivatives. Then the singularity properties of the kernels of integral equations are investigated and then the smoothing operation and constructing exponentially converging algorithms by means of a canonic function is explained and the limit values are examined. In Chapters 3.3 and 3.4, all these theoretical details are investigated by means of the numerical examples for impedance cylinders and dielectric cylinders.

3. APPLICATION OF ARM TO DIFFERENT SYSTEMS OF CIRCULAR CYLINDERS

3.1. Application of ARM to the Algebraic System of Series Solution of Two Parallel Circular Impedance Cylinders

The geometrical structure of the considered problem is given in Figure 3.1.

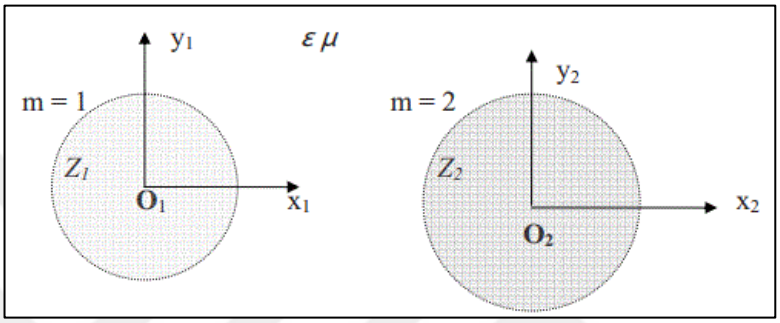

Figure 3.1: Geometrical structure of two parallel circular impedance cylinders.

The work of application of the ARM to two parallel circular impedance cylinders is published in [12] for $e^{-i\omega t}$ time dependency in comparison with the formulation that is given herein. In sense of formulation, it is just switching of $H_n^{(1)}(k\rho)$ to $H_n^{(2)}(k\rho)$ (and derivatives) in all formulas that are given in [12] and in numerical sense there is not qualitative difference. Here, the selected two-sided operator pair (L, R) that reduces the first kind system to a second kind one as $I + K$, the compactness of the operator K and the numerical results that are published in [12] which support the stability and reliability of new system are given once again. For more technical details the reader is referred to that publication.

Since the boundaries are modeled as impedance, then the inner fields of circles are null and there are just scattered fields. For TM-z case the z-component of the electric fields that are reflected from the boundaries are in form of (2.18) with unknown coefficients $R_n^{(1)}$ and $R_n^{(2)}$ and the relation of the tangential total electric and magnetic fields on the boundary with a surface impedance η_s is given as

$$E_z^{tot} = \eta_s H_\varphi^{tot} \tag{3.1}$$

where H_φ is as given in (2.24). If the boundary condition (3.1) is imposed on each boundary and the transformation of the local coordinates is achieved by the second row of the addition theorems in (2.23), then the following algebraic equation system is obtained.

$$\underbrace{\begin{bmatrix} \overline{H_n^{(2)}}(a) & \overline{J_{n,s}^{\{21\}}}(a) \\ \overline{J_{n,s}^{\{12\}}}(a) & \overline{H_n^{(2)}}(b) \end{bmatrix}}_{A} \underbrace{\begin{bmatrix} R_n^{(1)} \\ R_n^{(2)} \end{bmatrix}}_{x} = \underbrace{\begin{bmatrix} -T_n^{(0)}\overline{J_n}(a) \\ -T_n^{(0)}\overline{J_n}(b) \end{bmatrix}}_{b} \tag{3.2}$$

Here, all the entries of matrix A with top-line has the form

$$\overline{Z_n}(\rho_m) = Z_n(k_0\rho_m) - i\beta Z_n'(k_0\rho_m);\ m = 1,2 \tag{3.3}$$

where $Z_n(t)$ stands for $J_n(t)$ or $H_n^{(2)}(t)$, $\eta_0 = (\mu_0/\varepsilon_0)^{1/2}$ is free space intrinsic impedance and $\beta = \eta_s/\eta_0$. The off-diagonal elements with top-script $\{pq\}$ are interaction matrices similar to (2.42) and have the following form

$$\overline{Z_{n,s}^{\{pq\}}}(\rho_m) = \overline{Z_n}(\rho_m) \sum_{s=-\infty}^{\infty} e^{i(s-n)\theta_{pq}} H_{s-n}^{(2)}(k_0 d_{pq}) \tag{3.4}$$

As explained in Chapter 2.1, due to the bad behavior of the Bessel and Hankel functions, the system (3.2) is one of the first kind and it must be reduced to a second kind one by means of ARM algorithm. For this purpose, as a first step, according to the details given in Chapter 2.1, the right-side operator R^{-1} can be chosen as

$$R^{-1} = \begin{bmatrix} \left[\dfrac{1}{\overline{J_n}(a)}\right] & [0] \\ [0] & \left[\dfrac{1}{\overline{J_n}(b)}\right] \end{bmatrix} \tag{3.5}$$

where the functions with top-line are in form of (3.3). This choice, which is a combination of functions $J_n(t)$ and $J'_n(t)$ has the same asymptotic behavior as

possible choices of function $F_1(n)$ that are given in Table 2.1. In addition, it has another superiority to these choices because $J_n(t)$ and $J'_n(t)$ have not common root for arbitrary t which prevents division by zero.

Since the operator R^{-1} is identified as (3.5) now, the next step is to determine the left-side operator L as it yields a second kind system operator $I + K$. For the matrix operator A that is given in (3.2) and the diagonal operator R^{-1} in (3.5), the operator L^{-1} is obtained as

$$L^{-1} = \begin{bmatrix} \left[\dfrac{\overline{H_n^{(2)}}(a)}{\left(\overline{J_n}(a)\right)^{-1}}\right] & [0] \\ [0] & \left[\dfrac{\overline{H_n^{(2)}}(a)}{\left(\overline{J_n}(a)\right)^{-1}}\right] \end{bmatrix} \tag{3.6}$$

which yields a system in form of (2.17) with a compact, in space l_2, operator K as following.

$$K = \begin{bmatrix} [0] & K_1 \\ K_2 & [0] \end{bmatrix};\ K_1 = \left\{k_{ns}^{(1)}\right\}_{n,s=-\infty}^{\infty};\ K_2 = \left\{k_{ns}^{(2)}\right\}_{n,s=-\infty}^{\infty} \tag{3.7}$$

The compactness of the operator K can be shown easily by analyzing the entries $k_{ns}^{(1)}$ and $k_{ns}^{(2)}$ which have the following upper bounds for some real-valued constants $\Lambda_{1,2}$ of asymptotic analysis.

$$\begin{aligned} \left|k_{ns}^{(1)}\right| &< \Lambda_1 \times \left[\frac{(|n|+|s|)!}{|n-1|!|s-1|!}\right]\left(\frac{a}{d_{12}}\right)^{|n|}\left(\frac{b}{d_{12}}\right)^{|s|}; \\ \left|k_{ns}^{(2)}\right| &< \Lambda_2 \times \left[\frac{(|n|+|s|)!}{|n-1|!|s-1|!}\right]\left(\frac{b}{d_{21}}\right)^{|n|}\left(\frac{a}{d_{21}}\right)^{|s|} \end{aligned} \tag{3.8}$$

The equation (3.8) proves the compactness of the operator K for any $d_{pq} > a + b$ which is already satisfied for the configuration that is given in Figure 3.1.

If the operation LAR, with the above-given operators, is examined carefully it can be seen that the resultant identity operator has not exactly, but, asymptotically one on its diagonal. This is important if a spectral problem is under consideration and the roots of the determinant are searched. Because, when the diagonal becomes exactly one then the dependency to the frequency may be destroyed. Such an operator R and correspondent operator L is suggested in [12] and it is tested. In the sense of numerical results and the compactness of K it has the same qualitative properties as (3.5).

Let's now see, through the numerical results, the superiority of the obtained second kind system by the two-sided operator pair (L, R) that are given by (3.5) and (3.6) compared to the first kind system (3.2).

The following numerical results are given for the values of both surface impedances are equal $\eta_s = 100 + 100i$, the radius of the circles are $a = b = 1/k_0$ and the distance between two circles $d = 5/k_0$ where the center of both circles are posed on the *x*-axis. The incidence field is supposed as a TM-*z* polarized plane wave impinging on the circles with $\pi/2$ incidence angle.

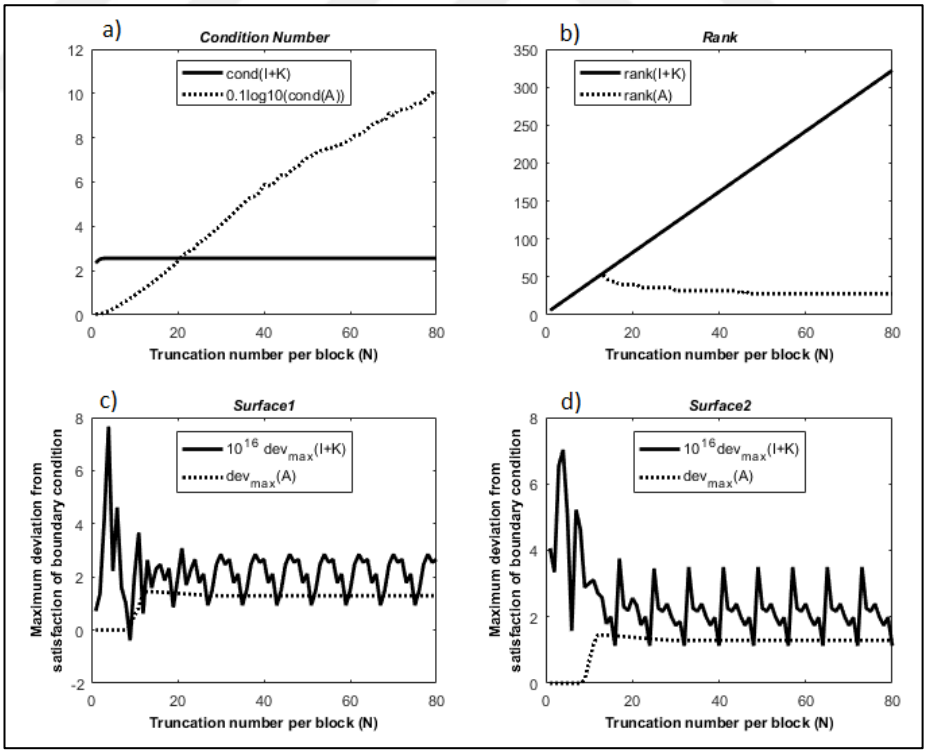

Figure 3.2: a) Condition number, b) Rank, c) On the boundary m=1, d) On the boundary m=2, maximum deviation from the satisfaction the boundary condition.

In Figure 3.2.a) and b), the condition number that is defined by (2.6), and the rank of both systems, i.e. before regularization and after regularization, are plotted. It is well known that a well-conditioned system has uniformly bounded condition number and its rank grows linearly with increasing truncation number. On the other side, the condition number of an ill-conditioned system grows dramatically, and it is rank-deficient while the truncation number increases. These facts are seen clearly from the plots. Here, the truncation number means for a value N the infinite series are truncated from $-N$ to N and thus the size of the algebraic system becomes $2(2N+1)$. In Figure 3.2.a), for a better view, the condition number of the first kind system is given in logarithmic scale and even scaled by a small factor.

In Figure 3.2.c) and d), the maximum deviation from the satisfaction of the boundary condition (3.1) on both boundaries is given. For a clear comparison, the values that are obtained from the solution of the second kind system are scaled by a very large value. These graphs show clearly that the solution of the first kind system is far from the satisfaction of the boundary condition which means the solution is not correct. On the other hand, the second kind system which is arrived at by the suggested regularization operation satisfy the boundary conditions perfectly with machine precision.

Figure 3.3.a) and b) shows the surface currents on both boundaries, m=1 and m=2, and Figure 3.3.c) shows the bistatic RCS of the scattered field from two circles for regularized and un-regularized systems. As seen from the graphs, the results that are obtained from the first kind and second kind systems are quite different as expected.

Notice that these results are not a validation but comparison of two systems. However, due to the facts that are shown in Figure 3.2 the regularized, i.e. second kind, system is reliable from the point of numerical results. Also, in [12] (in Figure 2) a verification of the bistatic RCS for several impedance values is made by a packaged program called as Ansoft HFSS.

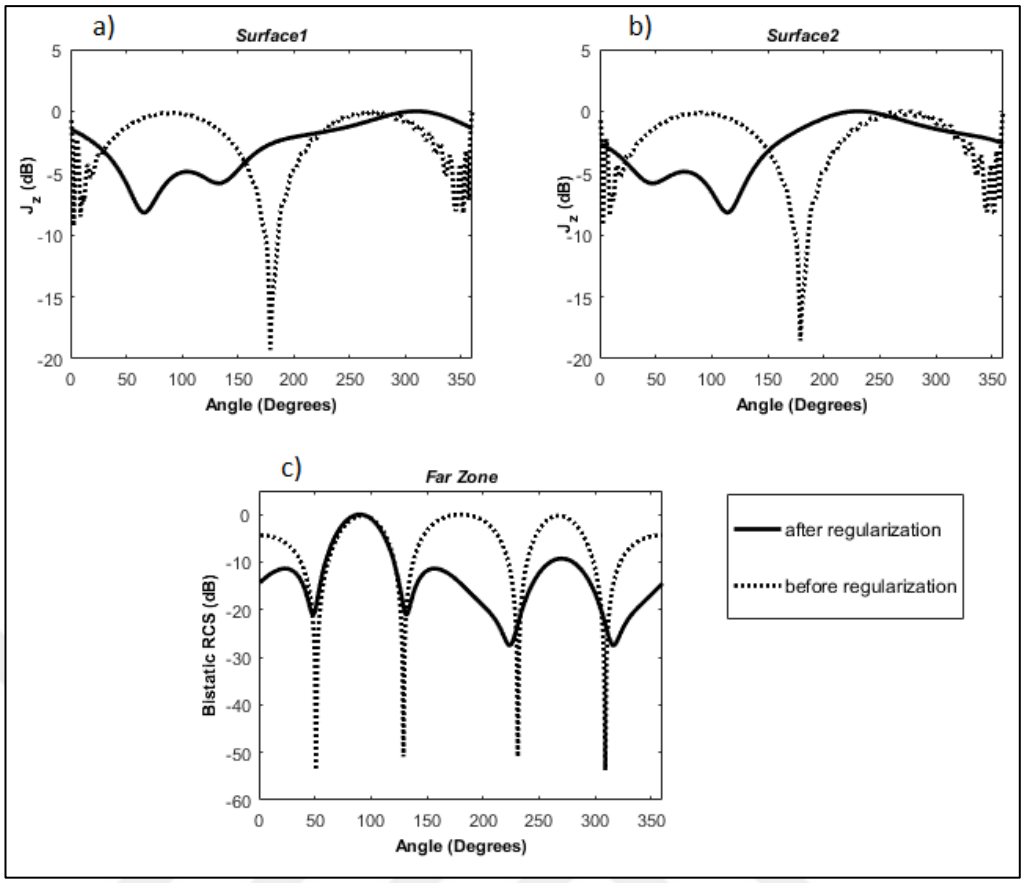

Figure 3.3: The values calculated at N=40; a) Surface currents on the boundary m=1, b) Surface currents on the boundary m=2, c) The bistatic RCS.

Now, it is clear that the LAES1, i.e. the algebraic system before regularization, is extremely ill-conditioned as shown Figure 3.2 by means of key indicators as the condition number and rank. In addition, in Figure 3.3 by means of physical quantities as surface current and RCS, the difference between two solutions is shown clearly. The calculations corresponding to these plots are performed in MATLAB environment by using the iterative solver "quasi-minimal residual" (qmr) method which is one of the many options of MATLAB. Because, even being extremely ill-conditioned and rank-deficient for N=40, the MATLAB's LU solver keeps working perfectly well for the system (3.2) contrary to the expectations. When the LU solver method of MATLAB has invoked, a warning about bad-conditioning of the matrix as "matrix is close to singular or badly scaled" is thrown and the value of reciprocal condition number (rcond) is displayed which is very close to zero. This means MATLAB is aware of the situation and makes something inside (might be the scaling of the matrix elements or implementing some preconditioning techniques) which masks the bad behavior of the LAES1. For the purpose of revealing the ill-conditioned behavior of

the LAES1, the solution of the system (3.2) is performed by an LU decomposition solver which is implemented in C++ with double precision (16 significant digits) and the maximum deviation from the satisfaction of the boundary condition is calculated. The results that are obtained for several truncation numbers on both surfaces are tabulated in Table 3.1. As seen from the values in the table, with increasing truncation number the boundary condition is far from being satisfied.

Table 3.1: Maximum deviation from the satisfaction of the boundary condition tested by an LU solver of mantissa length 10^{16} via the solution of the matrix A.

Truncation number per block (N)	Maximum deviation from satisfaction of the boundary condition	
	Surface 1	Surface 2
10	2.107708154721642e-08	2.110741476084647e-08
20	4.199639234666350e-02	2.110740774266010e-08
40	9.852222875038121e+11	2.110740707965443e-08
80	5.767939322592583e+39	1.592155168152142e+40
100	3.172408189417764e+64	5.632395455446972e+65

In this chapter, the numerical implementation of the suggested ARM algorithm for circular boundaries that is explained in Chapter 2.1 is applied to two parallel circular impedance scatterers and its achievement is shown in many aspects by means of illustrative numerical results.

3.2. Application of ARM to the Algebraic System of Series Solution of a Few Eccentrically Layered Circular Dielectric Cylinders

The considered configuration of the eccentrically layered dielectric circles is given in Figure 3.4.

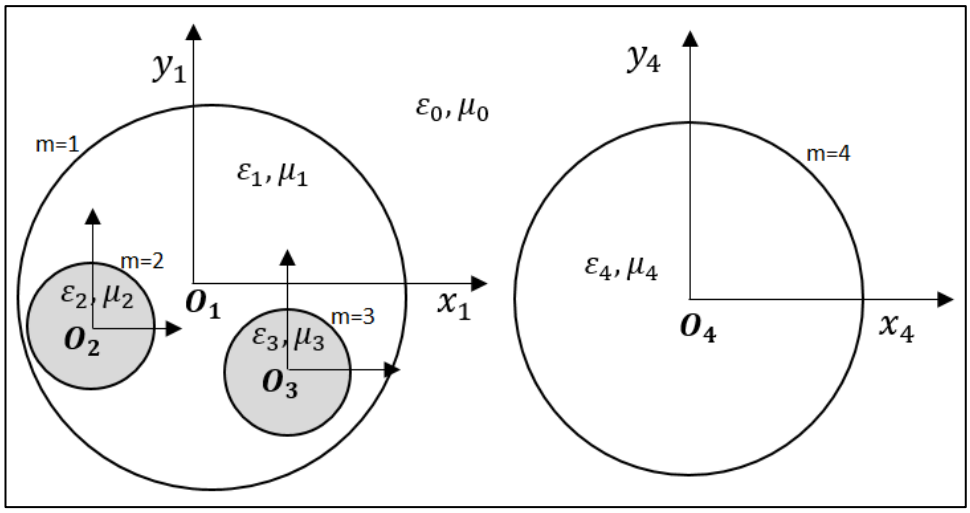

Figure 3.4: Geometrical structure of eccentrically layered dielectric circles.

This model can be used as a draft of power transmitter cables. That is why the analytical model of such a configuration has sense in real world. The ARM algorithm and remarkable numerical results that support the necessity of reducing the algebraic system to a second kind one for this configuration is published in [11]. Here, the algebraic system and the regularization operators are given for TM-z case and the same numerical results are repeated here once more.

Let us assume that a TM-z polarized incident plane wave that has the expression in form of (2.25) illuminates the system of the dielectric circles of Figure 3.4. If one applies the formulation steps, in a very similar manner, as in Chapter 2.1, then arrives at the following algebraic system $Ax = b$ which is a combination of the systems (2.41) and (2.44) similar to the representation that is given in form of (2.45).

$$\begin{bmatrix} [\Pi_1^0] & [\Upsilon_{2,1}^0] & [\Upsilon_{3,1}^0] & [\Upsilon_{4,1}^0] \\ [\Upsilon_{1,2}^1] & [\Pi_2^1] & [\Upsilon_{3,2}^1] & [0] \\ [\Upsilon_{1,3}^1] & [\Upsilon_{2,3}^1] & [\Pi_3^1] & [0] \\ [\Upsilon_{1,4}^0] & [0] & [0] & [\Pi_4^0] \end{bmatrix} \begin{bmatrix} [\xi_1] \\ [\xi_2] \\ [\xi_3] \\ [\xi_4] \end{bmatrix} = \begin{bmatrix} [\tau_1] \\ [\tau_2] \\ [\tau_3] \\ [\tau_4] \end{bmatrix} \tag{3.9}$$

In Chapter 2.1 it is explained mathematically for the general case, and in addition in Chapter 3.1 it is shown by numerical results of two parallel impedance cylinders, that such a system is one of the first kind and naturally ill-conditioned one for

numerical calculation since it is very much sensitive to the matrix inversion operations. Thus, it is clear that this system must be reduced to a second kind one for having a stable system and, as a result, reliable numerical results.

According to the given background in Chapter 2.1, the double-sided regulators for the system (3.9) are chosen as

$$R^{-1} = \begin{bmatrix} \left[\Gamma_1^0\right] & [0] & [0] & [0] \\ [0] & \left[\Gamma_2^1\right] & [0] & [0] \\ [0] & [0] & \left[\Gamma_3^1\right] & [0] \\ [0] & [0] & [0] & \left[\Gamma_4^0\right] \end{bmatrix} \tag{3.10}$$

where each block is in the form as $\Gamma_m^j = diag\left[H_n^{(1)}(k_j\rho_m),\ \left(H_n^{(1)}(k_m\rho_m)\right)^{-1}\right]$ and

$$L^{-1} = \begin{bmatrix} \left[\Lambda_1^0\right] & [0] & [0] & [0] \\ [0] & \left[\Lambda_2^1\right] & [0] & [0] \\ [0] & [0] & \left[\Lambda_3^1\right] & [0] \\ [0] & [0] & [0] & \left[\Lambda_4^0\right] \end{bmatrix} \tag{3.11}$$

with the form $\Lambda_m^j = diag\left[P_n^{(m,j)}(\rho_m)\left(H_n^{(1)}(k_j\rho_m)\right)^{-1},\ P_n^{(m,j)}(\rho_m)\left(H_n^{(1)}(k_m\rho_m)\right)\right]$.

After applying the regulators (3.10) and (3.11) to the system (3.9), then the second kind system $(I+K)y = Lb$ is obtained with the following compact operator

$$K = \begin{bmatrix} [0] & \left[K_{2,1}^0\right] & \left[K_{3,1}^0\right] & \left[K_{4,1}^0\right] \\ \left[K_{1,2}^1\right] & [0] & \left[K_{3,2}^1\right] & [0] \\ \left[K_{1,3}^1\right] & \left[K_{2,3}^1\right] & [0] & [0] \\ \left[K_{1,4}^0\right] & [0] & [0] & [0] \end{bmatrix} \tag{3.12}$$

The compactness of this operator, by means of (2.47)-(2.55), can be shown by the upper limits of its entries W, Q, T that are seen in (2.41) and (2.44) with the

interaction of the addition theorems as follows with some constants of asymptotic analysis $c_1, c_2 \ldots c_{10}$.

For the function $W_{n,s}^{mm\prime}$

$$\begin{aligned}
\left|k_{n,s}^{(W)12}\right| &< c_1\left[\frac{\left(|n|!+|s|!\right)}{|n|!|s|!}\right] \quad \left(\frac{b}{a}\right)^{|n|}\left(\frac{d_{12}}{a}\right)^{|s|};\\
\left|k_{n,s}^{(W)13}\right| &< c_2\left[\frac{\left(|n|!+|s|!\right)}{|n|!|s|!}\right] \quad \left(\frac{c}{a}\right)^{|n|}\left(\frac{d_{13}}{a}\right)^{|s|};\\
\left|k_{n,s}^{(W)14}\right| &< c_3\left[\frac{\left(|n|!+|s|!\right)}{|n|!|s|!}\right] \quad \left(\frac{a}{d_{14}}\right)^{|n|}\left(\frac{d}{d_{14}}\right)^{|s|};\\
\left|k_{n,s}^{(W)23}\right| &< c_4\left[\frac{\left(|n|!+|s|!\right)}{|n|!|s|!}\right] \quad \left(\frac{b}{d_{23}}\right)^{|n|}\left(\frac{c}{d_{23}}\right)^{|s|};
\end{aligned} \tag{3.13}$$

For the function $Q_{n,s}^{mm\prime}$

$$\begin{aligned}
\left|k_{n,s}^{(Q)12}\right| &< c_5\left[\frac{\left(|n|!+|s-1|!\right)}{|n|!|s|!}\right]\left(\frac{b}{a}\right)^{|n|}\left(\frac{d_{12}}{a}\right)^{|s|};\\
\left|k_{n,s}^{(Q)13}\right| &< c_6\left[\frac{\left(|n|!+|s-1|!\right)}{|n|!|s|!}\right]\left(\frac{b}{a}\right)^{|n|}\left(\frac{d_{13}}{a}\right)^{|s|};\\
\left|k_{n,s}^{(Q)14}\right| &< c_7\left[\frac{\left(|n|!+|s-1|!\right)}{|n|!|s|!}\right]\left(\frac{a}{d_{14}}\right)^{|n|}\left(\frac{d}{d_{14}}\right)^{|s|};\\
\left|k_{n,s}^{(Q)23}\right| &< c_8\left[\frac{\left(|n|!+|s-1|!\right)}{|n|!|s|!}\right]\left(\frac{b}{d_{23}}\right)^{|n|}\left(\frac{c}{d_{23}}\right)^{|s|};
\end{aligned} \tag{3.14}$$

For the function $T_{n,s}^{mm\prime}$

$$\begin{aligned}
\left|k_{n,s}^{(T)21}\right| &< c_9\left[\frac{\left(|n+1|!+|s|!\right)}{|n|!|s|!}\right]\left(\frac{b}{a}\right)^{|n|}\left(\frac{d_{21}}{a}\right)^{|s|};\\
\left|k_{n,s}^{(T)31}\right| &< c_{10}\left[\frac{\left(|n+1|!+|s|!\right)}{|n|!|s|!}\right]\left(\frac{b}{a}\right)^{|n|}\left(\frac{d_{31}}{a}\right)^{|s|};
\end{aligned} \tag{3.15}$$

Since the inequalities $d_{12}, d_{13} < a$, $d_{23} > b$, $d_{23} > c$, $d_{14} > a$, $d_{14} > d$ are already satisfied, then all the entries in (3.13)-(3.15) are uniformly bounded. That is why, it is

proved that the initial boundary value problem of a few eccentrically layered dielectric circular cylinders is equivalently reduced to one of the second kind successfully. Let's now see these facts by means of numerical results that are published in [11].

The numerical results are given for the values as $\varepsilon_{r1} = 4 + i\varepsilon'_{r1}$, $\varepsilon_{r2} = \varepsilon_{r3} = 16$ and $\varepsilon_{r4} = 4$ and $\mu_{rj} = 1$ for all regions and the imaginary part ε'_{r1} takes three different values as $0, 10, 100$. The center of the circles are posed as $O_m(k_0 x_m, k_0 y_m) = (0,0), (-1,0), (1.5,0), (6,0)$ and the radiuses are $k_0\rho_m = 2.5, 0.5, 0.5,$ and 2.5 for $m = 1, 2, 3, 4$ respectively.

For the configuration that is given in Figure 3.4 with above given parameters the comparison of LAES1 and LAES2 is shown in Figure 3.5.

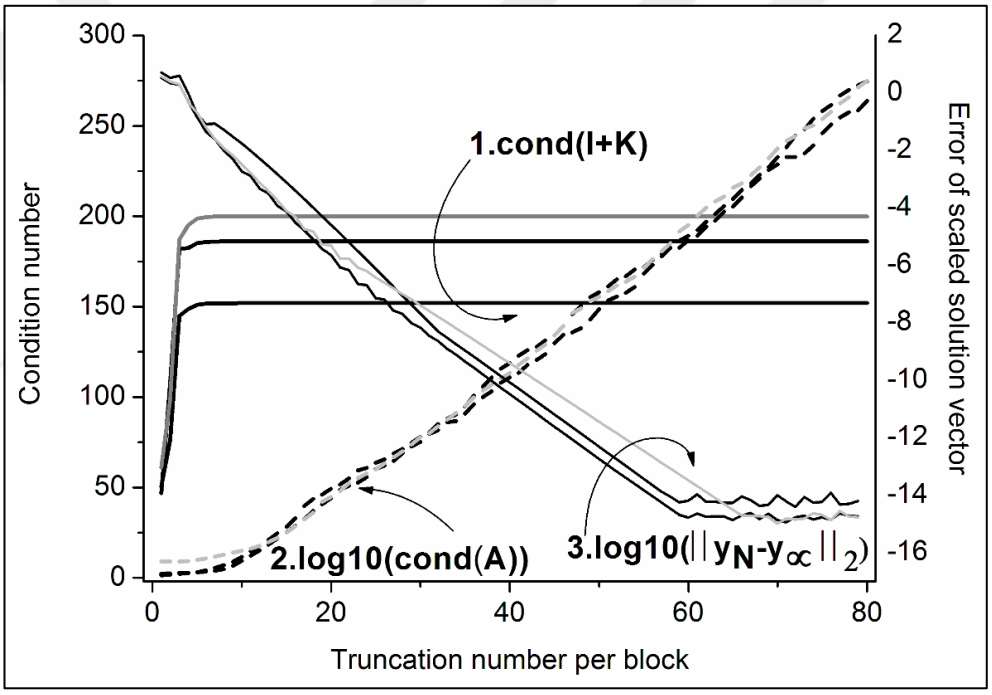

Figure 3.5: The condition numbers of the LAES1 and LAES2 and the absolute error of LAES2 for different values of imaginary part of the dielectric permittivity of the region *j*=1.

In Figure 3.5, the condition numbers of the LAES1 are shown in linear scale through the curves that are denoted by the number 1. The condition numbers of LAES2 are shown in logarithmic scale by the curves which are denoted by the number 2 and the absolute error of the solution of the LAES2 are shown, again in logarithmic scale, by the curves denoted by number 3 where in each curve group, the colors from lighter to darker are for the values of $\varepsilon'_{r1} = 0, 10, 100$ respectively. As seen from the figure,

the condition number, which is defined by (3.9), of the first kind system grows dramatically w.r.t. truncation number. On the other hand, the second kind system with compact operator (3.12), which is arrived by the operators (3.10) and (3.11), has extremely small and uniform condition numbers for increasing truncation number. In addition, the 3rd curve group shows the convergence of the LAES2 for increasing truncation number. In these curves, the solution of the LAES2 at $N = 80$ is taken as the solution of infinite system, i.e. $y_{80} = y_\infty$, and the norms $\|y_N - y_\infty\|_2$ are calculated for increasing N by padding $80 - N$ zeros to the vector y_N. These numerical result is consistent perfectly with the theoretically expected behavior of the second kind system that is given in Figure 2.1.

Another illustrative graphic that expresses the superiority of the LAES2 to LAES1 is shown in Figure 3.6. In this figure, the convergence of the systems and the maximum deviation from the satisfaction of the boundary condition on the boundary $m = 1$ is checked and the results are given in logarithmic scale.

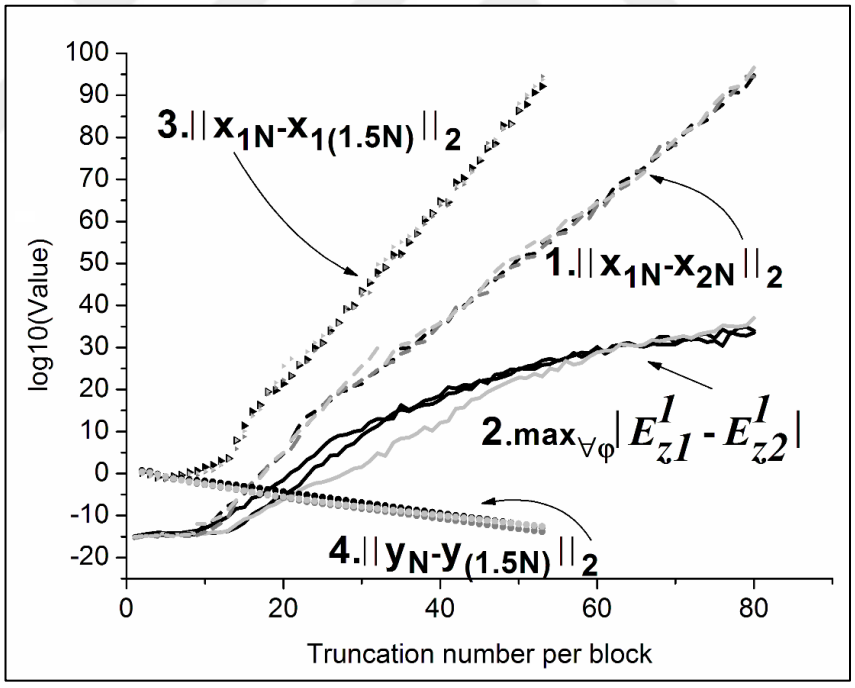

Figure 3.6: The change of the absolute errors with truncation number for (1) the solutions of LAES1 and LAES2, (2) the field at the two sides of the boundary, (3) the solutions of the LAES1 in itself, and (4) the solution of the LAES2 in itself.

Here, the curve group that is denoted by the number 1 shows the norm $\|x_{1N} - x_{2N}\|_2$ where x_{1N} is the solution of the LAES1 directly, and x_{2N} is obtained by the relation $x_{2N} = R_N y_N$ with the converging solution y_N which is displayed in Figure 3.5. The

values that are given in logarithmic scale shows the divergence of the solution of the LAES1 clearly.

The curve group in number 2, for the solution of the LAES1, shows the maximum deviation from the satisfaction of the boundary condition. For this purpose, the maximum value of the absolute differences of the tangential electric fields that are calculated at 36 equidistant polar angles on the boundary $m = 1$ is picked for each N. As seen clearly from the figure, the deviation gets bigger for increasing truncation number. These numerical results show the bad behavior of LAES1 from another aspect.

The curves in group number 3 and number 4 shows the absolute error between the two solutions for the truncation numbers N and $\lfloor 1.5N \rceil$ of the LAES1 and LAES2, respectively (here $\lfloor 1.5N \rceil$ means the nearest integer number to $1.5N$). Actually, to understand whether the solution of the truncated system LAES1 is convergent, it is a common practice to look at the absolute error of the solutions for N and $N + 1$, i.e. $\delta_N = |a_{N+1} - a_N|$ to see whether $\delta_N \to 0$ with increasing N (here a_N is the Nth entry to the solution vector x_{1N}). But, in the case considered here, this common practice can be misleading because of the dramatically growing behavior of the coefficients a_N. To avoid from such a circumstance, calculating $\delta_N = |a_{\kappa N} - a_N| (\kappa = 1.5 \sim 2)$ for the investigation of the convergence of the LAES1 gives the correct insight and is realized here. For the solution of the LAES2 similar to in Figure 3.5, the norm $\|y_N - y_{1.5N}\|_2$ converges to zero for increasing N. On the other hand, and as expected, for the solution of the LAES1 the result of $\|x_N - x_{1.5N}\|_2$ is divergent.

Figure 3.7.a)-d) displays the measure of the boundary conditions on each boundary m=1, 2, 3, and 4 respectively, for the solutions of LAES1 and LAES2. On each boundary, the boundary condition is tested at 60 equidistant polar angles for the tangential electric field E_z and tangential magnetic field H_φ and the maximum deviation is picked for each truncation number. It is clear from the numerical results that the fields calculated by the reflection and transmission coefficients which are obtained from the solution of LAES1 do not satisfy the boundary condition while N increases. On the contrary, the fields that are calculated by the solution of the LAES2 satisfy the boundary conditions at any truncation number.

It is worth to note that none of the behaviors of the numerical results given in Figure 3.5-3.7 change due to the variation of the value of the imaginary part ε'_{r1}.

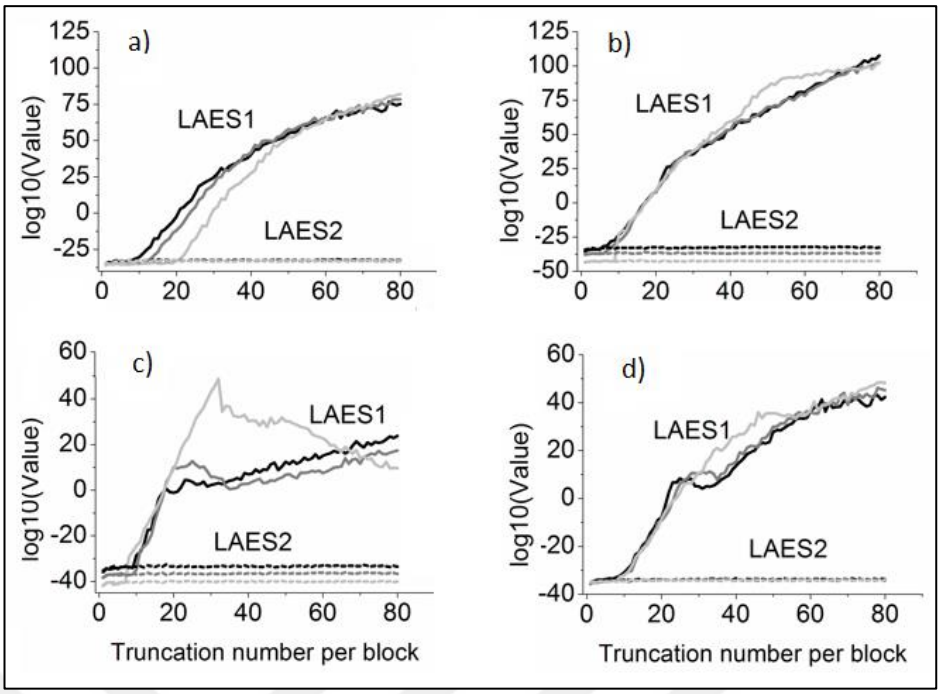

Figure 3.7: The absolute error between the tangential field; a) On the boundary m=1, b) On the boundary m=2, c) On the boundary m=3, d) On the boundary m=4.

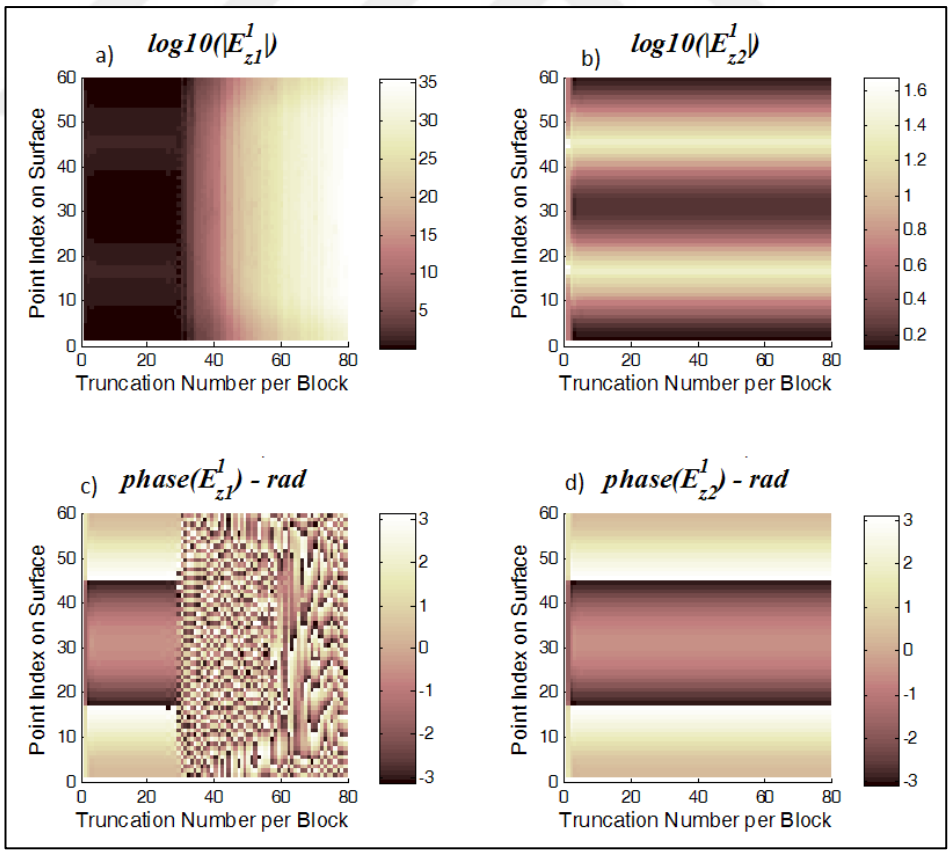

Figure 3.8: On the circular boundary m=1 for $\varepsilon'_{r1} = 4$; The modulus of electric field obtained from a) LAES1, b) LAES2; The phase of electric field obtained from c) LAES1, d) LAES2.

The disadvantage of using the solutions of LAES1 from a different perspective is shown in Figure 3.8. This is another view of the information which is given in Figure 3.6 by the curves in group number 2. Here, the 2-dimensional plots w.r.t. the truncation number (*x*-axis) and point index on the surface (*y*-axis) shows the modulus and the phase of the tangential electric field that is obtained from the LAES1 (E_{z1}^{1}) and LAES2 (E_{z2}^{1}) on the boundary m=1.

According to these figures, the check of the boundary condition is inevitable if the solution of LAES1 is used. In addition, this check is necessary for each different values of ε'_{r1}. However, it is clearly seen from all those plots such a control is not required if the system that is reduced to a second kind one by the ARM is considered.

3.3. Application of ARM to the Algebraic System of Integral Equation of Circular Dielectric Cylinders

This chapter is devoted to the implementation of the theoretical information that is given in Chapter 2.2.4 of the ARM for the boundary integral equation of dielectric BVP. The kernels of the boundary integral equations are split into parts as infinitely smooth and singular. Then the singular parts are subjected to a smoothing operation by means of the canonic function (2.170) which has the same singularity behavior of the kernels as explained in Chapter 2.2.5. This smoothing operation results in a kernel that consists of infinitely smooth parts and the Fourier coefficients of these parts can be calculated quite efficiently by means of the Fast Fourier Transform (FFT), which is the exact implementation of the Discrete Fourier Transform (DFT) for complex exponentials.

The considered geometrical structure of dielectric boundaries is given in Figure 3.9 as nested in a) and parallel in b). Even if the circular boundaries are under consideration, the construction of the algorithm is for the general case of arbitrarily shaped obstacles whose boundary satisfy some certain conditions.

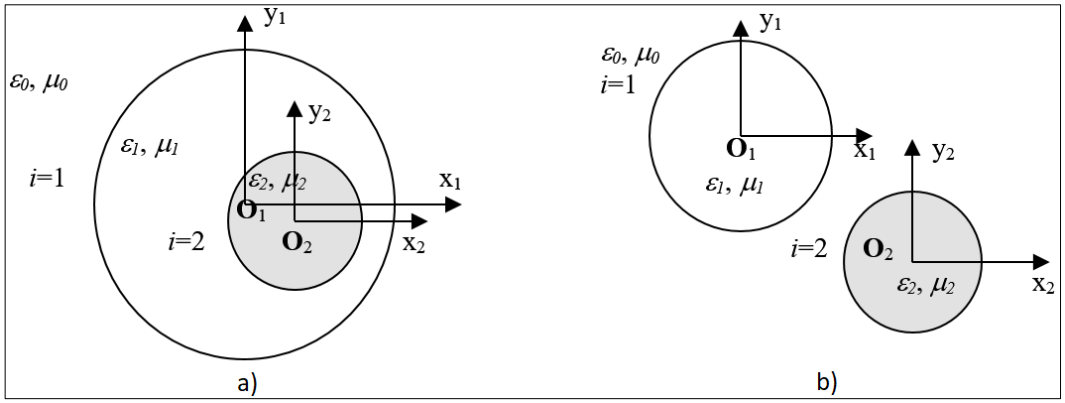

Figure 3.9: The considered circular dielectric boundaries: a) Inclusion, b) Neighbor.

The algorithm and the numerical results that are going to be given here are a repetition of the publication [19]. Here, the integral equations and the formulation are given explicitly which are given in a compact form in that publication. However, most of the explanation is not repeated here for the sake of brevity. For this purpose, the reader is referred to the publication.

The integral equations regarding to the multiple dielectric boundaries that are considered here are obtained by means of the equivalence principle by generalizing the boundary integral equations which are given for a single dielectric boundary in Chapter 3 of [17]. Therein, the field formulation [22] is used which results in, naturally, four equations for two unknown surface currents where two of them are the EFIE and the other two are the MFIE. The corresponding unknowns are the vector electric surface current $\vec{K}$ and the vector magnetic surface current $\overrightarrow{K_m}$ that, for infinitely long cylinders along the O_z axis, have the expressions

$$\vec{K} = K_z \hat{z} + K_l \hat{l};\ \vec{K}_m = K_{mz} \hat{z} + K_{ml} \hat{l} \tag{3.16}$$

where $\hat{z}$ and $\hat{l}$ denotes the tangential unit vectors and K_z/K_{mz} and K_l/K_{ml} are the corresponding components. The relations of these surface currents with the total surface electric fields $\vec{E}$ and magnetic field $\vec{H}$ are

$$\vec{K} = \hat{n} \times \vec{H};\ \vec{K}_m = -\hat{n} \times \vec{E} \tag{3.17}$$

where $\hat{n}$ is the outward unit normal vector.

In the formulation that is given here, the unknown surface currents $\vec{K}_i$ and $\vec{K}_{mi}$ are put on each boundary where i denotes the related boundary and the integral equations are obtained in terms of these unknowns for TM-*z* and TE-*z* polarization. For TM-*z* polarization, which is the case that all the fields can be represented in terms of the *z*-component of the electric field, the relation between tangential fields, for infinitely long cylinder along the *z*-axis, are

$$E_l = H_z = 0;\ H_l = \frac{1}{i\omega\mu}\frac{\partial E_z}{\partial n} \tag{3.18}$$

and the relation between the total tangential fields and the surface currents that are obtained by substituting the (3.16) into (3.17) and using the relations (3.18) are obtained as

$$K_{mz} = K_l = 0;\ K_{ml} = E_z;\ K_z = H_l \tag{3.19}$$

On the other hand, for TE-*z* polarization, which is the case that all the fields can be represented in terms of the *z*-component of the magnetic field, the relation between tangential fields are

$$H_l = E_z = 0;\ E_l = -\frac{1}{i\omega\varepsilon}\frac{\partial H_z}{\partial n} \tag{3.20}$$

and similar to (3.19) the relations of the surface currents and the total tangential fields are obtained as

$$K_z = K_{ml} = 0;\ K_l = -H_z;\ K_{mz} = -E_l \tag{3.21}$$

Now, it is evident from (3.19) and (3.21) that in the case of TM-*z* polarization the unknowns are K_{ml} and K_z but for TE-*z* polarization K_l and K_{mz} are the related unknowns that have to be found.

After applying the equivalence principle, similar to done in [17] for a single boundary, and putting the unknowns $\vec{K}_1$ and $\vec{K}_{m1}$ on the boundary C_1 and $\vec{K}_2$ and $\vec{K}_{m2}$

on the boundary C_2 then the following integral equations regarding to the outer vicinity and the inner vicinity of each boundary (for $e^{i\omega t}$ time dependency) are obtained.

EFIE system for the configuration Figure 3.9.a) for TM-z polarization are obtained on the related boundaries (where the superscript $(\pm)$ means the outer and inner side of the boundary, respectively) as

$$\begin{aligned}&\frac{1}{2}K_{m1l}(q)+i\omega\mu_0\int_{C_1}K_{1z}(p)G_2\left(k_0R_{qp}\right)dl_p\\&-\int_{C_1}K_{m1l}(p)\frac{\partial G_2\left(k_0R_{qp}\right)}{\partial n_p}dl_p=E_z^{inc}(q);\ q\in C_1^+\end{aligned}\tag{3.22}$$

$$\begin{aligned}&-\frac{1}{2}K_{m1l}(q)+i\omega\mu_1\left[\int_{C_1}K_{1z}(p)G_2\left(k_1R_{qp}\right)dl_p+\int_{C_2}K_{2z}(p)G_2\left(k_1R_{qp}\right)dl_p\right]\\&-\left[\int_{C_1}K_{m1l}(p)\frac{\partial G_2\left(k_1R_{qp}\right)}{\partial n_p}dl_p+\int_{C_2}K_{m2l}(p)\frac{\partial G_2\left(k_1R_{qp}\right)}{\partial n_p}dl_p\right]=0;\ q\in C_1^-\end{aligned}\tag{3.23}$$

$$\begin{aligned}&\frac{1}{2}K_{m2l}(q)+i\omega\mu_1\left[\int_{C_1}K_{1z}(p)G_2\left(k_1R_{qp}\right)dl_p+\int_{C_2}K_{2z}(p)G_2\left(k_1R_{qp}\right)dl_p\right]\\&-\left[\int_{C_1}K_{m1l}(p)\frac{\partial G_2\left(k_1R_{qp}\right)}{\partial n_p}dl_p+\int_{C_2}K_{m2l}(p)\frac{\partial G_2\left(k_1R_{qp}\right)}{\partial n_p}dl_p\right]=0;\ q\in C_2^+\end{aligned}\tag{3.24}$$

$$\begin{aligned}&-\frac{1}{2}K_{m2l}(q)+i\omega\mu_2\int_{C_2}K_{2z}(p)G_2\left(k_2R_{qp}\right)dl_p\\&-\int_{C_2}K_{m2l}(p)\frac{\partial G_2\left(k_2R_{qp}\right)}{\partial n_p}dl_p=E_z^{inc}(q);\ q\in C_2^-\end{aligned}\tag{3.25}$$

As seen the from the EFIE set (3.22)-(3.25), there are four unknowns and four equations, so the unknowns can be calculated by solving this system of equations. These equations are in the same structure of (2.144) and (2.145) which are given for a single dielectric boundary in terms of the total fields on the boundary. But it is evident

that by means of the relations (3.18) and (3.19) one can be transformed to each other quite simply by considering the definitions (2.59) and (2.60).

In the same manner, the MFIE system that has the same unknowns is obtained on the related boundaries as

$$\begin{aligned}&\frac{1}{2}K_{1z}(q)+\int_{C_1}K_{1z}(p)\frac{\partial G_2\left(k_0R_{qp}\right)}{\partial n_q}dl_p\\&-\frac{1}{i\omega\mu_0}\int_{C_1}K_{m1l}(p)\frac{\partial^2 G_2\left(k_0R_{qp}\right)}{\partial n_q\partial n_p}dl_p=H_l^{inc}(q);\ \ q\in C_1^+\end{aligned}\tag{3.26}$$

$$\begin{aligned}&-\frac{1}{2}K_{1z}(q)+\left[\int_{C_1}K_{1z}(p)\frac{\partial G_2\left(k_1R_{qp}\right)}{\partial n_q}dl_p+\int_{C_2}K_{2z}(p)\frac{\partial G_2\left(k_1R_{qp}\right)}{\partial n_q}dl_p\right]\\&-\frac{1}{i\omega\mu_1}\left[\int_{C_1}K_{m1l}(p)\frac{\partial^2 G_2\left(k_1R_{qp}\right)}{\partial n_q\partial n_p}dl_p+\int_{C_2}K_{m2l}(p)\frac{\partial^2 G_2\left(k_1R_{qp}\right)}{\partial n_q\partial n_p}dl_p\right]=0;\\&\qquad\qquad q\in C_1^-\end{aligned}\tag{3.27}$$

$$\begin{aligned}&\frac{1}{2}K_{1z}(q)+\left[\int_{C_1}K_{1z}(p)\frac{\partial G_2\left(k_1R_{qp}\right)}{\partial n_q}dl_p+\int_{C_2}K_{2z}(p)\frac{\partial G_2\left(k_1R_{qp}\right)}{\partial n_q}dl_p\right]\\&-\frac{1}{i\omega\mu_1}\left[\int_{C_1}K_{m1l}(p)\frac{\partial^2 G_2\left(k_1R_{qp}\right)}{\partial n_q\partial n_p}dl_p+\int_{C_2}K_{m2l}(p)\frac{\partial^2 G_2\left(k_1R_{qp}\right)}{\partial n_q\partial n_p}dl_p\right]=0;\\&\qquad\qquad q\in C_2^+\end{aligned}\tag{3.28}$$

$$\begin{aligned}&-\frac{1}{2}K_{2z}(q)+\int_{C_1}K_{2z}(p)\frac{\partial G_2\left(k_2R_{qp}\right)}{\partial n_q}dl_p\\&-\frac{1}{i\omega\mu_2}\int_{C_1}K_{m2l}(p)\frac{\partial^2 G_2\left(k_2R_{qp}\right)}{\partial n_q\partial n_p}dl_p=0;\ \ q\in C_2^-\end{aligned}\tag{3.29}$$

Similar to the EFIE system, the MFIE system has four unknowns that are the same as the unknowns of EFIE and four equations (3.26)-(3.29) that are enough to solve the system. These equations are in the same form of (2.146) and (2.147), and by

means of the relations (3.18) and (3.19) one can be transformed to the other one by considering the definitions (2.61) and (2.62).

Since both equation systems, i.e. EFIE and MFIE, have the same unknowns but completely different kernels, the solution of one can be compared to the other. In numerical results, this comparison is done in addition to the comparison by the rigorous solution of the SoV which is obtained by means of the stable algorithm that is suggested in the former chapters for circular boundaries.

For TE-*z* polarization case the integral equations of the configuration Figure 3.9.a) can be obtained simply by considering the relations (3.20), (3.21) instead of (3.18), (3.19) and (2.146), (2.147) instead of (2.144), (2.145) and thus the potentials (2.61) and (2.62) with the properties (2.66) and (2.68) respectively.

Let's now obtain the integral equations for the configuration b) but now for the case of the TE-*z* polarization. Again, similar to done in [17] for a single dielectric boundary, the following integral equations are obtained for two parallel boundaries that are given in Figure 3.9.b).

EFIE system:

$$-\frac{1}{2}K_{m1z}(q)-\left[\int_{C_1}K_{m1z}(p)\frac{\partial G_2\left(k_0R_{qp}\right)}{\partial n_q}dl_p+\int_{C_2}K_{m2z}(p)\frac{\partial G_2\left(k_0R_{qp}\right)}{\partial n_q}dl_p\right]$$
$$-\frac{1}{i\omega\varepsilon_0}\left[\int_{C_1}K_{1l}(p)\frac{\partial^2 G_2\left(k_0R_{qp}\right)}{\partial n_q\partial n_p}dl_p+\int_{C_2}K_{2l}(p)\frac{\partial^2 G_2\left(k_0R_{qp}\right)}{\partial n_q\partial n_p}dl_p\right]=E_l^{inc}(q);\quad q\in C_1^+ \tag{3.30}$$

$$\frac{1}{2}K_{m1z}(q)+\int_{C_1}K_{m1z}(p)\frac{\partial G_2\left(k_1R_{qp}\right)}{\partial n_q}dl_p$$
$$-\frac{1}{i\omega\varepsilon_1}\int_{C_1}K_{1l}(p)\frac{\partial^2 G_2\left(k_1R_{qp}\right)}{\partial n_q\partial n_p}dl_p=0;\quad q\in C_1^- \tag{3.31}$$

$$-\frac{1}{2}K_{m2z}(q)-\left[\int_{C_1}K_{m1z}(p)\frac{\partial G_2\left(k_0R_{qp}\right)}{\partial n_q}dl_p+\int_{C_2}K_{m2z}(p)\frac{\partial G_2\left(k_0R_{qp}\right)}{\partial n_q}dl_p\right]$$
$$-\frac{1}{i\omega\varepsilon_0}\left[\int_{C_1}K_{1l}(p)\frac{\partial^2 G_2\left(k_0R_{qp}\right)}{\partial n_q\partial n_p}dl_p+\int_{C_2}K_{2l}(p)\frac{\partial^2 G_2\left(k_0R_{qp}\right)}{\partial n_q\partial n_p}dl_p\right]=E_l^{inc}(q);\quad (3.32)$$
$$q\in C_2^+$$

$$\frac{1}{2}K_{m2z}(q)+\int_{C_1}K_{m2z}(p)\frac{\partial G_2\left(k_2R_{qp}\right)}{\partial n_q}dl_p$$
$$-\frac{1}{i\omega\varepsilon_2}\int_{C_1}K_{2l}(p)\frac{\partial^2 G_2\left(k_2R_{qp}\right)}{\partial n_q\partial n_p}dl_p=0;\quad q\in C_2^- \quad (3.33)$$

MFIE system:

$$-\frac{1}{2}K_{1l}(q)+i\omega\varepsilon_0\left[\int_{C_1}K_{m1z}(p)G_2\left(k_0R_{qp}\right)dl_p+\int_{C_2}K_{m2z}(p)G_2\left(k_0R_{qp}\right)dl_p\right]$$
$$+\left[\int_{C_1}K_{1l}(p)\frac{\partial G_2\left(k_0R_{qp}\right)}{\partial n_p}dl_p+\int_{C_2}K_{2l}(p)\frac{\partial G_2\left(k_0R_{qp}\right)}{\partial n_p}dl_p\right]=H_z^{inc}(q);\quad q\in C_1^+ \quad (3.34)$$

$$\frac{1}{2}K_{1l}(q)+i\omega\varepsilon_1\int_{C_1}K_{m1z}(p)G_2\left(k_1R_{qp}\right)dl_p$$
$$+\int_{C_1}K_{1l}(p)\frac{\partial G_2\left(k_1R_{qp}\right)}{\partial n_p}dl_p=0;\quad q\in C_1^- \quad (3.35)$$

$$-\frac{1}{2}K_{2l}(q)+i\omega\varepsilon_0\left[\int_{C_1}K_{m1z}(p)G_2\left(k_0R_{qp}\right)dl_p+\int_{C_2}K_{m2z}(p)G_2\left(k_0R_{qp}\right)dl_p\right]$$
$$+\left[\int_{C_1}K_{1l}(p)\frac{\partial G_2\left(k_0R_{qp}\right)}{\partial n_p}dl_p+\int_{C_2}K_{2l}(p)\frac{\partial G_2\left(k_0R_{qp}\right)}{\partial n_p}dl_p\right]=H_z^{inc}(q);\quad (3.36)$$
$$q\in C_2^+$$

$$\frac{1}{2}K_{2l}(q)+i\omega\varepsilon_2\int_{C_2}K_{m2z}(p)G_2\left(k_2R_{qp}\right)dl_p$$
$$+\int_{C_2}K_{2l}(p)\frac{\partial G_2\left(k_2R_{qp}\right)}{\partial n_p}dl_p=0;\ q\in C_2^- \tag{3.37}$$

Analogously, there are two systems, i.e. EFIE and MFIE, with same unknowns but with different kernels. Thus, the solutions can be compared to each other. This comparison is done in numerical results. The similarity of these equations with the equations (2.144)-(2.147) is clear similar to the others as explained above.

Now let us consider these equations from the point of ARM algorithm. The first step of the algorithm is making the parametrization of the boundary by means of the smooth vector function $\eta(\theta)=\left(x(\theta),y(\theta)\right)$ that has the property (2.69) that ensures the periodicity of all functions where θ is uniformly sampled in the interval $(-\pi,\pi]$. After the parametrization of the contour, the integral expressions that are in form of the potentials (2.59)-(2.62) with the kernels (2.159), (2.184), (2.187), (2.198) for an unknown denoted as $\zeta(\tau)$ seem as

$$\int_{-\pi}^{\pi}\zeta(\tau)\left\{\tilde{K}_P(\theta,\tau)-\frac{1}{2\pi}\ln\left|2\sin\left(\frac{\theta-\tau}{2}\right)\right|J_0(kR)\right\}l(\tau)\,d\tau \tag{3.38}$$

$$\int_{-\pi}^{\pi}\zeta(\tau)\left\{\tilde{K}_Q(\theta,\tau)+\frac{k^2}{2\pi}\ln\left|2\sin\left(\frac{\theta-\tau}{2}\right)\right|\frac{J_1(kR)}{kR}\vec{R}\cdot\hat{n}_p\right\}l(\tau)\,d\tau \tag{3.39}$$

$$\int_{-\pi}^{\pi}\zeta(\tau)\left\{\tilde{K}_{\partial_n P}(\theta,\tau)-\frac{k^2}{2\pi}\ln\left|2\sin\left(\frac{\theta-\tau}{2}\right)\right|\frac{J_1(kR)}{kR}\vec{R}\cdot\hat{n}_q\right\}l(\tau)\,d\tau \tag{3.40}$$

$$\int_{-\pi}^{\pi}\zeta(\tau)\left\{\begin{array}{l}\tilde{K}_{\partial_n Q}(\theta,\tau)-\frac{k^2}{2\pi}\ln\left|2\sin\left(\frac{\theta-\tau}{2}\right)\right|\left(\hat{n}_q\cdot\hat{n}_p\right)\frac{J_1(kR)}{kR}+\\ \frac{1}{2\pi l(\theta)l(\tau)}\left[2\sin\left(\frac{\theta-\tau}{2}\right)\right]^{-2}\end{array}\right\}l(\tau)\,d\tau \tag{3.41}$$

where the notation of a function as $f(\theta)$ means the value at the observation point $q(\theta) = \{x(\theta), y(\theta)\}$ and in similar manner the notation $f(\tau)$ means the value of the function at the integration point $p(\tau) = \{x(\tau), y(\tau)\}$ and $l(\tau)d\tau$ is the differential arc-length.

All of the functions in (3.38)-(3.41) that are denoted by tilde are infinitely smooth functions. They are obtained by extracting the canonic singularities of the kernels $P, Q, \partial_n P$ and $\partial_n Q$ where the remainder parts are the additions corresponding to the extracted parts. These parts consist of infinitely smooth functions multiplied by singular functions whose Fourier coefficients are known analytically. Construction of the kernels as splitting them into additive and multiplicative smooth and singular parts gives a very important chance to overcome the singularity of the kernels. The discretization of the integrals is achieved via the Galerkin method where the base functions are complex exponentials and all the related functions are expanded into one- or two-dimensional Fourier series. The Fourier spectrum of infinitely smooth functions can be calculated efficiently by the DFT which is well-known as Gauss quadrature for trigonometric polynomials and its error tends to zero super-algebraically for infinitely smooth functions. That is why, the FFT routine can be employed to calculate the Fourier coefficients of infinitely smooth functions. But for singular parts, of course, it is not possible to obtain the Fourier spectrum and not efficiently. But, as explained before, the used canonic functions have analytically known Fourier spectrums as (2.171) and (2.201). Thus, one- or two-dimensional FFT is employed to calculate the Fourier spectrum of infinitely smooth functions and then the convolution theorem is applied between the Fourier coefficients of the singular functions and their factors. The application of the convolution theorem in such a manner brings a fast converging algorithm [55], [56].

After expressing all the functions into Fourier series, and then through the orthogonality of the complex exponentials the integral equations are reduced to algebraic equation system [5], [24], [54] and the numerical implementation is done by a truncation procedure. For the truncation number denoted by N, each block has Fourier indices form $-N+1$ to N where $(-N)^{\text{th}}$ term is excluded because of the periodicity of Fourier coefficients. After applying such truncation procedure, the Fourier spectrum of each potential that are given by (3.38)-(3.41)seems as

$$2\pi\left[\left[k_{n,-s}^{(\tilde{P})}\right]_{2N\times 2N}+\left(\left[diag\left\{\tau_n\right\}\right]_{n=-N+1}^{N}\right)*\left[j_{n,-s}^{(0)}\right]_{2N\times 2N}\right]\left[z_n\right]_{2N\times 1} \tag{3.42}$$

$$\left[2\pi\left[k_{n,-s}^{(\tilde{Q})}\right]_{2N\times 2N}+k^2\left(\left[diag\left\{\tau_n\right\}\right]_{n=-N+1}^{N}\right)*\left[j'^{(1)}_{n,-s}\right]_{2N\times 2N}\right]\left[z_n\right]_{2N\times 1} \tag{3.43}$$

$$\left[2\pi\left[k_{n,-s}^{(\partial_n\tilde{P})}\right]_{2N\times 2N}-k^2\left(\left[diag\left\{\tau_n\right\}\right]_{n=-N+1}^{N}\right)*\left[j_{n,-s}^{(1)}\right]_{2N\times 2N}\right]\left[z_n\right]_{2N\times 1} \tag{3.44}$$

$$\tilde{k}_{n,-s}^{(D)}-k^2\left[diag\left\{\tau_n\right\}\right]_{n=-N+1}^{N}*\left[\tilde{j}_{n,-s}^{(1)}\right]_{2N\times 2N}+\left[diag\left\{\frac{1}{\tau_n}\right\}\right]_{n=-N+1}^{N} \tag{3.45}$$

with the fact that

$$\int_{-\pi}^{\pi}e^{i(n+s)\tau}=2\pi\delta_{n,-s};\ \delta_{n,-s}=\begin{cases}1, & n=-s\\ 0, & n\neq -s\end{cases} \tag{3.46}$$

and the corresponding definition of truncated Fourier series expansions

$$\zeta(\tau)=\sum_{n=-N+1}^{N}z_n e^{in\tau} \tag{3.47}$$

$$\tilde{K}_P(\theta,\tau)l(\tau)=\sum_{n=-N+1}^{N}\sum_{s=-N+1}^{N}k_{n,s}^{(\tilde{P})}e^{i(n\theta+s\tau)} \tag{3.48}$$

$$J_0\left(kR(\theta,\tau)\right)l(\tau)=\sum_{n=-N+1}^{N}\sum_{s=-N+1}^{N}j_{n,s}^{(0)}e^{i(n\theta+s\tau)} \tag{3.49}$$

$$\tilde{K}_Q(\theta,\tau)l(\tau)=\sum_{n=-N+1}^{N}\sum_{s=-N+1}^{N}k_{s,n}^{(\tilde{Q})}e^{i(n\theta+s\tau)} \tag{3.50}$$

$$\frac{J_1(kR)}{kR}\vec{R}\cdot\hat{n}_p l(\tau)=\sum_{n=-N+1}^{N}\sum_{s=-N+1}^{N} j_{n,s}^{(1)} e^{i(n\theta+s\tau)} \tag{3.51}$$

$$\tilde{K}_{\partial_n P}(\theta,\tau)l(\tau)=\sum_{n=-N+1}^{N}\sum_{s=-N+1}^{N} k_{n,s}^{(\partial_n \tilde{P})} e^{i(n\theta+s\tau)} \tag{3.52}$$

$$\frac{J_1(kR)}{kR}\vec{R}\cdot\hat{n}_q l(\tau)=\sum_{n=-N+1}^{N}\sum_{s=-N+1}^{N} j_{n,s}^{(1)} e^{i(n\theta+s\tau)} \tag{3.53}$$

$$2\pi l(\theta)l(\tau)\tilde{K}_{\partial_n Q}(\theta,\tau)=\sum_{n=-N+1}^{N}\sum_{s=-N+1}^{N} \tilde{k}_{n,s}^{(D)} e^{i(n\theta+s\tau)} \tag{3.54}$$

$$2\pi l(\theta)l(\tau)\frac{J_1(kR)}{kR}\left(\hat{n}_q\cdot\hat{n}_p\right)\sum_{n=-N+1}^{N}\sum_{s=-N+1}^{N} \tilde{j}_{n,s}^{(1)} e^{i(n\theta+s\tau)} \tag{3.55}$$

The algebraic system that is obtained by reducing the integral equations by means of the Fourier coefficients of any system, i.e. of EFIE or MFIE that are given above, in matrix form seems as

$$\begin{bmatrix} \frac{1}{2}I+A_{11} & A_{12} & A_{13} & A_{14} \\ \frac{1}{2}I+A_{21} & A_{22} & A_{23} & A_{24} \\ A_{31} & A_{32} & \frac{1}{2}I+A_{33} & A_{34} \\ A_{41} & A_{42} & \frac{1}{2}I+A_{43} & A_{44} \end{bmatrix} \begin{bmatrix} x_1 \\ x_2 \\ x_3 \\ x_4 \end{bmatrix} = \begin{bmatrix} b_1 \\ b_2 \\ b_3 \\ b_4 \end{bmatrix} \tag{3.56}$$

where $x=\left[k_n^{(1z)},k_n^{(m1l)},k_n^{(2z)},k_n^{(m2l)}\right]^T$ are the Fourier coefficients of the unknown surface currents K_{1z}, K_{m1l}, K_{2z} and K_{m2l} for TM-z polarization case and $x=\left[k_n^{(1l)},k_n^{(m1z)},k_n^{(2l)},k_n^{(m2z)}\right]^T$ are the Fourier coefficients of the unknown surface currents K_{1l}, K_{m1z}, K_{2l} and K_{m2z} for TE-z polarization case. It is clear that the system (3.56) is not a second kind one because, as seen, the matrix is not a diagonal one. That

is why, at first glance, a regularization operation with the block operators (2.151) and (2.153) seems as necessary. However, in numerical results it will be shown that for this configuration, thanks to the fast converging algorithm the condition number remains bounded. Also, it is checked that a regularization operation does not change the situation very much. Nevertheless, the super-algebraically converging algorithm does not mean a regularized system. In any case, it is better to have a second kind system by applying properly, i.e. according to the structure of the kernels, the double-sided regulator blocks that are given by (2.151) and (2.153) for dielectric boundaries.

Let us now see the implementation of the constructed algorithm. The numerical results that are going to be given here are already published in [19] and represented here once more for the purpose of discussion of the suggested algorithm. The parameters for numerical results regarding to the considered problems that are given in Figure 3.9.a) and Figure 3.9.b) are tabulated in the columns of the Table 3.2 column a) and column b) respectively.

Table 3.2: The parameters of the dielectric cylinders and mediums for numerical results of the solution of the boundary integral equation of dielectrics.

a)	b)
$O_1(x,y) = (0,0)$ $O_2(x,y) = \left(-\frac{\lambda_0}{2}, 0\right)$ $\rho_1 = \frac{3\lambda_0}{2}, \rho_2 = \frac{\lambda_0}{2}$	$O_1(x,y) = \left(-\frac{\lambda_0}{2}, 0\right)$ $O_2(x,y) = \left(-\frac{\lambda_0}{2}, 0\right)$ $\rho_1 = \rho_2 = \frac{\lambda_0}{2}$
$\mu_1 = \mu_1 = \mu_0, \varepsilon_1 = 4\varepsilon_0, \varepsilon_1 = 16\varepsilon_0$	

All the numerical results are given for a unit amplitude plane wave incidence along the negative *x*-axis. For the geometrical structure of Figure 3.9.a), the numerical results are given for TM-*z* polarized wave incidence, but for Figure 3.9.b) a TE-*z* wave incidence is assumed.

The first numerical result is the validation of the algorithm by comparison of the solutions of the systems of the EFIE and MFIE and the SoV solution that is obtained by means of the rigorous well-conditioned algorithm constructed by means of the ARM algorithm for circular dielectric cylinders. For a TM-*z* polarized wave impinging on the dielectric scatterers in Figure 3.9.a) the results are given in Figure 3.10.

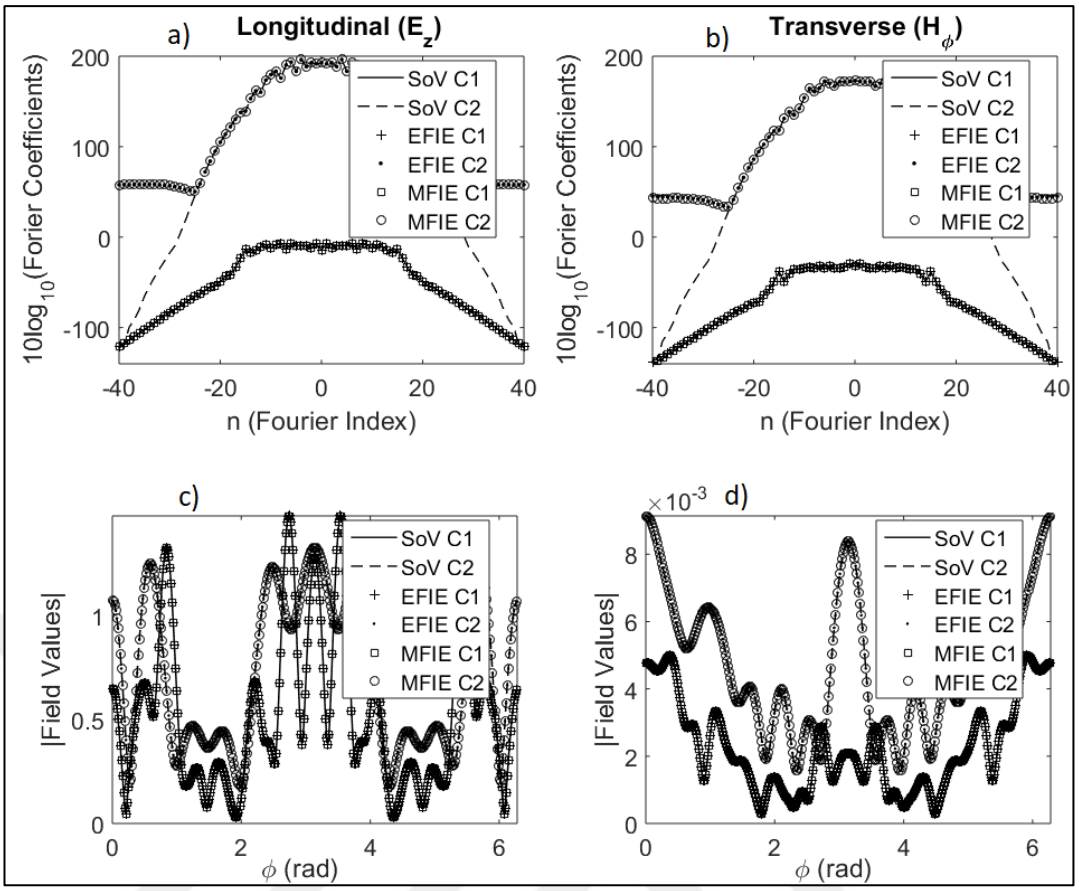

Figure 3.10: Validation of the solutions of the EFIE and MFIE systems for double layered dielectric circular cylinders; a) Fourier coefficients of the electric fields, b) Fourier coefficients of the magnetic fields, c) Electric fields, d) Magnetic fields.

In Figure 3.10.a) and b) the Fourier coefficients of the total tangential fields, i.e. the solution of the systems that are obtained from EFIE, MFIE and SoV, are compared on the outer boundary C_1 and inner boundary C_2.

The relation of the surface currents and the total longitudinal and transverse tangential fields (E_z and $H_l = H_\varphi$ for circular boundary) are given by (3.19). It is clear that the solution, i.e. the Fourier coefficients of the currents, are the same as of the tangential fields. However, for the solution of SoV where the reflection and transmission coefficients are obtained, a translation of these coefficients to the Fourier coefficients of the total fields as of the integral equations is necessary. For this purpose, the total fields on the boundaries are calculated and then the Fourier coefficients are equated as

$$E_z^{tot}\Big|_{C_1} = \sum_{n=-\infty}^{\infty}\left[T_n^{(0)}J_n\left(k_0\rho_1\right)+R_n^{(1)}H_n^{(2)}\left(k_0\rho_1\right)\right]e^{in\theta} = \sum_{n=-\infty}^{\infty}\left[k_n^{(m1l)}\right]e^{in\theta} \tag{3.57}$$

$$H_\varphi^{tot}\Big|_{C_1} = \frac{1}{i\omega\mu_0}\frac{\partial E_z^{tot}}{\partial\rho}\Big|_{C_1} = \sum_{n=-\infty}^{\infty}\left[\frac{1}{i\eta_0}\left(T_n^{(0)}J_n'\left(k_0\rho_1\right)+R_n^{(1)}H_n'^{(2)}\left(k_0\rho_1\right)\right)\right]e^{in\theta} = \sum_{n=-\infty}^{\infty}\left[k_n^{(1z)}\right]e^{in\theta} \tag{3.58}$$

$$E_z^{tot}\Big|_{C_2} = \sum_{n=-\infty}^{\infty}\left[T_n^{(12)}J_n\left(k_1\rho_2\right)+R_n^{(2)}H_n^{(2)}\left(k_1\rho_2\right)\right]e^{in\theta} = \sum_{n=-\infty}^{\infty}\left[k_n^{(m2l)}\right]e^{in\theta} \tag{3.59}$$

$$H_\varphi^{tot}\Big|_{C_2} = \frac{1}{i\omega\mu_1}\frac{\partial E_z^{tot}}{\partial\rho}\Big|_{C_2} = \sum_{n=-\infty}^{\infty}\left[\frac{1}{i\eta_1}\left(T_n^{(12)}J_n'\left(k_1\rho_2\right)+R_n^{(2)}H_n'^{(2)}\left(k_1\rho_2\right)\right)\right]e^{in\theta} = \sum_{n=-\infty}^{\infty}\left[k_n^{(2z)}\right]e^{in\theta} \tag{3.60}$$

Here the coefficients $R_n^{(m)}$ and $T_n^{(m)}$ are the coefficients of the reflection and transmission fields from the boundaries that are formulated in series solution as discussed in Chapter 2.1.

In Figure 3.10.c) and d) the corresponding total tangential fields that are calculated via the Fourier coefficients of the systems are given. As seen from Figure 3.10.a)-d), the solutions of three different systems are well consistent. The Fourier coefficients that are obtained from the solution of the integral equations can be calculated until the machine epsilon ($\sim 10^{-16}$) due to the numerical saturation.

The same quantities for a TE-*z* polarized wave incidence on two parallel dielectric scatterers that have the parameters of Table 3.2 in column b) are given in Figure 3.11.

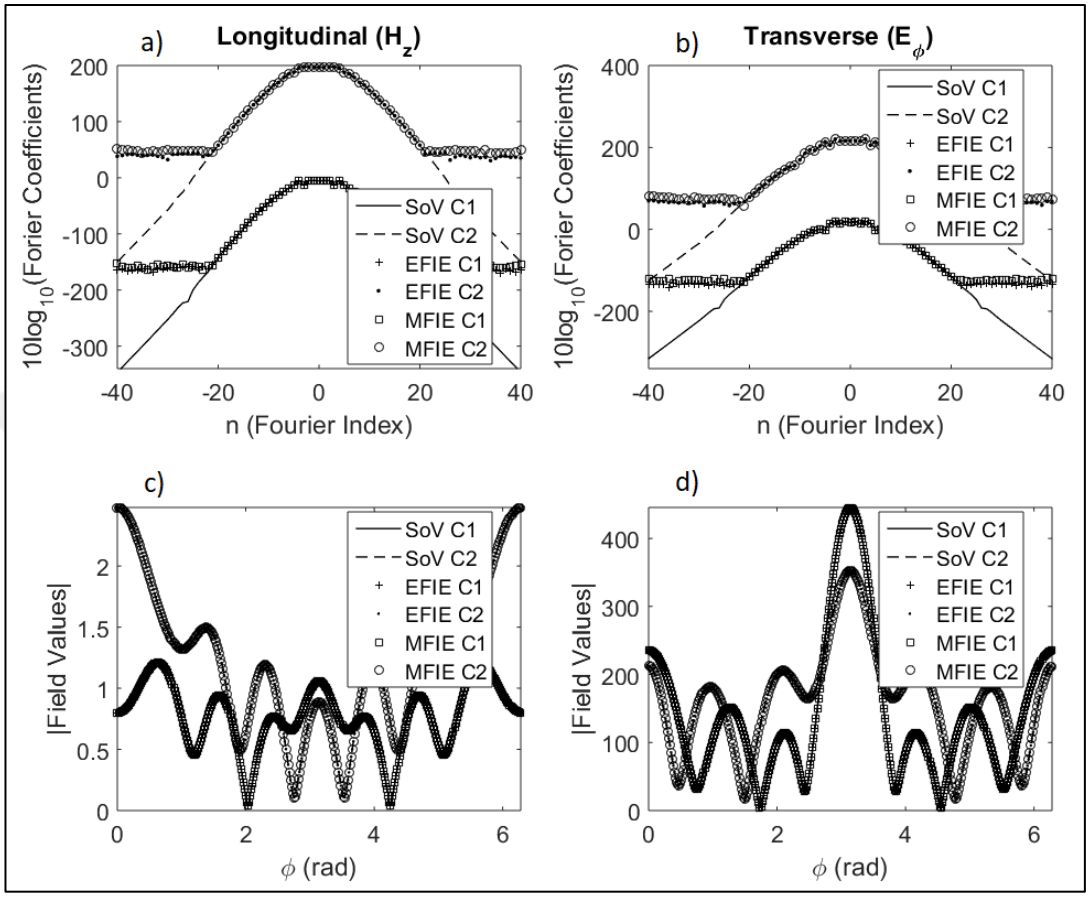

Figure 3.11: Validation of the solutions of the EFIE and MFIE systems for two parallel circular cylinders; a) Fourier coefficients of the magnetic fields, b) Fourier coefficients of electric fields, c) Magnetic fields, d) Electric fields.

As seen from Figure 3.11.a)-d), similar to the results in that are shown in Figure 3.10, the solutions of three different systems are consistent which proves the reliability of the suggested algorithm.

The plots in Figure 3.12 shows the key points of the suggested algorithm. Because the stability and super-algebraically convergence is the main aim of this work. For the purpose of disclosing the super-algebraically or even exponentially convergence, by doubling the size of the algebraic system and zero padding to the previous solutions and right-hand sides, the relative difference between two consecutive solutions

$$\left\| x_{2N} - x_N \right\|_C / \left\| x_{2N} \right\|_C \tag{3.61}$$

and the residuals of the algebraic system

$$\left\| A_{2N} x_N - b_N \right\|_C / \left\| b_{2N} \right\|_C \tag{3.62}$$

are calculated via the norm that is defined as

$$\left\| f_\infty \right\|_C = \sum_{m=-\infty}^{\infty} |f_m|^2 \left(1+|m|^2\right) \tag{3.63}$$

that guarantees the convergence by means of the Sobolev's embedding theorem in continuous metric.

The numerical results corresponding to the formula (3.61) and (3.62) are shown in Figure 3.12.a) and b) respectively. In these plots, the notations [I] is used to indicate the double layered circles that is given in Figure 3.9.a) and [N] is used for the geometry of in Figure 3.9.b) with related parameters that are given in Table 3.2. In addition, the polarization type is specified by subscript as TM and TE.

In Figure 3.12.c) the relative error of the solutions of integral equations w.r.t. the solutions obtained from SoV are given in l_2 norm. The solutions that used in these plots are the Fourier coefficients that are given in Figure 3.10 and Figure 3.11. The plots of Figure 3.12.a)-c) clearly shows the super-algebraically convergent algorithm. In addition to these plots, in Figure 3.12.d) the condition numbers of the algebraic systems of the integral equations are shown. As seen from the nature of the matrix in (3.56) these systems are not one of the second kind. But thanks to the super-algebraically convergence, the ill-conditioned behavior of such system is shifted to larger truncation numbers and not encountered at the considered levels. But, as discussed before, by a proper combination of the equations (3.22)-(3.25) and (3.26)-(3.29) or the equations (3.30)-(3.33) and (3.34)-(3.37) a second kind system can be constructed. However, here they are used just as they are and such combinations are out of the scope of this thesis.

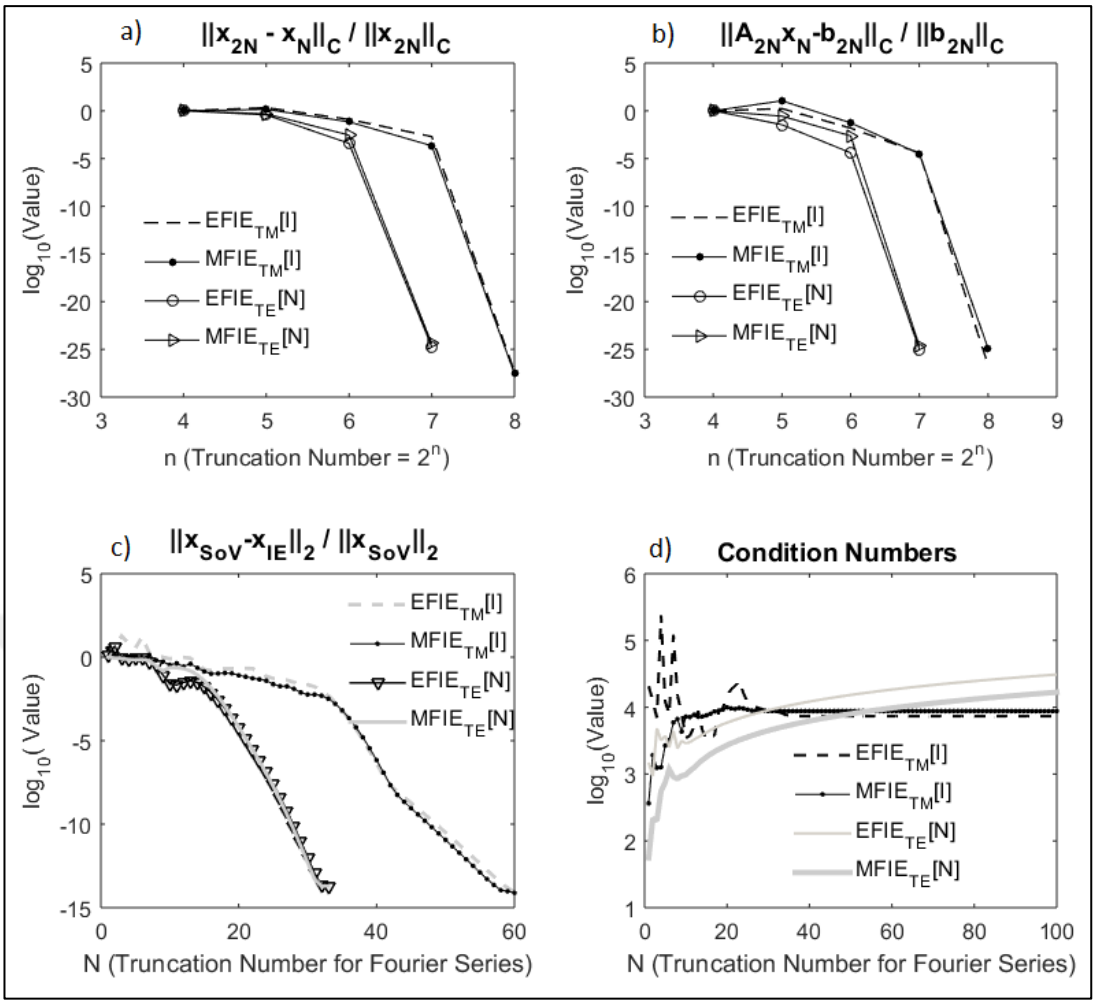

Figure 3.12: Qualitative data for performed calculations of double layered circles and two parallel circles; a) Relative norm w.r.t. doubled size, b) Residual norm w.r.t. doubled size, c) Relative error w.r.t. SoV, d) Condition numbers.

In this chapter the theoretical information which is given in Chapter 2.2 and in its subchapters are applied to two different geometrical structure of dielectric circular cylinders and thanks to the singularity extraction and the convolution theorem, a super-algebraically convergent algorithm is constructed and its proof is shown by means of various numerical results.

3.4. Application of ARM to the Algebraic System of Integral Equation of Two Parallel Circular Impedance Cylinders

In this subchapter, the results of the numerical implementation of the ARM that is explained in Chapter 2.2.3 for integral equations of the third kind BVP is going to be presented for two parallel circular impedance cylinders whose configuration and

corresponding values are given in Figure 3.13. The center of both cylinders are posing on the *x*-axis and the distance between two boundaries is equal to the free space wavelength that denoted by λ_0. The numerical results that are going to be presented here are already published in [18]. The formulation is given here in details but for more explanation of the motivation, the reader is referred to that publication.

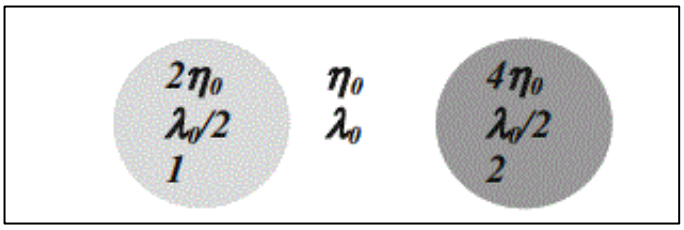

Figure 3.13: Two circular impedance cylinders.

Here, the integral equations which is obtained in Chapter 3.3 for dielectric boundaries are re-arranged for two impedance cylinders by means of the impedance boundary conditions also called as third kind boundary condition or mixed boundary condition. The standard impedance boundary condition is expressed as [57]

$$\hat{n}\times\vec{E}=\eta\hat{n}\times\left(\hat{n}\times\vec{H}\right) \tag{3.64}$$

where $\vec{E}$ is the electric and $\vec{H}$ is the magnetic field in vector form, η is the surface impedance and $\hat{n}$ is the unit outward normal vector. By means of the relations (3.17) between the fields and surface currents, the condition (3.64) can be rewritten in terms of surface currents as

$$\vec{K}_m=-\eta\hat{n}\times\vec{K} \tag{3.65}$$

For TM-*z* polarization case, substitution of (3.16) into (3.65) and using the related expressions from (3.19) results in

$$K_{ml}=\eta K_z \tag{3.66}$$

In a similar manner, by substituting zero values that are given in (3.21) into (3.65), for TE-*z* polarization case the relation

$$K_{mz} = -\eta K_l \tag{3.67}$$

is obtained.

Now, it is clear that by means of the relations (3.66) and (3.67), the four integral equations for BVP of two dielectrics can be reduced to two integral equations when the surface is modeled by an impedance value η and the determination of one is sufficient since the other can be obtained from (3.66) and (3.67). By doing so, the following integral equation systems are obtained.

For TM-*z* polarization;

EFIE system:

$$\begin{aligned}&\frac{1}{2}\eta_1 K_{1z}(q) + i\omega\mu_0\left[\int_{C_1} K_{1z}(p)G_2\left(k_0R_{qp}\right)dl_p + \int_{C_2} K_{2z}(p)G_2\left(k_0R_{qp}\right)dl_p\right]\\ &-\left[\int_{C_1}\eta_1 K_{1z}(p)\frac{\partial G_2\left(k_0R_{qp}\right)}{\partial n_p}dl_p + \int_{C_2}\eta_2 K_{2z}(p)\frac{\partial G_2\left(k_0R_{qp}\right)}{\partial n_p}dl_p\right] = E_z^{inc}(q); \qquad q\in C_1^+\end{aligned} \tag{3.68}$$

$$\begin{aligned}&\frac{1}{2}\eta_2 K_{2z}(q) + i\omega\mu_0\left[\int_{C_1} K_{1z}(p)G_2\left(k_0R_{qp}\right)dl_p + \int_{C_2} K_{2z}(p)G_2\left(k_0R_{qp}\right)dl_p\right]\\ &-\left[\int_{C_1}\eta_1 K_{1z}(p)\frac{\partial G_2\left(k_0R_{qp}\right)}{\partial n_p}dl_p + \int_{C_2}\eta_2 K_{2z}(p)\frac{\partial G_2\left(k_0R_{qp}\right)}{\partial n_p}dl_p\right] = E_z^{inc}(q); \qquad q\in C_2^+\end{aligned} \tag{3.69}$$

MFIE system:

$$\frac{1}{2}K_{1z}(q)+\left[\int_{C_1}K_{1z}(p)\frac{\partial G_2\left(k_0R_{qp}\right)}{\partial n_q}dl_p+\int_{C_2}K_{2z}(p)\frac{\partial G_2\left(k_0R_{qp}\right)}{\partial n_q}dl_p\right]$$
$$-\frac{1}{i\omega\mu_0}\left[\int_{C_1}\eta_1K_{1z}(p)\frac{\partial^2 G_2\left(k_0R_{qp}\right)}{\partial n_q\partial n_p}dl_p+\int_{C_2}\eta_2K_{2z}(p)\frac{\partial^2 G_2\left(k_0R_{qp}\right)}{\partial n_q\partial n_p}dl_p\right] \qquad (3.70)$$
$$=H_l^{inc}(q);\ q\in C_1^+$$

$$\frac{1}{2}K_{2z}(q)+\left[\int_{C_1}K_{1z}(p)\frac{\partial G_2\left(k_0R_{qp}\right)}{\partial n_q}dl_p+\int_{C_2}K_{2z}(p)\frac{\partial G_2\left(k_0R_{qp}\right)}{\partial n_q}dl_p\right]$$
$$-\frac{1}{i\omega\mu_0}\left[\int_{C_1}\eta_1K_{1z}(p)\frac{\partial^2 G_2\left(k_0R_{qp}\right)}{\partial n_q\partial n_p}dl_p+\int_{C_2}\eta_2K_{2z}(p)\frac{\partial^2 G_2\left(k_0R_{qp}\right)}{\partial n_q\partial n_p}dl_p\right] \qquad (3.71)$$
$$=H_l^{inc}(q);\ q\in C_2^+$$

For TE-z polarization;

EFIE system:

$$\frac{1}{2}\eta_1K_{1l}(q)+\left[\int_{C_1}\eta_1K_{1l}(p)\frac{\partial G_2\left(k_0R_{qp}\right)}{\partial n_q}dl_p-\int_{C_2}\eta_2K_{2l}(p)\frac{\partial G_2\left(k_0R_{qp}\right)}{\partial n_q}dl_p\right]$$
$$-\frac{1}{i\omega\varepsilon_0}\left[\int_{C_1}K_{1l}(p)\frac{\partial^2 G_2\left(k_0R_{qp}\right)}{\partial n_q\partial n_p}dl_p+\int_{C_2}K_{2l}(p)\frac{\partial^2 G_2\left(k_0R_{qp}\right)}{\partial n_q\partial n_p}dl_p\right] \qquad (3.72)$$
$$=E_l^{inc}(q);\ q\in C_1^+$$

$$\frac{1}{2}\eta_2K_{2l}(q)+\left[\int_{C_1}\eta_1K_{1l}(p)\frac{\partial G_2\left(k_0R_{qp}\right)}{\partial n_q}dl_p-\int_{C_2}\eta_2K_{2l}(p)\frac{\partial G_2\left(k_0R_{qp}\right)}{\partial n_q}dl_p\right]$$
$$-\frac{1}{i\omega\varepsilon_0}\left[\int_{C_1}K_{1l}(p)\frac{\partial^2 G_2\left(k_0R_{qp}\right)}{\partial n_q\partial n_p}dl_p+\int_{C_2}K_{2l}(p)\frac{\partial^2 G_2\left(k_0R_{qp}\right)}{\partial n_q\partial n_p}dl_p\right] \qquad (3.73)$$
$$=E_l^{inc}(q);\ q\in C_2^+$$

MFIE system:

$$-\frac{1}{2}K_{1l}(q)-i\omega\varepsilon_0\left[\int_{C_1}\eta_1 K_{1l}(p)G_2\left(k_0R_{qp}\right)dl_p-\int_{C_2}\eta_2 K_{2l}(p)G_2\left(k_0R_{qp}\right)dl_p\right]$$
$$+\left[\int_{C_1}K_{1l}(p)\frac{\partial G_2\left(k_0R_{qp}\right)}{\partial n_p}dl_p+\int_{C_2}K_{2l}(p)\frac{\partial G_2\left(k_0R_{qp}\right)}{\partial n_p}dl_p\right]=H_z^{inc}(q);\ q\in C_1^+ \tag{3.74}$$

$$-\frac{1}{2}K_{2l}(q)-i\omega\varepsilon_0\left[\int_{C_1}\eta_1 K_{1l}(p)G_2\left(k_0R_{qp}\right)dl_p-\int_{C_2}\eta_2 K_{2l}(p)G_2\left(k_0R_{qp}\right)dl_p\right]$$
$$+\left[\int_{C_1}K_{1l}(p)\frac{\partial G_2\left(k_0R_{qp}\right)}{\partial n_p}dl_p+\int_{C_2}K_{2l}(p)\frac{\partial G_2\left(k_0R_{qp}\right)}{\partial n_p}dl_p\right]=H_z^{inc}(q);\ q\in C_2^+ \tag{3.75}$$

It is evident from the equations (3.70)-(3.75) that the algebraic systems of the EFIE and MFIE of both polarization may be an equation of the first kind or equation of the second kind depends on the value of the surface impedance. Thus, a regularization operation may be necessary or unnecessary. As discussed in Chapter 2.2.3 where ARM for third kind boundaries is considered, depends on the value of the impedance which is defined by (2.124), a regularization procedure with the operators (2.151) or (2.153) may be necessary. This is the case when η_1 or η_2 has very small or very large values and this cases are considered in numerical results for various values of the surface impedances.

In Figure 3.14-3.15, the validation of the solutions of integral equations is done by means of the SoV solution that is achieved via a stable and reliable algorithm for circular impedance cylinders that is suggested in [12]. In these figures, the numbers 1 and 2 denote the values regarding the boundaries C_1 (the left-hand-side circle) and C_2 (the right-hand-side circle).

Figure 3.14.a) and b) shows the exponentially converging Fourier coefficients of tangential fields and c) and d) shows the related tangential fields on the boundaries that are obtained for a TM-z polarized plane wave incidence from the solution of three different systems as EFIE, MFIE and SoV. The similar results are shown in Figure 3.15.a)-d) for a TE-*z* plane wave incidence on the impedance cylinders. These plots, as well, shows the consistency between the solutions and the exponentially converging behavior of the solutions.

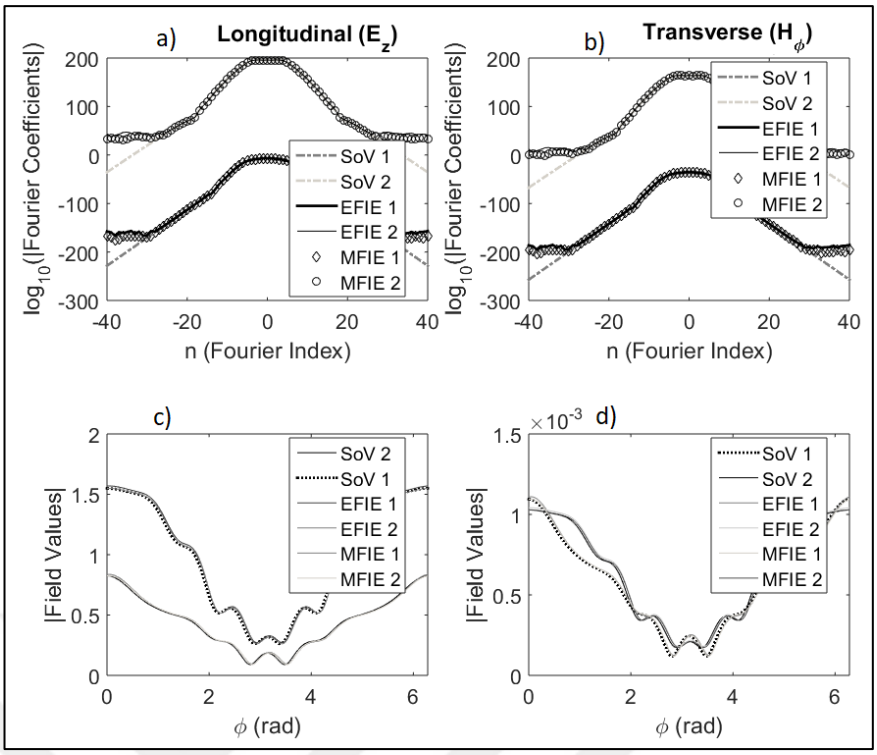

Figure 3.14: Validation of the solutions of the EFIE and MFIE systems for TM-z plane wave illumination; a) Fourier coefficients of the electric fields, b) Fourier coefficients of the magnetic fields, c) Electric fields, d) Magnetic fields.

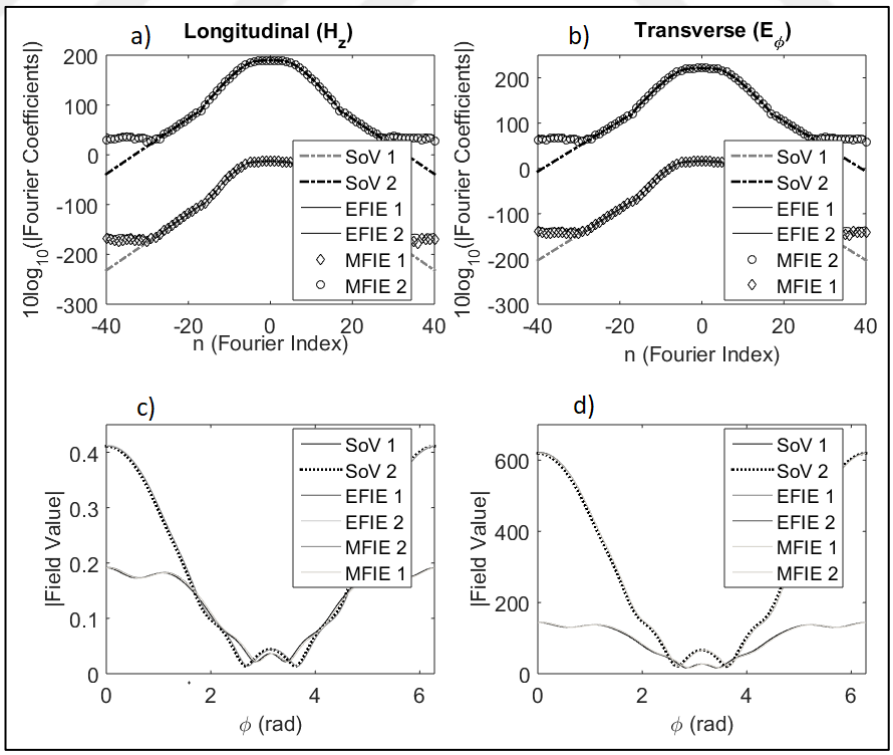

Figure 3.15: Validation of the solutions of the EFIE and MFIE systems for TE-z plane wave illumination; a) Fourier coefficients of the magnetic fields, b) Fourier coefficients of the electric fields, c) Magnetic fields, d) Electric fields.

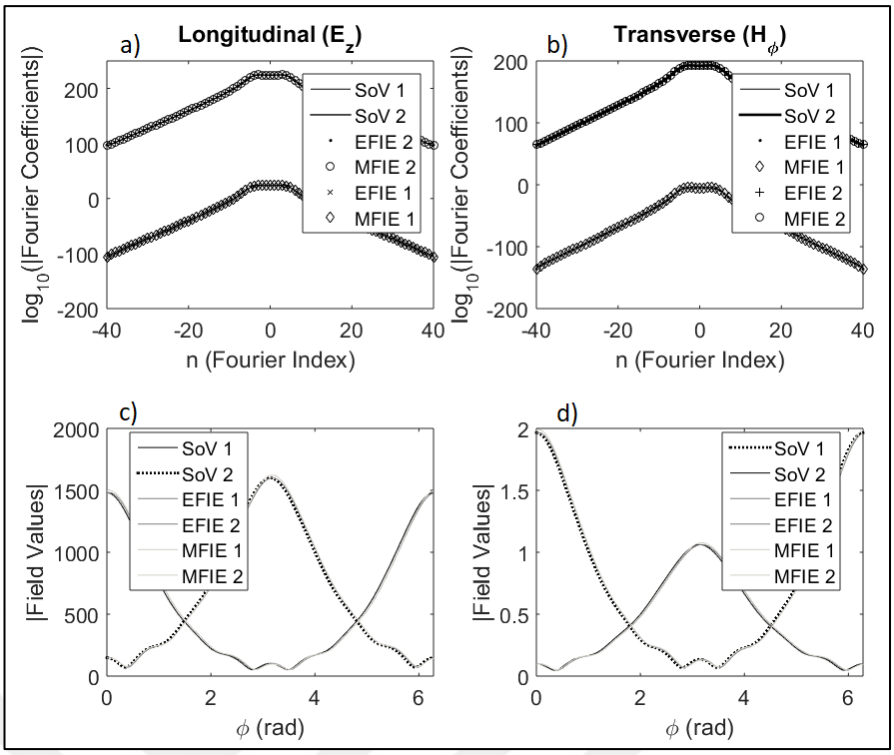

Figure 3.16: Validation of the solutions of the EFIE and MFIE systems for TM-z line source illumination; a) Fourier coefficients of the electric fields, b) Fourier coefficients of the magnetic fields, c) Electric fields, d) Magnetic fields.

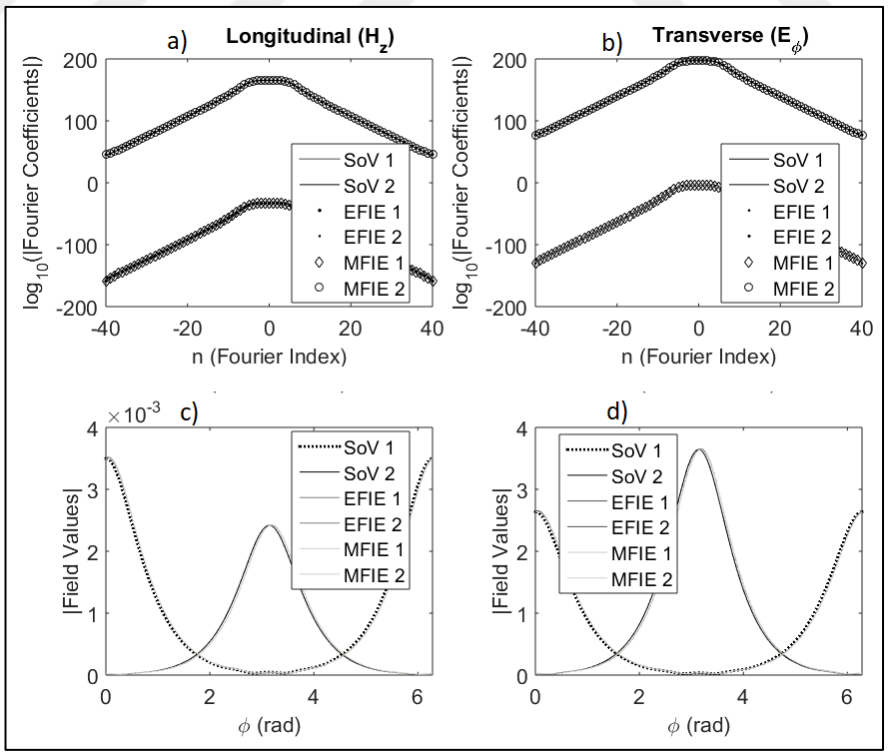

Figure 3.17: Validation of the solutions of the EFIE and MFIE systems for TE-z line source illumination; a) Fourier coefficients of the magnetic fields, b) Fourier coefficients of the electric fields, c) Magnetic fields, d) Electric fields.

The same validation is achieved for the values calculated on the boundary impedance cylinders under the electric line source (TM-z polarization) and magnetic line source (TE-z polarization) illuminations. The results of these validations are plotted in Figure 3.16.a)-d) and Figure 3.17.a)-d) respectively.

The following figures (Figure 3.18-Figure 3.22) shows the condition numbers of the considered systems. In Figure 3.18, the condition numbers of the systems regarding the configuration of impedance cylinder given in Figure 3.13 are plotted. It is clear from the plots that some systems have bounded condition numbers for the corresponding surface impedance values, but on the other side, some systems have condition numbers in growing trend and the only way to make them bounded is applying the suggested ARM as discussed in 0. This is indicated in figure by the curves with the same name but with the postfix LAES1 and LAES2 where LAES2 is the regularized version of LAES1.

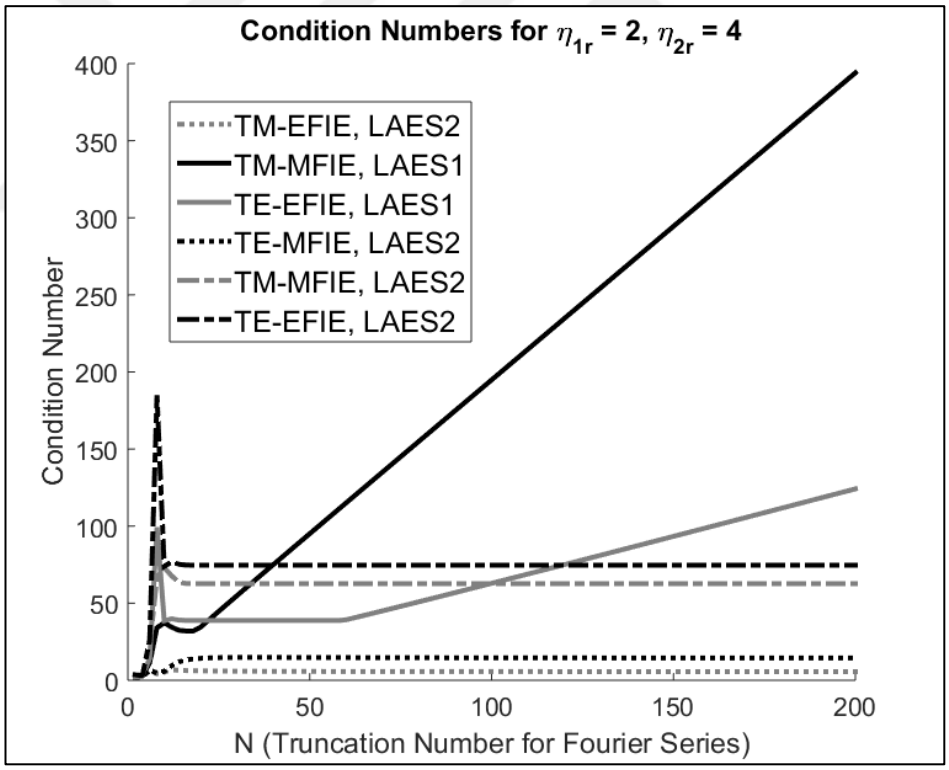

Figure 3.18: Condition numbers of linear algebraic systems.

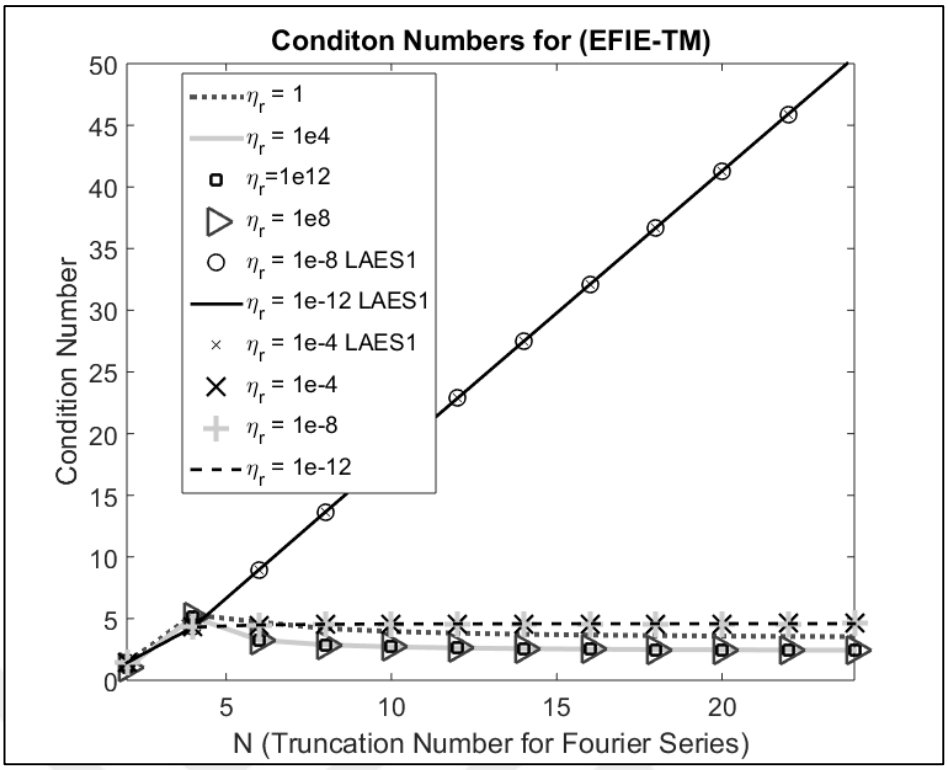

Figure 3.19: Condition numbers for varying surface impedances for the algebraic system of EFIEs of TM-z wave incidence.

Figure 3.19 shows the condition numbers of the EFIE for TM-z polarization for various surface impedance values where both surface impedances are taken equally. By considering the equations (3.68) and (3.69) of the EFIE for TM-z polarization it is evident that for very small values of the relative surface impedances $\eta_r = \eta_i/\eta_0$ $(i = 1, 2)$, the diagonalized structure of the system is corrupted and thus, it becomes one of the first kind. This situation is seen clearly from the curves that labelled by the values of $\eta_r = 10^{-4}, 10^{-8}, 10^{-12}$ and continuing by LAES1. The curves given for the same values and labelled by LAES2 are the condition numbers of the regularized versions of the corresponding systems of LAES1. It is clear that after regularization the system behaves as a second kind whose condition numbers are smooth for growing truncation numbers. Also, it is evident that for larger values of the relative surface impedance, the algebraic equations system (3.68) and (3.69) remain as a second kind and its condition numbers are uniformly bounded for increasing size of the algebraic system

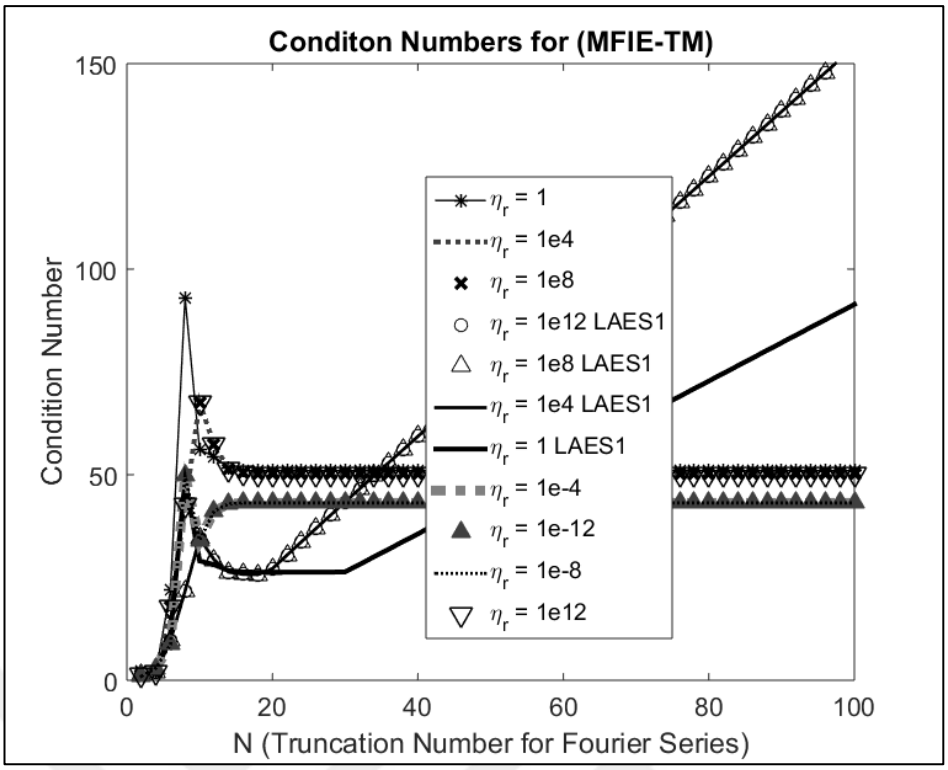

Figure 3.20: Condition numbers for varying surface impedances for the algebraic system of MFIEs of TM-z wave incidence.

Figure 3.20 shows the condition numbers of the algebraic system of the MFIEs of TM-*z* polarization given by the equations (3.70) and (3.71) for various values of the impedance. Unlike the plots that are given in Figure 3.19, in this case, the system becomes one of the first kind for large values and remains as a second kind for very small values of the surface impedance. It is clear from the figure, by the regularization procedure which is discussed in 0 the ill-conditioned trend of the system LAES1 can be fixed and a system with uniformly bounded condition numbers can be constructed.

In Figure 3.21 and Figure 3.22, the numerical results of the same discussions are plotted for the systems of the EFIE and MFIE of TE-*z* polarization that are given by the equations (3.72), (3.73) and (3.74), (3.75) respectively. In this case, the results opposite to the TM-*z* case are observed because of the similarity of the structure of EFIE-TM and MFIE-TE equations and the MFIE-TM and EFIE-TE equations.

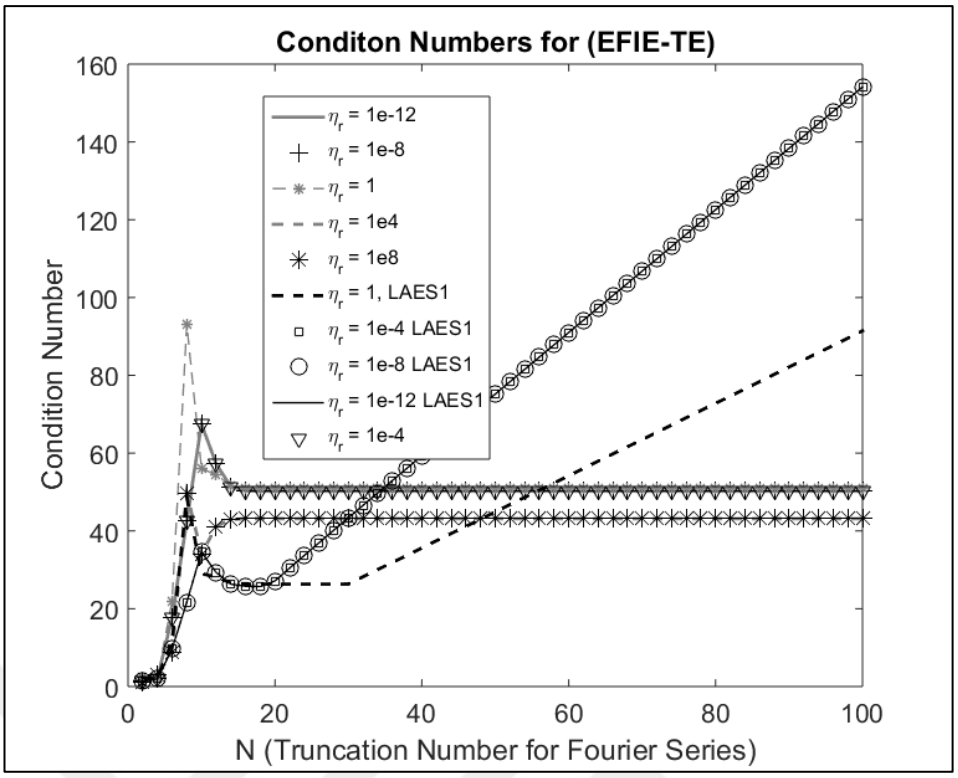

Figure 3.21: Condition numbers for varying surface impedances for the algebraic system of EFIEs of TE-z wave incidence.

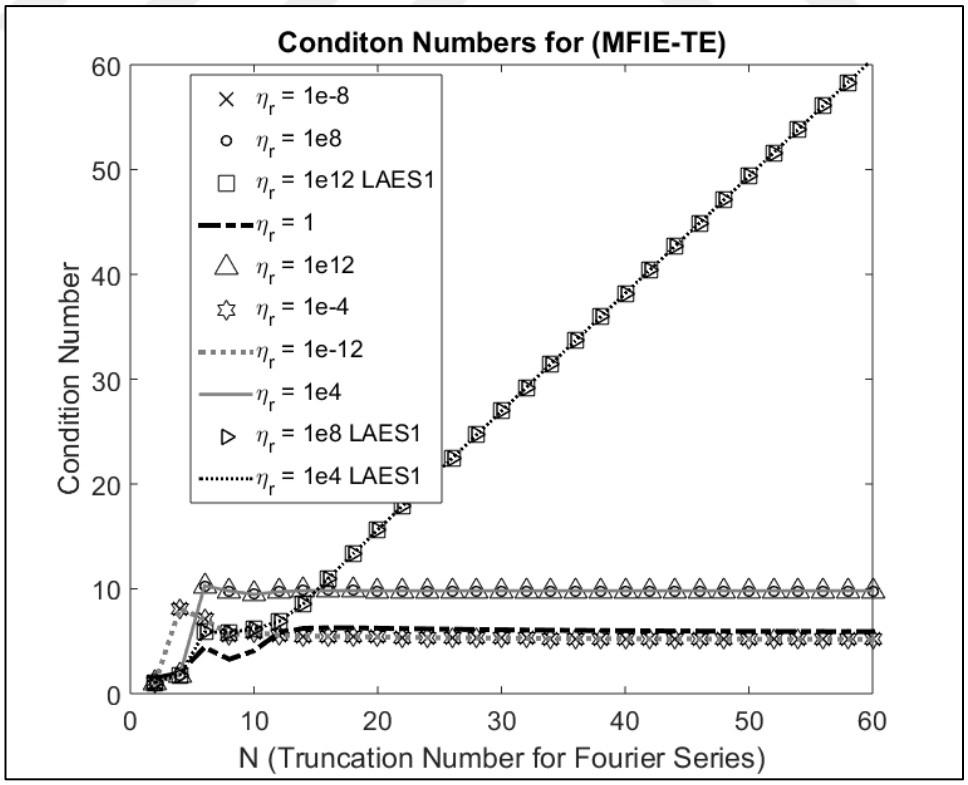

Figure 3.22: Condition numbers for varying surface impedances for the algebraic system of MFIEs of TE-z wave incidence.

In this chapter, the integral equations regarding two parallel impedance cylinders are reduced to the linear algebraic equations by means of the entire domain Galerkin method where all the quantities are expanded as Fourier series. Then the systems are analyzed for various values of the surface impedance and the ARM algorithm that is discussed in Chapter 2.2.3 is applied if necessary. Also, it is shown that by means of the suggested algorithm super-algebraically convergent solutions can be obtained.

4. CONCLUSION

In two-dimensional boundary value problems, where the field variations along one axis are neglected, the scattered field that satisfies the homogeneous Helmholtz equation is sought. In circular coordinates, by means of the separation of variables method, the Helmholtz equation results in the expression of the fields into infinite series with unknown coefficients. The corresponding unknowns are calculated by imposing the boundary conditions of the related boundary. This operation yields to an infinite size algebraic equation system which is, in general, one of the first kind. For the obstacles that have arbitrary shape, by means of the Green's identities, the Helmholtz equation yields to an integral equation and the algebraization of this integral, in general, yields to an infinite size algebraic equation of the first kind. The numerical solution of such a system can be achieved through a truncation procedure. However, it is well known that numerical solution of such system is error-prone due to its sensitivity to the matrix inversion depending on the truncation number, i.e. it is an ill-conditioned system. If the solution of such a system is considered then, as a rule, the condition number of the matrix and the satisfaction of the boundary condition must be checked to make sure of the numerical results. Otherwise, the solutions obtained may be completely wrong. In Chapter 2, from the theoretical point of view and in Chapter 3, by means of the various illustrative numerical results, this drawback of the first kind system is revealed. One of the ways to avoid such a hazard is to transform this ill-conditioned system to a well-conditioned algebraic equation of the second kind through a regularization operation. In this thesis, the Analytical Regularization Method is used for such a regularization. In this method a left-hand-side operator L and a right hand-side operator R is used to transform the first kind system in form of $Ax = b$ to a second kind one as $(I + K)y = g$. It is shown, in Chapter 2 mathematically and in Chapter 3 numerically, that a system obtained by subjecting the ARM algorithm is numerically stable and reliable. Thus, if the solution of such a system is under consideration, then its numerical implementation can be achieved without any extra check.

In this thesis, at first, the ARM algorithm is implemented to algebraic systems of the two neighbor circular impedance boundaries and eccentrically layered dielectric boundaries where the fields are expanded into infinite series. Secondly, the ARM

algorithm is implemented to the boundary integral equations of the two neighbor circular impedance boundaries, two eccentrically layered circular dielectric boundaries and two neighbor dielectric boundaries with the entire domain Galerkin method. It is shown that such a construction brings exponentially converging algorithm, which is very efficient from the point of numerical implementation. The necessity and the success of this algorithm are expressed clearly from many aspects. This algorithm can be used for a wide class of the 2-dimensional boundary value diffraction problems. The plans for future are to expand the scope of its application further by including the contour smoothing through spline interpolation and other smooth parametrically presented contours.

REFERENCES

[1] Ergül Ö., (2012), "Analysis of composite nanoparticles with surface integral equations and the multilevel fast multipole algorithm", Journal of Optics, 14 (6), 1-4.

[2] Pagnetti A., Xemard A., Paladian F., Nucci C. A., (2012), "An improved method for the calculation of the internal impedances of solid and hollow conductors with the inclusion of proximity effect", IEEE Transactions on Power Delivery, 27 (4), 2063-2072.

[3] Ramm A., (2013), "Scattering of electromagnetic waves by many nano-wires", Mathematics, 1 (3), 89-99.

[4] Bates R., (1975), "Analytic constraints on electromagnetic field computations", IEEE Transactions on Microwave Theory and Techniques, 23 (8), 605-623.

[5] Poyedinchuk A. Y., Tuchkin Y. A., Shestopalov V., (2000), "New numerical-analytical methods in diffraction theory", Mathematical and Computer Modeling, 32 (9), 1029-1046.

[6] Ivanov Y. A., (1970), "Diffraction of Electromagnetic Waves on Two Bodies", 1st Edition, National Aeronautics and Space Administration.

[7] Ioannidou M., Kapsalas K., Chrissoulidis D., (2004), "Electromagnetic-wave scattering by an eccentrically stratified, dielectric cylinder with multiple, eccentrically stratified, cylindrical, dielectric inclusions", Journal of Electromagnetic Waves and Applications, 18 (4), 495-516.

[8] Kishk A. A., Parrikar R. P., Elsherbeni A. Z., (1992), "Electromagnetic scattering from an eccentric multilayered circular cylinder", IEEE Transactions on Antennas and Propagation, 40 (3), 295-303.

[9] Toyama H., Yasumoto K., Iwasaki T., (2003), "Electromagnetic scattering from a dielectric cylinder with multiple eccentric cylindrical inclusions", Progress in Electromagnetics Research, 40, 113-129.

[10] S. Vatansever, (2013), "Eksantrik Katmanlı ve Komşu Dielektrik Silindirlerden Dalga Saçılması", Master Thesis, Gebze Technical University.

[11] Dikmen F., Sever E., Vatansever S., Tuchkin Y. A., (2015), "Well-conditioned algorithm for scattering by a few eccentrically multilayered dielectric circular cylinders", Radio Science, 50 (2), 99-110.

[12] Sever E., Dikmen F., Suvorova O. A., Tuchkin Y. A., (2016), "An analytical formulation with ill-conditioned numerical scheme and its remedy: scattering

by two circular impedance cylinders", Turkish Journal of Electrical Engineering and Computer Sciences, 24 (3), 1194-1207.

[13] Dikmen F., Sever E., Tuchkin Y. A., Sabah C., (2016), "A numerically stable algorithm for eccentrically metamaterial covered circular cylinders", URSI International Symposium on Electromagnetic Theory, 515-517, Espoo, Finland, 14-18 August.

[14] Güler S., Önol. C., Ergül Ö., Hatipoğlu M. E., Sever E., Dikmen F., Tuchkin Y., (2016), "Elektrik-Alan integral denkleminin genetik algoritma ile optimize edilmiş modifiye süperformül ile iki boyuttaki hızlı yakınsayan çözümleri", International Union Of Radio Science Türkiye Bilimsel Kongresi, ODTÜ, Akara, Türkiye, 1-3 Eylül.

[15] Hatipoglu M. E., Suvorova O. A., Dikmen F., Tuchkin Y. A., (2016), "İki boyutta Teğet Elektrik (TE) durumda elektrik alan integral denkleminin çözümüne üç yaklaşım ve analitik regülerleştirilmeleri", International Union Of Radio Science Türkiye Bilimsel Kongresi, ODTÜ, Ankara, Türkiye, 1-3 Eylül.

[16] Dikmen F., Sever E., Tuchkin Y., (2016), "İki boyutta manyetik alan integral denkleminin tüm bölge Galerkin yöntemi ile çözümleri", International Union Of Radio Science Türkiye Bilimsel Kongresi, ODTÜ, Ankara, Türkiye, 1-3 Eylül.

[17] Nagayoshi M., K. Nobuaki H., Mautz J. R., (1991), "Integral Equation Methods for Electromagnetics", 1st Edition, Artec House.

[18] Sever E., Tuchkin Y. A., Dikmen F., (2018), "On a super-algebraically converging, numerically stable solving strategy for electromagnetic scattering by impedance cylinders", Journal of Computational Electronics, 17 (1), 427-435.

[19] Sever E., Dikmen F., Tuchkin Y. A., (2017), "Superalgebraically converging Galerkin method for electromagnetic scattering by dielectric cylinders", Radio Science, 52 (10), 1282-1292.

[20] Carl M., (1969), "Foundations of Mathematical Theory of Electromagnetic Waves", 1st Edition, Springer.

[21] Mautz J. R., Harrington R. F., (1979), "Electromagnetic scattering from a homogeneous material body of revolution", Archiv Elektronik und Uebertragungstechnik, 33, 71-80.

[22] Harrington R. F., (1989), "Boundary integral formulations for homogeneous material bodies", Journal of Electromagnetic Waves and Applications, 3 (1), 1-15.

[23] Huddleston P., Medgyesi-Mitschang L. N., J. Putnam J. M., (1986) "Combined field integral equation formulation for scattering by dielectrically coated

conducting bodies", IEEE Transactions on Antennas and Propagation, 34 (4), 510-520.

[24] Tuchkin Y. A., (1997), "Regularization of one class of system of integral-differential equations of mathematical physics", Doclady of The Ukrainian National Academy of Sciences, A (10), 47-51.

[25] Vinogradov S. S., Vinogradova E. D., Wilson C., Sharp I., Y. A. Tuchkin, (2009), "Scattering of an E-polarized plane wave by two-dimensional airfoils", Electromagnetics, 29 (3), 268-282.

[26] Abramowitz M., Irene A. S., (1972) "Handbook of Mathematical Functions with Formulas, Graphs, and Mathematical Tables", 3rd Edition, Dover Publications.

[27] Tuchkin Y. A., (1985), "The wave scattering by an unclosed arbitrarily shaped cylindrical screen with Dirichlet boundary condition", Reports of Science Academy, USSR, 285 (6), 1370-1373.

[28] Tuchkin Y. A., (1987), "Derivation of one integral-differential equation of theory of diffraction", (in Russian), Reports of The Ukrainian National Academy of Sciences, A (4), 21-25.

[29] Tuchkin Y. A., (1987), "The wave scattering by an unclosed arbitrarily shaped cylindrical screen with Neumann boundary condition", Reports of Science Academy, USSR, 293 (2), 343-345.

[30] Vinogradov S., Smith P., Vinogradova E., (2001), "Canonical Problems in Scattering and Potential Theory, Part 1: Canonical Structures in Potential Theory, Part 2: Acoustic and Electromagnetic Diffraction by Canonical Structures", 1st Edition, CRC Press.

[31] Tuchkin Y. A., (2002), "Analytical regularization method for wave diffraction by bowl-shaped screen of revolution", In: Smith P. D., Cloude S. R., Editors, "Ultra-Wideband, Short-Pulse Electromagnetics 5", Kluwer Academic Publisher.

[32] Tuchkin Y. A., (2006), "Method of analytical regularization: state of art and new approaches", 4th International Workshop on Electromagnetic Wave Scattering, 43-49, Gebze, Turkey, 18-22 September.

[33] Panin S. B., Smith P. D., Vinogradova E. D., Tuchkin Y. A., Vinogradov S. S., (2009), "Regularization of the Dirichlet problem for Laplace's equation: surfaces of revolution", Electromagnetics, 29 (1), 53-76.

[34] Tuchkin Y. A., (2018), "On analytical regularization method", In: Kobayashi K, Smith P., Editors, "Advances in Mathematical Methods for Electromagnetics", Instution of Engineering and Technology.

[35] Tuchkin Y. A., (2010), “Analytic Regularization Methods”, In: Ström. S., Sirenko Y. K., Editors, “Modern Theory of Gratings”, Springer.

[36] Mitra R., Lee S. W., (1971), “Analytical Techniques in The Theory of Guided Waves”, 1st Edition, Macmillan Company.

[37] Wilkinson J. H., (1965), “The Algebraic Eigenvalue Problem”, 1st Edition, Clarendon Press.

[38] Bakhvalov N. S., (1977), “Numerical Methods: Analysis, Algebra, Ordinary Differential Equations”, 1st Edition, MIR Publisher.

[39] Tikhonov A. N., Arsenin V. Y., John F., (1977), “Solutions of ill-posed Problems”, 1st Edition, Winston.

[40] Krein S., (1982), “Linear Equations in Banach Spaces”, 1st Edition, Springer.

[41] Kantorovich L., Akilov G., (1964), “Functional Analysis in Normed Spaces, International Series of Monographs in Pure and Applied Mathematics”, 1st Edition, Pergamon Press.

[42] Kolmogorov A., Fomin S., (1957), “Elements of Function Theory and Functional Analysis”, 1st Edition, Graylock Press.

[43] Valagiannopoulos C. A., (2008), “Electromagnetic scattering from two eccentric metamaterial cylinders with frequency-dependent permittivities differing slightly each other”, Progress In Electromagnetics Research, 3, 23-34.

[44] Chew W. C., (1995), “Waves and Fields in Inhomogeneous Media”, 1st Edition, IEEE Press.

[45] Balanis C. A., (1989), “Advanced Electromagnetic Engineering”, 1st Edition, John Wiley & Sons.Inc.

[46] Eom H. J., (2004), “Electromagnetic Wave Theory for Boundary-Value Problems: An Advanced Course on Analytical Methods”, 1st Edition, Springer.

[47] Colton D., Kress R., (2013), “Integral Equation Methods in Scattering Theory”, 2nd Edition, SIAM Press.

[48] Gi͡unter N. M., (1967), “Potential Theory, and Its Applications to Basic Problems of Mathematical Physics”, 1st Edition, Burns & Oates.

[49] Tikhonov A. N., Samarskii A. A., (2013), “Equations of Mathematical Physics”, 1st Edition, Courier Corporation.

[50] Shestopalov V. P., Tuchkin Y. A., Poyedinchuk A. Y., Sirenko Y. K., (1997), “New methods for solving direct and inverse problems of diffraction theory,

Part 1: Analytical Regularization of Boundary Value Problems of Electromagnetics", (in Russian), Osnova Publishing House.

[51] Tuchkin Y. A., (2004), "Electromagnetic wave scattering by a smooth imperfectly conducting cylindrical obstacle", 10th International Conference on Mathematical Methods in Electromagnetic Theory, 106-110, Dniepropetrovsk, Ukraine, 14-17 September.

[52] Luke Y. L., (1975), "Mathematical Functions and Their Approximations", 1st Edition, Academic Press.

[53] Prudnikov A. P., Brychkov Y. A., Marichev O. I., Romer R. H., (1992), "Integrals and Series", 1st Edition, Gordon & Breach Science.

[54] Vinogradova E., (2017), "Reflectivity of two-dimensional airfoils illuminated by H-polarized plane wave: Rigorous approach", Electromagnetics, 37 (6), 377-397.

[55] Hu F. Q., (1994) F. "A Spectral Boundary Integral Equation Method, A fast numerical solution of scattering by a circular cylinder", Technical Report No: VA 23529, Department of Mathematics and Statistics, Old Dominion University, Norfolk.

[56] Hu F. Q., (1995), "A spectral boundary integral-equation method for the 2nd Helmholtz-equation", Journal of Computational Physics, 120 (2), 340-347.

[57] Senior T. B., Volakis J. L., (1995), "Approximate Boundary Conditions in Electromagnetics", 1st Edition, The Institution of Electrical Engineers.

BIOGRAPHY

Emrah Sever received his B.Sc. degree from Istanbul University Electrical and Electronics Engineering department in 2008 and M.Sc. degree from Istanbul Technical University Electronics and Telecommunication Engineering department in 2011. He started his Ph.D. studies at Gebze Technical University Graduate School of Natural and Applied Science department of Electronics Engineering in September 2011 and became a member of this department in 2013 as a research assistant. He is currently a research assistant in the department and interested in the research areas of the boundary value problems in diffraction theory. He is particularly interested in regularization of the systems of boundary value problems.